INVESTIGATION OF TRANSIENT OPERATION ON TUMBLE DRYERS
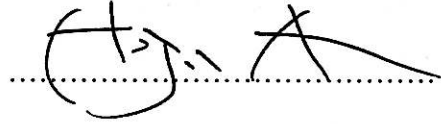
by

Burak Ukuşer

Submitted to the Institute of Graduate Studies in
Science and Engineering in partial fulfillment of
the requirements for the degree of
Master of Science
in
Mechanical Engineering

Yeditepe University
2010

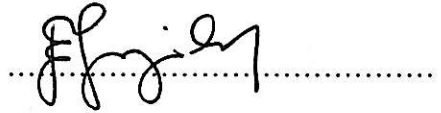# INVESTIGATION OF TRANSIENT OPERATION ON TUMBLE DRYERS

APPROVED BY:

Assoc. Prof. Dr. Hojin Ahn (Erdem An)      ......................................................
(Thesis Supervisor)

Prof. Dr. Oktay Özcan      ......................................................

Asst. Prof. Esra Sorgüven      ......................................................

DATE OF APPROVAL: …. /…. /….

# ACKNOWLEDGEMENTS

# ABSTRACT

## INVESTIGATION OF TRANSIENT OPERATION ON TUMBLE DRYERS

In this project, the start transient, steady-state operation and shutdown transient of a tumble dryer are experimentally investigated and a transient simulation model is developed using FORTRAN program. Both air-vented and air-condenser tumble dryers are employed in the present experiments. Relative humidity and temperature are measured at the drum outlet, also at the upstream of the heater that is located near the inlet of the drum. Using these measurements, the total mass transfer coefficient is calculated during the drying process. Several factors, which influence the characteristics of the total mass transfer coefficient, are investigated by the design of experiment method. The results show that the total mass transfer coefficient mainly depends on the amount of water remaining at the surface of the clothes. The experimental results have aided to the modeling of the tumble dryer operation. The main components of a tumble dryer such as fan, condenser, drum and heater are modeled, and the entire drying process from the start to the shutdown period is simulated. The simulation results are found to be in good agreement with the experimental data. The simulation model may be employed in the process of a new tumble dryer design.

# ÖZET

## TAMBURLU KURUTUCULARDA GEÇİCİ REJİM SÜRECİNİN ARAŞTIRILMASI

Bu projede, tamburlu kurutucunun başlangıç geçici rejimi, kararlı hal ve kapanma geçici rejimi deneysel olarak incelenmiştir ve FORTRAN programı kullanılarak geçici rejim simülasyon modeli geliştirilmiştir. Mevcut deneylerde hem bacalı, hem de hava kondenserli tamburlu kurutucular kullanılmıştır. Tambur çıkışında ve ayrıca tambur girişine yakın bir yerde bulunan ısıtıcı akış girişinde bağıl nem ve sıcaklık ölçülmüştür. Bu ölçümler kullanılarak kurutma süreci boyunca kütle transferi katsayısı hesaplanmıştır. Kütle transfer katsayısını etkileyen bir çok faktör, deney tasarımı yöntemi (Design of Experiment) kullanılarak incelenmiştir. Sonuçlar göstermiştir ki; kütle transfer katsayısı esas olarak çamaşır üzerinde kalan su miktarına bağlıdır. Deneysel sonuçlar, tamburlu kurutma süreci modellemesine yardımcı olmuştur. Fan, kondenser, tambur ve ısıtıcı gibi tamburlu bir kurutucunun temel bileşenleri modellenmiş ve başlangıçtan havalandırma periyoduna kadar tüm kurutma süreci simüle edilmiştir. Simülasyon sonuçları ile deneysel veriler arasında iyi bir uyum vardır. Oluşturulan simülasyon modeli yeni tamburlu kurutucu tasarımı sürecinde kullanılabilir.

# TABLE OF CONTENTS

# LIST OF FIGURES

# LIST OF TABLES

## LIST OF SYMBOLS

| | |
|---|---|
| $A$ | Surface area (m$^2$) |
| $a$ | Water activity parameter |
| $C$ | Molar concentration (kmol/m$^3$) |
| $C_c$ | Heat capacity of cold fluid (kj/kgK) |
| $C_{max}$ | Maximum heat capacity (kj/kg) |
| $C_{min}$ | Minimum heat capacity (kj/kg) |
| $C_h$ | Heat capacity of hot fluid (kj/kgK) |
| $C_r$ | Heat capacity ratio |
| $Cp$ | Specific heat at constant pressure (kj/kgK) |
| $Cp_{air}$ | Specific heat at constant pressure for dry air (kj/kgK) |
| $Cp_c$ | Specific heat at constant pressure for cold fluid (kj/kgK) |
| | Specific heat at constant pressure for clothes (kj/kgK) |
| $Cp_h$ | Specific heat at constant pressure for hot fluid (kj/kgK) |
| $Cp_w$ | Specific heat at constant pressure for water (kj/kgK) |
| $Cv$ | Specific heat at constant volume (kj/kgK) |
| $Cv_c$ | Specific heat at constant volume for cold fluid (kj/kgK) |
| $Cv_h$ | Specific heat at constant volume for hot fluid (kj/kgK) |
| $D$ | Diffusivity (m$^2$/s) |
| $F$ | Condenser correction factor |
| $FR_c$ | Mass flow rate of cooling air (L/s) |
| $FR_p$ | Mass flow rate of process air (L/s) |
| $g$ | Gravitational acceleration (m/s$^2$) |
| $h$ | Convectional heat transfer coefficient (W/m$^2$K) |
| $h_{cond}$ | Enthalpy at condenser (kj/kg) |
| $h_{drum}$ | Enthalpy at drum (kj/kg) |
| $h_f$ | Enthalpy of fluid phase (kj/kg) |
| $h_{fg}$ | Enthalpy of fluid-gas mixture (kj/kg) |
| $h_g$ | Enthalpy of gas phase (kj/kg) |
| $h_{heat}$ | Enthalpy at heater (kj/kg) |

| | |
|---|---|
| $h_m$ | Mass transfer coefficient (m/s) |
| $(hA)_m$ | Total mass transfer coefficient (m³/s) |
| $(hA)_{m_{overall}}$ | Total mass transfer coefficient at overall period (m³/s) |
| $(hA)_{m_{ss}}$ | Total mass transfer coefficient at steady state (m³/s) |
| $(hA)_{m_t}$ | Total mass transfer coefficient at transient period (m³/s) |
| $(hA_{ch})_{in}$ | Heat transfer coefficient times area at the channel inlet between the drum and the condenser entrance (W/K) |
| $(hA_{ch})_{out}$ | Heat transfer coefficient times area at the channel outlet between the drum and the condenser entrance (W/K) |
| $hA_{loss,heater}$ | Heat transfer coefficient times area for heater (kW/°C) |
| $hA_{loss,drum}$ | Heat transfer coefficient times area for the heat loss at drum (kW/°C) |
| $hA_{loss,heater}$ | Heat transfer coefficient times area for the heat loss at heater (kW/°C) |
| $J$ | Jacobian matrix |
| $j$ | Components of jacobian matrix |
| $k$ | Thermal conductivity (W/Km) |
| $Le$ | Lewis number |
| $L_v$ | Leakage of water vapor (%) |
| $m_a$ | Mass of dry air (kg) |
| $m_c$ | Mass of clothes (kg) |
| $m_w$ | Mass of water (kg) |
| $m\_c$ | Moisture content at the surface of the clothes (%) |
| $\dot{m}_{a\_in}$ | Mass flow rate of air leakage entering the drum (kg/s) |
| $\dot{m}_{a\_leak1}$ | Mass flow rate of air leakage leaving the drum (kg/s) |
| $\dot{m}_{a\_leak2}$ | Mass flow rate of air leakage entering the drum (kg/s) |
| $\dot{m}_{air}$ | Mass flow rate of air (kg/s) |
| $\dot{m}_{air,fan}$ | Mass flow rate of air at fan (kg/s) |
| $\dot{m}_{leak,fan}$ | Mass flow rate of air leakage at fan (kg/s) |
| $\dot{m}_c$ | Mass flow rate of cold fluid (kg/s) |
| $\dot{m}_h$ | Mass flow rate of hot fluid (kg/s) |
| $\dot{m}_v$ | Evaporation rate (g/s) |
| $NTU$ | Number of transfer units |
| $P$ | Total pressure (kPa) |

| | |
|---|---|
| $P_a$ | Dry air pressure (kPa) |
| $P_{atm}$ | Atmospheric air pressure (kPa) |
| $P_{air}$ | Dry air pressure (kPa) |
| $Pr$ | Prandtl number |
| $P_v$ | Vapor pressure (kPa) |
| $P_s$ | Saturation pressure (kPa) |
| $P_0$ | Atmospheric air pressure (kPa) |
| $q$ | The amount of heat transfer (kj) |
| $q_{max}$ | Maximum amount of allowable heat transfer (kj) |
| $Q$ | The amount of heat transfer (kj) |
| $Q_{total}$ | Total amount of heat transfer (kj) |
| $Q_{heater}$ | Total amount of heat transfer at heater (kj) |
| $\dot{Q}$ | Heat transfer rate (W) |
| $\dot{Q}_{CV}$ | Heat transfer rate of control volume (W) |
| $\dot{Q}_L$ | Rate of heat loss (W) |
| $R$ | Universal gas constant (J/Kmol) |
| $R_a$ | Dry air gas constant (J/Kmol) |
| $R_{cooling\ air}$ | Ratio of air leakage for cooling air from chassis into the condenser entrance |
| $R_{fan}$ | Ratio of air leakage at fan |
| $R_{heater}$ | Ratio of air leakage for heater at drum entrance |
| $R_v$ | Vapor gas constant (J/Kmol) |
| $Re$ | Reynolds number |
| $RH_{coeff}$ | Relative humidity coefficient |
| $RH_{cond}$ | Relative humidity at condenser |
| $RH_{drum}$ | Relative humidity at drum |
| $RH_{heat}$ | Relative humidity at heater |
| $RH_\infty$ | Relative humidity of ambient air |
| $T$ | Temperature (°C) |
| $t$ | Time (s) |
| $T_c$ | Temperature of cold fluid (°C) |
| $T_{cond}$ | Temperature at condenser (°C) |
| $T_{drum}$ | Temperature at drum (°C) |

| | |
|---|---|
| $T_h$ | Temperature of hot fluid (°C) |
| $T_{heat}$ | Temperature at heater (°C) |
| $T_{heater}$ | Temperature of the heater hardware (°C) |
| $T_m$ | Mean temperature (°C) |
| $T_\infty$ | Temperature of ambient air (°C) |
| $T_w$ | Temperature at the surface of the clothes (°C) |
| $U$ | Overall heat transfer coefficient (W/m$^2$K) |
| $u$ | Internal energy (kj/kg) |
| $u_c$ | Internal energy of clothes (kj/kg) |
| $u_w$ | Internal energy of water (kj/kg) |
| $Sc$ | Schmidt number |
| $Sh$ | Sherwood number |
| $SMER$ | Specific moisture extraction rate (g/kj) |
| $V$ | Volume (m$^3$) |
| | Velocity (m/s) |
| $V_E$ | External air flow (m$^3$/h) |
| $V_I$ | Internal air flow (m$^3$/h) |
| $w$ | Specific humidity (kg water vapor/kg dry air) |
| $w_{cloth}$ | Specific humidity at the surface of the clothes (g water vapor/kg dry air) |
| $w_{cond}$ | Specific humidity at condenser (g water vapor/kg dry air) |
| $w_{drum,i}$ | Specific humidity at drum inlet (g water vapor/kg dry air) |
| $w_{drum,e}$ | Specific humidity at drum exit (g water vapor/kg dry air) |
| $w_w$ | Specific humidity at the surface of the clothes (g water vapor/kg dry air) |
| $\dot{W}_{CV}$ | Work at control volume (W) |
| $X$ | Root of the solution set |
| | |
| $\alpha$ | Thermal diffusivity (m$^2$/s) |
| $\beta$ | Water activity constant |
| $\gamma$ | Water activity constant |
| $\delta$ | Water activity constant |
| $\Delta T_{lm}$ | Logarithmic mean temperature difference |
| $\varepsilon$ | Effectiveness ratio |

| | |
|---|---|
| $\eta$ | Efficiency |
| $\mu$ | Dynamic viscosity (Ns/m$^2$) |
| $\nu$ | Kinematic viscosity (m$^2$/s) |
| $\rho$ | Density (kg/m$^3$) |
| $\Phi$ | Relative humidity |
| $\Phi_{drum}$ | Relative humidity at the drum |
| $\hat{X}_n$ | Solution set of jacobian matrix |
| | |
| AV | Air-vented |
| CV | Control volume |
| EC | Energy consumption |
| EN | European Nation |
| EU | European Union |
| DOE | Design of experiment |
| LMTD | Logarithmic mean temperature difference |
| NTU | Number of units |
| SMER | Specific moisture extraction rate |
| RH | Relative humidity |
| VBA | Excel Visual Basic |
| VTS | Data collecting system |

# 1. INTRODUCTION

## 1.1. DRYING TECHONOLOGY

Since the beginning of the civilization, washing and drying of laundry has become a daily routine of human life. For centuries, washing and drying are performed by hands or by the help of the sunlight. Thereby, cleaning with the assistance of washing and drying had been a very labor and time intensive process.



Figure 1.1. Historical background of washing & drying technology [1]

After the washing process, water has been extracted from clothes by two well-known methods; mechanically and thermally or the combination of these two methods. Until the beginning of the 19th century, wringing clothes by hand had been the only mechanical way for extracting water from the clothes.

The first machine to extract water from fabrics was called a "mangle (in U.K.)" or "wringer (in the U.S.A.)" invented in 1850 by Robert Tasker in Lancashire shown in Figure 1.2. The mangle simply consisted of two rollers in a rotary frame and powered by a hand crank or electricity. The main aim of this old-fashioned machine was to extract excess water content from the textile fibers prior to ironing while pressed laundry was passing across the rollers.

Figure 1.2. The mangle machine [2]

When home washing machines were first invented, they were simply a bucket on legs or wheels. The hand-cranked mangle appeared on top of the washing machine after 1843 when John E. Turnbull of Saint John, New Brunswick patented a "Clothes Washer with Wringer Rolls." In the 1940s, electric mangles were developed and they are still a feature of many laundry rooms. They consist of a rotating padded drum that revolves against a heating element. The heating element can be stationary, or can also be a rotating drum.

The Germans later invented a centrifuging technique to remove the moisture content from and to dry clothes. A new concept was later refined by the Americans and is incorporated in vertical axis washing machines available today. The first and even today most commonly used method for extracting water from laundry is to benefit from the sunlight.
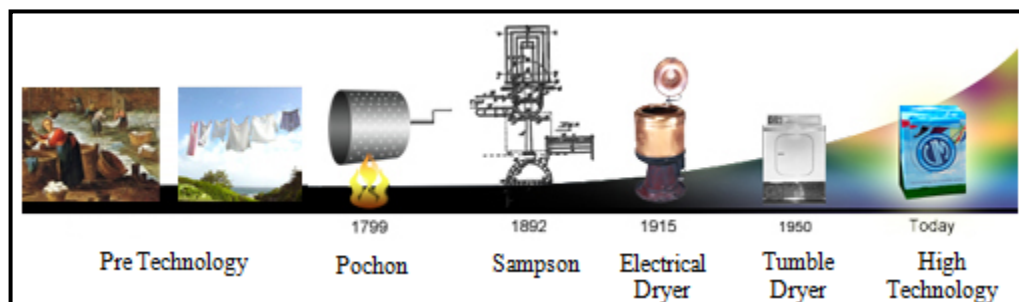


Figure 1.3. Historical evaluation of the drying technology [3]

In the early 1800s, clothes dryers were first being invented in England and France. One common kind of early clothes dryer was the ventilator; the first one known to be built was made by a Frenchman named Pochon. The ventilator was a barrel-shaped metal drum with holes in it and turned by hand over a fire. One early American patent for clothes dryer was granted to George T. Sampson on June 7, 1892. Sampson's dryer was an example of ventilator type machine and used the heat from a stove to dry clothes. In 1915, the first electrical drying machine was invented. Nowadays, with the assistance of developments on drying technology, latest high-tech dryers are on the market.

## 1.2. COMMERCIAL TUMBLE DRYERS

Cleaning and drying takes time with former technology. As technology grows up, people started to change their lifestyle in a much comfortable way. Since time requirement for cleaning decreases, people wash clothes more frequently. Home appliance companies try to facilitate their consumers' life by producing washing machines with higher capacities, shorter washing programs and faster spinning cycles.

The need for commercial tumble dryers increases day by day because of the shorter time advantage, more hygienic drying and less space requirement than hanging out the laundry. On the other hand, newly built apartments in metropolis with no appropriate space like balcony trigger more people to buy tumble dryers every day. Estimated number of tumble dryers for EU in the future is given in Figure 1.4.
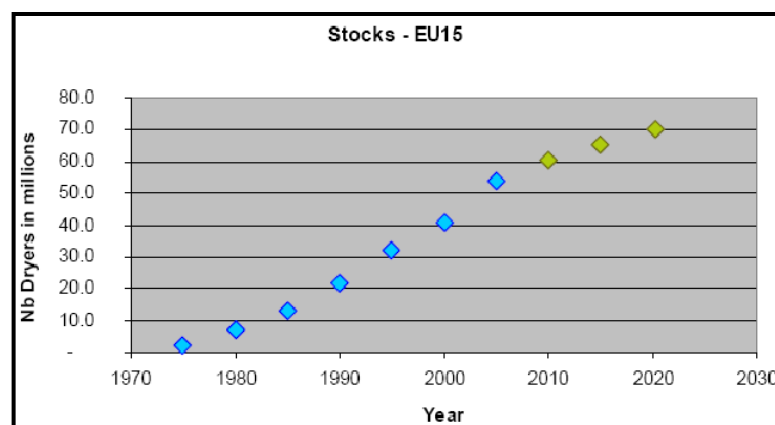


Figure 1.4. Estimated number of the tumble dryers in EU [4]

Tumble dryers are mainly divided into two groups according to the system involved in the drying process; open systems and closed systems. Classification of the tumble dryers is given in Figure 1.5.
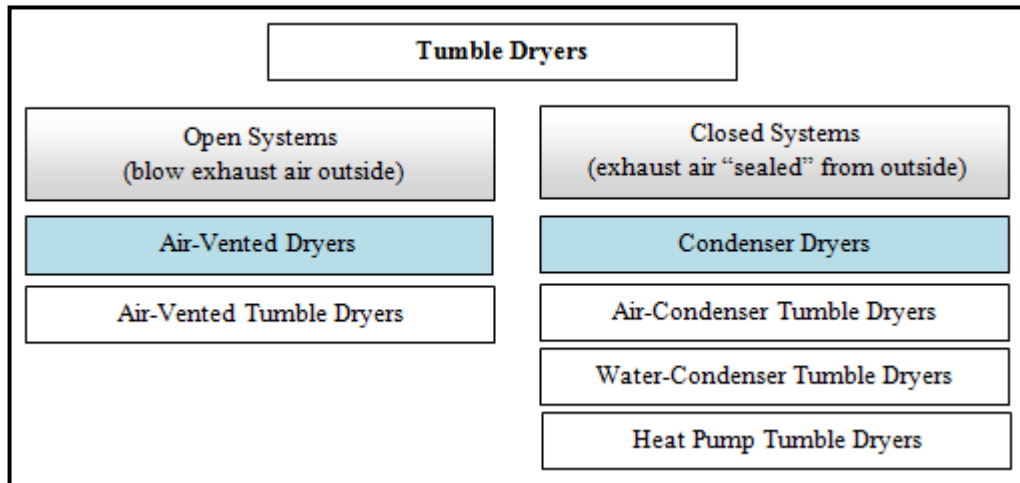


Figure 1.5. Classification of the tumble dryers [5]

### 1.2.1. Air-Vented Tumble Dryers

A typical air-vented tumble dryer consists of a drum, a fan and a heater, which are shown schematically in Figure 1.6. Drum is the main component of the dryer for holding and turning upside down the wet clothes during the drying. Heater is used for providing hot air for drying process. Fan is used for blowing the air inside the drum. An electric motor is used for powering fan and rotating the drum. Moreover, a lint filter is located on the door of the dryer to prevent lint from reaching undesirable places inside the machine.
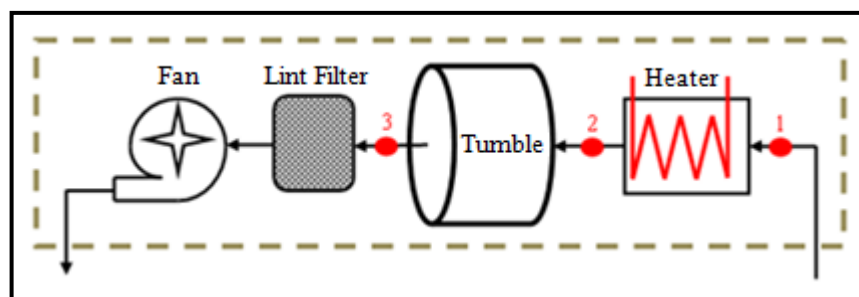


Figure 1.6. Air-vented tumble dryer cycle [3]

The working principle of an air-vented tumble dryer is also given in Figure 1.6. In air-vented tumble dryers, room air (nearly at 25 °C) is blown through the heater by a fan. Most of the dry air is inhaled from the free space under the drum. Room air is heated while passing through the channels of the heater (1-2). The heated air enters the drum, where dry air is brought into contact with the cold wet clothes. During this process, hot dry air with high moisture removal capacity facilitates the evaporation of water from the surface of the textiles (2-3). The humid air passes through a lint filter while leaving the drum. Exhaust humid air is evacuated outside through a flexible pipe by the fan.

If we would like to analyze the process thermodynamically on the psychometric chart in Figure 1.7, heating the room air increases the driving potential for the evaporation process of the moisture in the clothes. During the heating process at the heater, only the temperature of the air is increased. The humidification process within the drum is an isenthalpic process where the energy required for the evaporation is supplied by the heated air. Relative humidity of the air is increased according to the decrease in the temperature of the exit air relative to the inlet air.
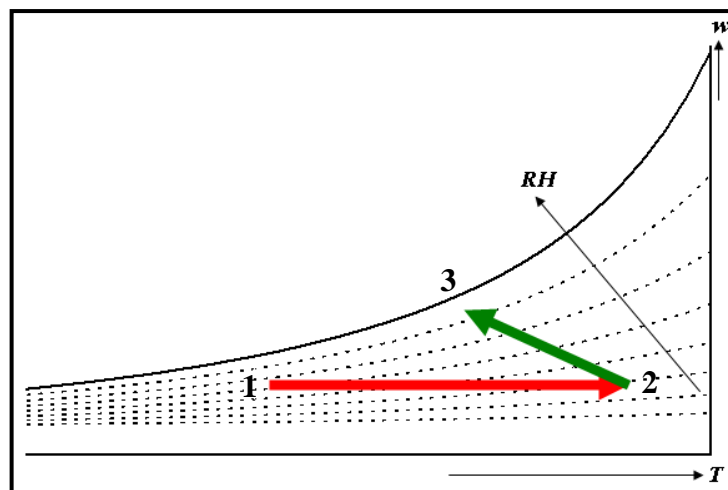
Figure 1.7. Thermodynamic process of the air-vented tumble dryer cycle [3]

The conventional process of air-vented tumble dryer is simple, effective, reliable and relatively fast. Nevertheless, since the excess energy is wasted through the duct, efficiency of an air-vented tumble dryer is much more less than the other types of the tumble dryers.

In addition, the requirement for a duct system to exhaust the air to the outdoor makes this technology inefficient. Especially in cold climates, household heating system must compensate for the exhausted air by additional heating. Moreover, in some applications of this method, it is impossible to locate a duct, thus the exhaust humid air is vented to the bathroom. In such cases, the humidity of the room is increased rapidly and that is not desirable for health.

In order to reduce the heating cost, a heat exchanger could be installed between the hot exhaust air and inlet room ambient air. In same applications, heat recovery can be applied between the exhaust air and inlet room air via air-air heat exchangers. However, humidity removal capacity of the air may be decreased in such applications.

### 1.2.2.  Condenser Tumble Dryers

Designers considered that the energy potential of the exhaust air in air-vented tumble dryers should not be underestimated. Thus, condenser tumble dryers came forward in the tumble dryer market.  Instead of exhausting the humid air outside, in this new technology a heat exchanger (namely, a condenser) is installed. Inside the heat exchanger, water vapor in the humid air condenses and which is collected by either a drainpipe or a collection tank.

Condenser tumble dryer technology includes a closed cycle and does not require a venting duct to the exterior of the house. Hence, this type of dryers can be placed at any location within the house.

#### 1.2.2.1.  *Air-Condenser Tumble Dryers*

Air-condenser tumble dryers are preferred to the air-vented tumble dryers, because of their low energy consumption and relatively high efficient drying performance in comparison. In this type of condenser dryer, room air is used as a cooling fluid inside the cycle, which will be explained later on.

Air-condenser tumble dryer is composed of a heater, a drum and a filter similar to the air-vented dryer as shown in Figure 1.8 schematically.
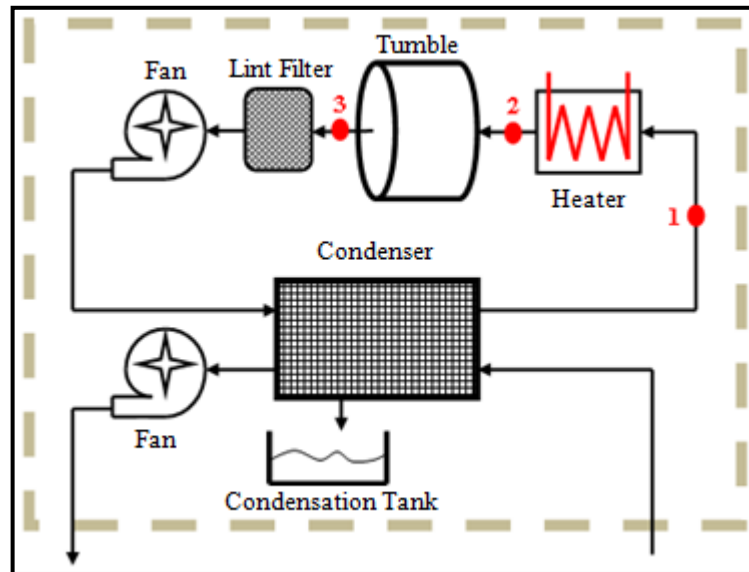
Figure 1.8. Air-condenser tumble dryer cycle [3]

In addition, there are two fans on the system. One of them is responsible for providing the fresh cool air to the condenser, and the other one is used for blowing the hot air through the clothes inside the tumble. The other main component of the system is condenser where the condensation process takes place.

A heater heats up the process air before entering the drum as in air-vented tumble dryers. As the temperature of the air increases, relative humidity decreases, and thus the evaporating potential of the process air increases (1-2) as shown on the psychometric chart in Figure 1.9. Inside the drum, the hot and dry air contacts with the cold wet clothes thus, moisture is evaporated from the clothes (2-3). The process air with high potential of humidity that exits the tumble is blown through the condenser by a process fan after passing through the filter. Then the second fan steps up and the ambient cold air is also blown through the condenser. In the condenser, the humid process air is cooled by contacting with the ambient air (3-1). Briefly, condensation process of the water vapor in takes place inside the condenser channels.

The condensed water is either pumped to a tank installed on the machine for manual removal or directly pumped to drain so that users may not have to unload the large condensate-holding tank periodically.
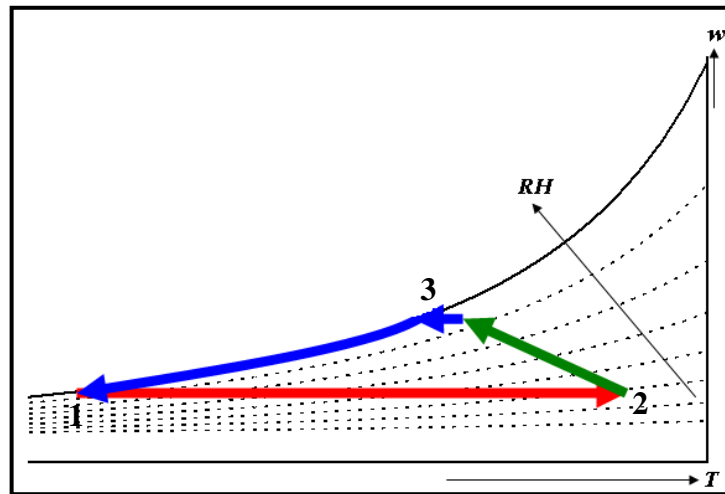
Figure 1.9. Thermodynamic process of the air-condenser tumble dryer cycle [3]

Air-condenser dryers are more expensive than the air-vented dryers. In addition, they have disadvantages on maintenance such as the requirement of manual water drainage removal and cleaning of the condenser from accumulated lint. Moreover, it should be taken into consideration that the air-condenser tumble dryers consume less energy and can be installed anywhere in the house. They also fit to the new trend by consuming less energy, if we consider that the natural sources are in danger of depletion.

### 1.2.2.2. *Water-Condenser Tumble Dryers*

Water condenser dryer uses water as a cooling fluid and condensing moisture instead of air. So far, it seemed that there is no tumble dryer on the market using this technology. However, it is usually what washer/dryers rely on for their "drying" function.

In washer/dryers, the ventless condenser system is also widely used, but in these cases, condensers are water-cooled. During a dry cycle, several gallons of cold water are used to condense the moisture evaporated from the clothes, which again is pumped away through the drain line. Most of the washer/dryers are currently available in North America use this method. Note that unlike the air-cooled design, these models do not significantly heat the indoor air in the laundry room. On the other hand, the fact that they use extra water during the dry cycle must be taken into consideration, especially for limited (or expensive) water supply areas.

### *1.2.2.3.  Heat Pump Tumble Dryers*

The heat pump dryer is relatively a new concept in the dryer market. The first heat pump dryer was introduced by Electrolux in 1997 [6]. As shown in Table 1.1, heat pump dryers have not been able to grab a large market share in Europe [5]. However, the market share of heat pump dryers is increasing in China compared to EU in a significant manner, as it can be understood from Figure 1.10 [4].

Table 1.1. Sales distribution of the heat pump dryers [5]

| Region | Western Europe | | Eastern Europe | |
|---|---|---|---|---|
| Year | 2002 | 2005 | 2002 | 2005 |
| Market Share (per cent) | 0,4 | 0,5 | 0,1 | 0,5 |
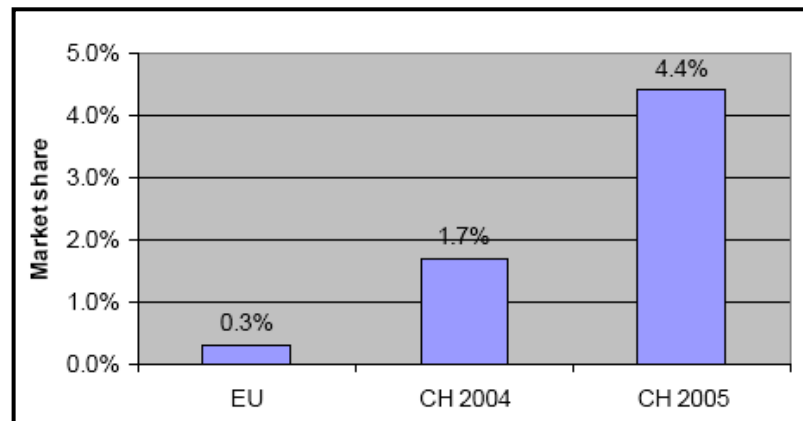


Figure 1.10. Market share of the heat pump tumble dryers [4]

Heat pump dryer is also similarly consists of a drum, filter and fan within the process cycle. The only difference in the concept is within the cooling cycle that contains a condenser, evaporator, expansion valve and compressor as in Figure 1.11.

The condenser in heat pump dryers replaces heater. After passing through the tumble and the filter (1-2), humidified air is blown through the evaporator. Inside the evaporator, the temperature of the humid air is reduced below the dew point. Moreover, condensation of the humid water vapor is takes place inside the evaporator (2-3). After the evaporator, the process air is transferred through the condenser. In the condenser, air is heated before being blown back to the tumble (3-1).
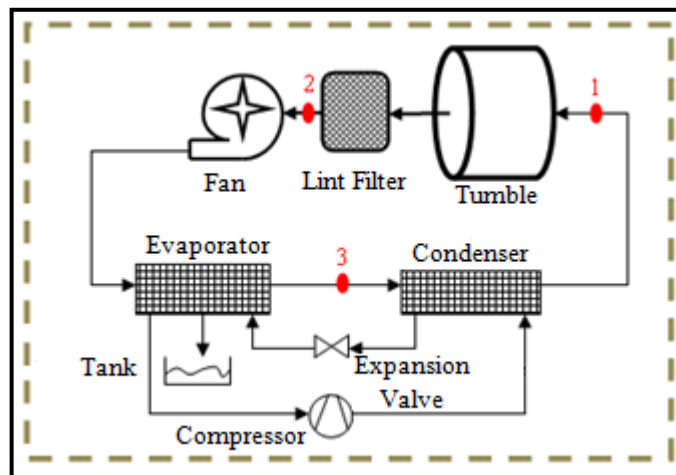
Figure 1.11. Heat pump tumble dryer cycle [3]

Thanks to the heat recovery system provided by the cooling cycle via compressor, condenser, evaporator and the expansion valve, heat pump dryers consume much less energy than the other technologies in the market.

### 1.2.3. Energy Classification of Tumble Dryers

According to the harsh downside potential of energy resources, world energy becomes more significant than ever. This situation also affects the standardization of the tumble dryers, which consume huge amount of energy compared to other home appliances. The valid standard within the EU is EN 61121:2005 and given in Table 1.2.

Table 1.2. EU energy label of the tumble dryers according to EN 61121:2005 [5]

| EU Energy Label | Condensing Dryer Energy Consumption (kWh/kg) | Air-Vented Dryer Energy Consumption (kWh/kg) |
|---|---|---|
| A | EC <= 0.55 | EC>=0.51 |
| B | 0.55 < EC <= 0.64 | 0.51 < EC <= 0.59 |
| C | 0.64 < EC <= 0.73 | 0.59 < EC <= 0.67 |
| D | 0.73 < EC <= 0.82 | 0.67 < EC <= 0.75 |
| E | 0.82 < EC <= 0.91 | 0.75 < EC <= 0.83 |
| F | 0.91 < EC <= 1.00 | 0.83 < EC <= 0.91 |
| G | EC > 1.00 | EC > 0.91 |

## 2. LITERATURE SURVEY

The main aim of this project is constructing a simulation model of tumble dryers in order to observe the drying process during the whole drying cycle. According to the objective of the project, studies that are performed in the literature are investigated and explained briefly.

## 2.1. MODELING OF HEATING AND DRYING PROCESSES IN A CLOTHES DRYER

In this project, diffusion coefficient of sample cloth is investigated. Author stated that this data would be useful in determining the correlation of the area mass transfer coefficient of sample cloth inside the tumble.
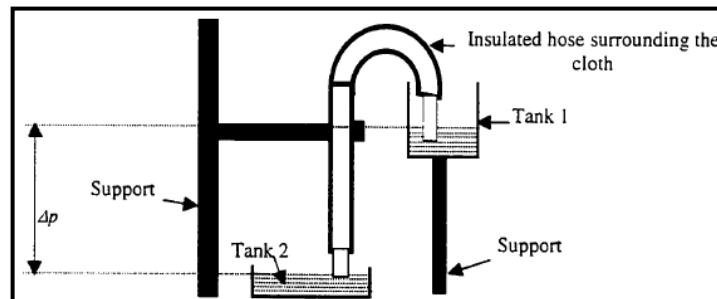


Figure 2.1. Experimental setup for the flow conductivity [7]
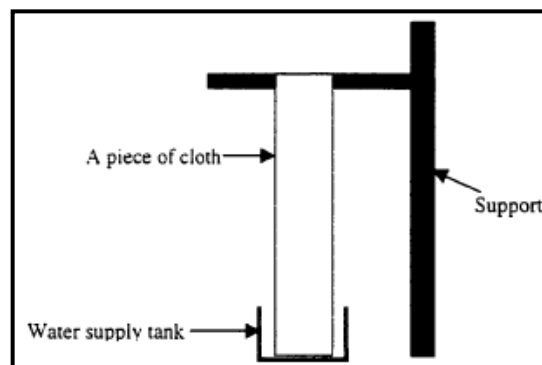


Figure 2.2. Experimental setup for the diffusion coefficient of the sample [7]
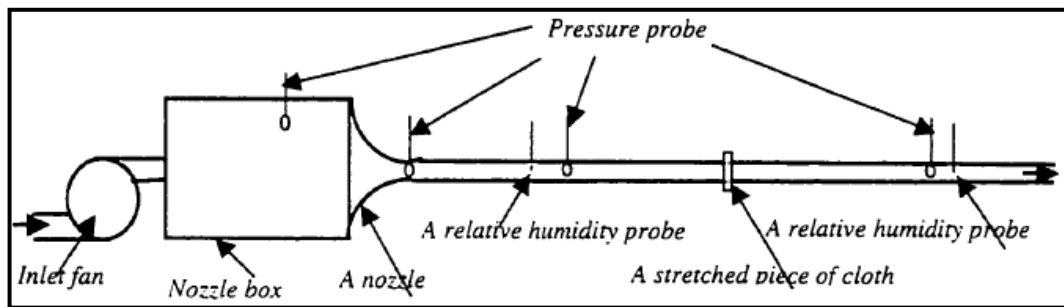
Figure 2.3. Experimental setup for the mass transfer from a piece of cloth [7]

Time dependent flow conductivity and the diffusivity of the sample cloth are determined via the constructed setups. The author also explains detailed mathematical calculations. In this project, factors that affect the area mass transfer coefficient are investigated by series of experiments performed on an air-vented tumble dryer. These factors are; the drum speed, fan speed, weight of the clothes, heater power and the theoretical movement of the clothes inside the drum.
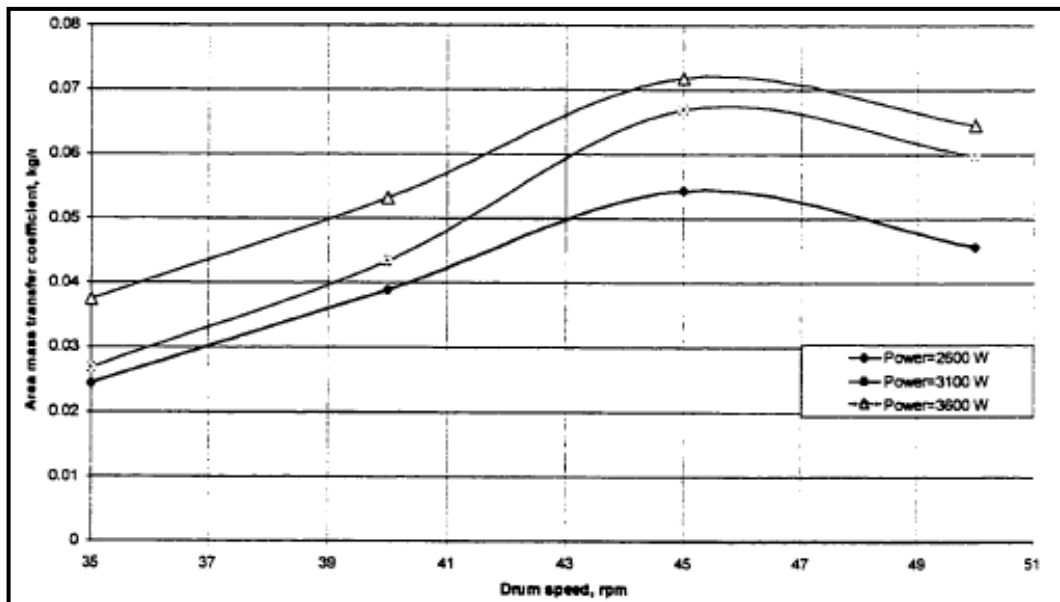


Figure 2.4. Effect of drum speed and variable heater power on the area mass transfer coefficient [7]
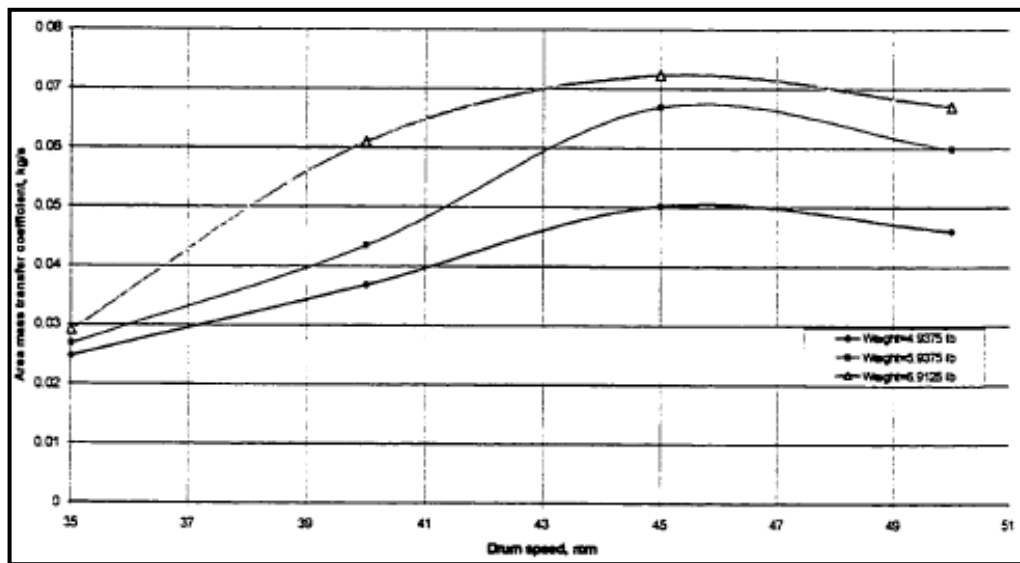
Figure 2.5. Effect of drum speed and variable weight of the clothes on the area mass transfer coefficient [7]

In summary, the area mass transfer correlation coefficient is both experimentally theoretically and determined. Author focused on the conic angle of the heater and the optimization of the heater parameters. The correlation equation showed that the area of mass transfer is a function of the weight of clothes and drum speed. However, the mass transfer coefficient is a function of the air flow rate, the relative humidity at the dryer outlet, the dry bulb temperature at the dryer outlet, and the material of clothes.

## 2.2. A MATHEMATICAL MODEL OF DRYING PROCESS

This study investigates the convectional heat transfer involved in the drying process of leather industry. The mathematical model is derived by Nordon, and after the modifications below, differential equations are obtained.

$$D\frac{\partial C_A}{\partial x^2} - \frac{\partial C_F}{\partial t} + \frac{\partial C_A}{\partial t} \tag{2.1}$$

$$k\frac{\partial^2 T}{\partial x^2} - \rho C_p \frac{\partial T}{\partial t} - \lambda \frac{\partial C_F}{\partial t} \tag{2.2}$$

Moisture content and the temperature of the leather are calculated using the required parameters, which are also indicated in the paper. First graph in Figure 2.6 represents the moisture content of leather with respect to relative humidity and time at the locations of center and surface.
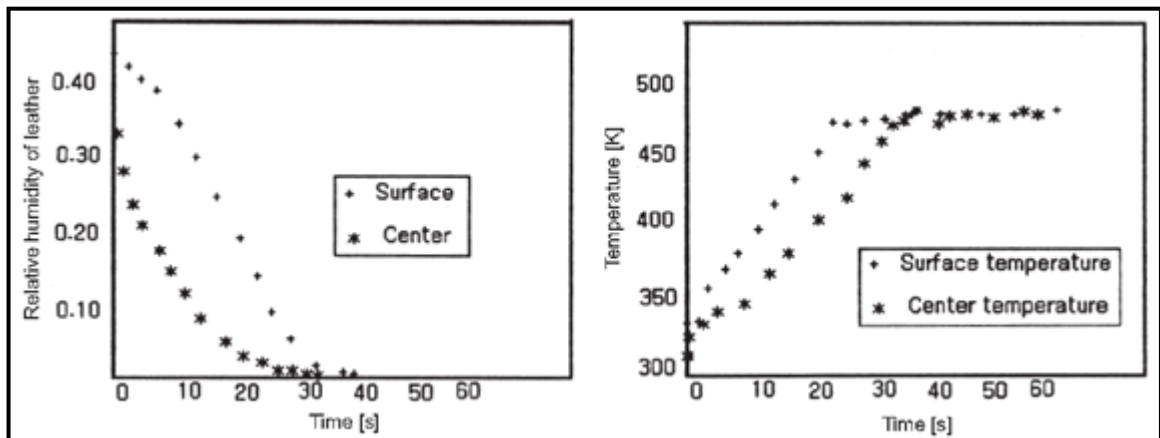


Figure 2.6. Change in moisture content & temperature with respect to time: effects of factors are investigated both for surface and center temperature [8]

It can be seen that the surface and the center temperatures increase up to the saturation point, at that point moisture of the leather starts to evaporate. From that point, the difference between the surface temperature and the center temperature increases due to the different moisture contents of the surface and the center. The mathematical model developed in this study can be used to predict transient variations in temperature and moisture content distribution of leather in the dryer.

## 2.3. FABRIC DRYING PROCESS IN DOMESTIC DRYERS

This study includes the mathematical modeling of the flow across the blower, across the drum external surface, across the heater, across the drum. For the experimental study, temperature relative humidity and flow rate measurements are performed for an air-vented tumble dryer. K – type thermocouples are used for temperature measurement. A 2000 W heater is used and the algorithm of the heater is set to be terminated by the humidity sensors inside the dryer. The weight of the dryer is also controlled during the experiment with the help of the calibrated weighing instrument.
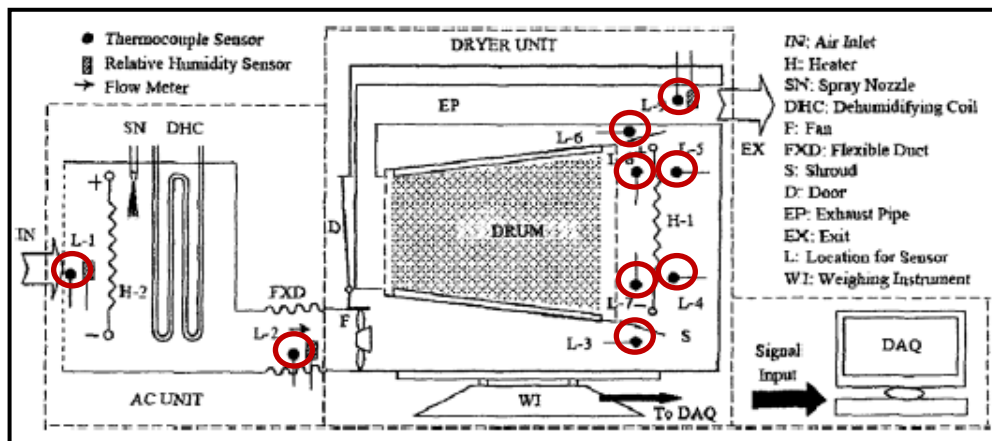
Figure 2.7. Experimental setup for the study: sensor locations are indicated with red colored circles [9]

Sensors positions are circled in red to indicate them clearly. Flow rate is determined by using a flow meter. Shielding is performed in order to avoid the effects of radiation from the heater. Various factors affecting the performance of the machine are discussed in this study. It can be understood that the experimental and simulation results were in fair agreement by investigating Figure 2.8.
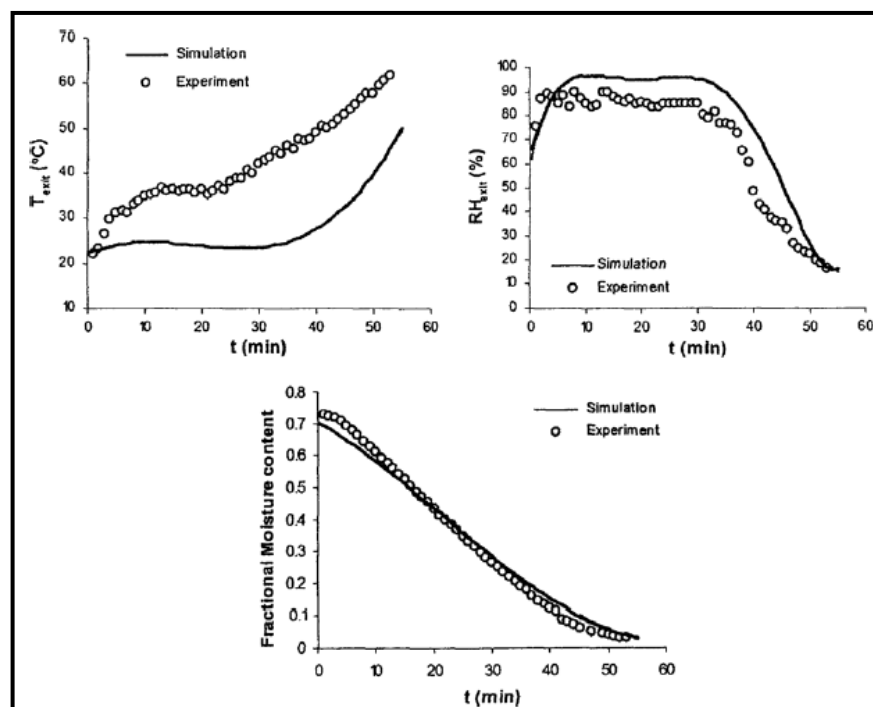


Figure 2.8. Data comparison for the simulation & experimental results [9]

## 2.4. PERFORMANCE ANALYSIS OF A TUMBLE DRYER

In this project, experiments are performed on an air-condenser tumble dryer with a heater of 2500 W power. Cotton is selected as textile type. The internal airflow was measured before and after the fan to estimate the proportion of leakage. Velocity profiles were determined in each cross section.

Energy performance, particularly energy consumption of the machine is taken into consideration during this study. Several modifications are set and tested on the machine and its components. Some of the results are given in Figure 2.9.
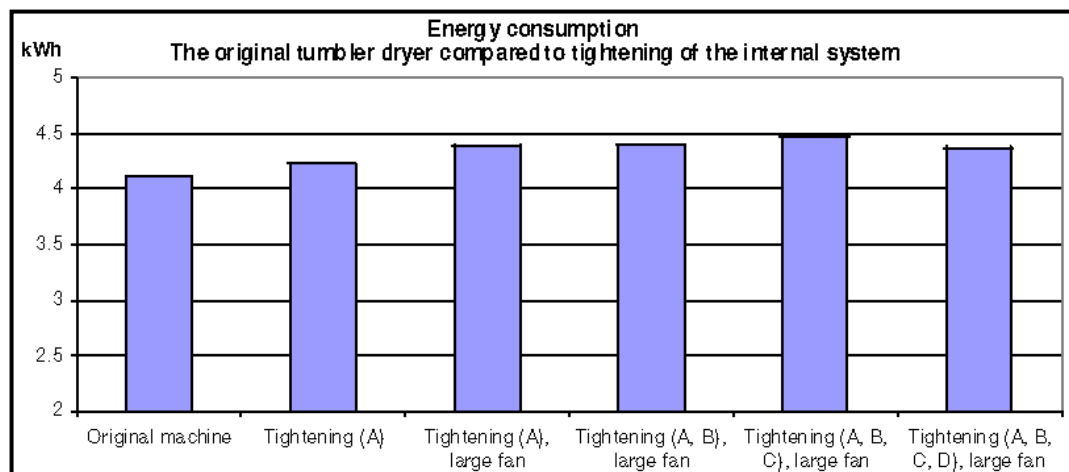


Figure 2.9. Energy consumptions for several rearrangements in the setup [10]

The back of the drum was tightened with an extra sealing (A). A return tube, transporting condensed moisture from a condensation water container to the water pump, has been sealed (B). The condenser was tightened in both ends to decrease leakage between internal and external flows (C). Finally, the shaft of the fan was tightened with a radial sealing (D). Distribution of energy consumption for the modifications performed on the setup is given in Figure 2.9.

The leakage of humid air from the closed system ranges between 20 and 40 per cent of the total airflow in the closed system. The main leakage is located at the entrance of the drum, and between the heat exchanger and the electric heater.

## 2.5. MATHEMATICAL MODELING AND COMPUTER SIMULATION OF A DRUM DRYER

A mathematical model based on the principles of heat and mass transfer taking place during the drying process has been developed during this study. Element material and energy balance equations are solved simultaneously using the modified Euler's method with time step variation. In addition, this study resembles the investigation of the drying process in food industry by three separated sections of drying. In the first part, temperature of the material increases up to boiling, in the second part where evaporation takes place from the outer surface at the boiling point and in the final part surface temperature increases again from boiling point to the final temperature.
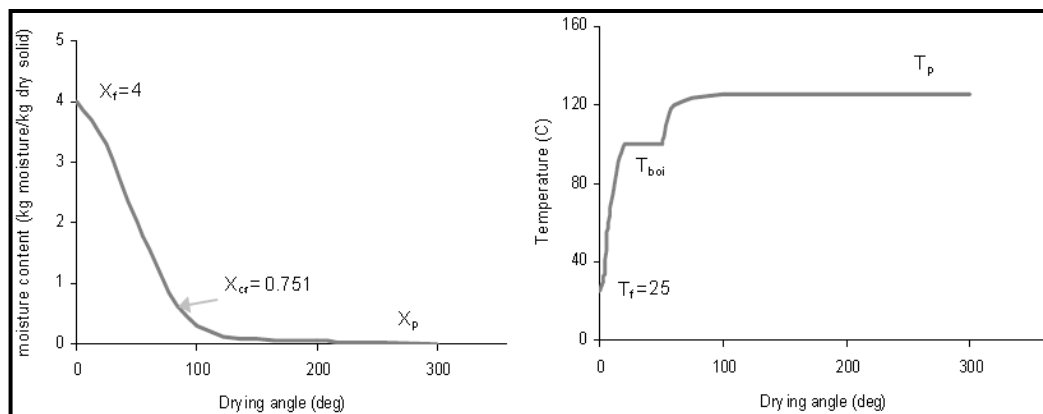


Figure 2.10. Distribution of temperature & moisture content on drying angle [11]

## 2.6. MODELING THE PROCESS OF DRYING STATIONARY OBJECTS INSIDE A TUMBLE DRYER USING COSMOL MULTIPHYSICS

This study contains the 2D model simulation of temperature and residual moisture content of stationary textile in a home tumble dryer with COMSOL Multiphysics. The drying air energy, mass and momentum transport were coupled to the textile model simulation but not included in the model validation. First model (textile domain) couples energy and mass transport in and out of the textile during the drying process where the air temperature and relative humidity are predetermined by the measurements. In the second model (air domain), air temperature and quality are modeled.
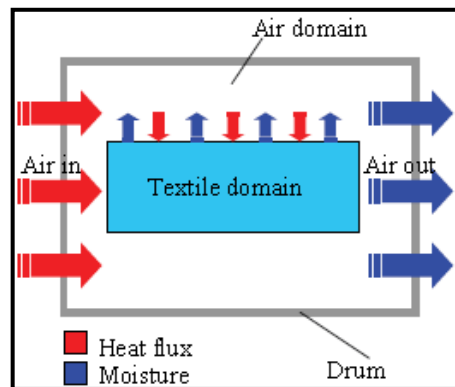
Figure 2.11. Schematics of the drying process inside the drum [12]

The energy passing into the textile helps the moisture overcome the binding forces, raises the vapor pressure and drives the moisture out to the surface.
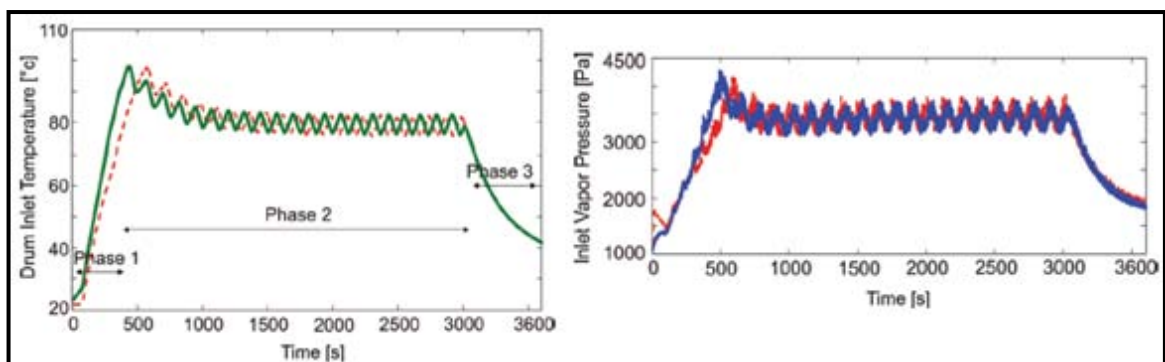


Figure 2.12. Measurements of the temperature & vapor pressure at the drum inlet [12]

The cycle starts with an increase in the drum inlet temperature. In the second phase, the inlet temperature stays almost constant. At the end, there is a cooling phase where room temperature is achieved. In all three phases, air enters with a low vapor pressure to create a higher concentration gradient at the textile surface.

In Figure 2.13, the difference between simulation and experimental results arise from that reasons, the sensor used to measure the air relative humidity (for calculating the air vapor pressure) delivers false values once water drops condense on its surface. Moreover, the model outputs a simulated temperature at a certain point, while the temperature sensor measures the temperature at many points along its surface and the output is an average.
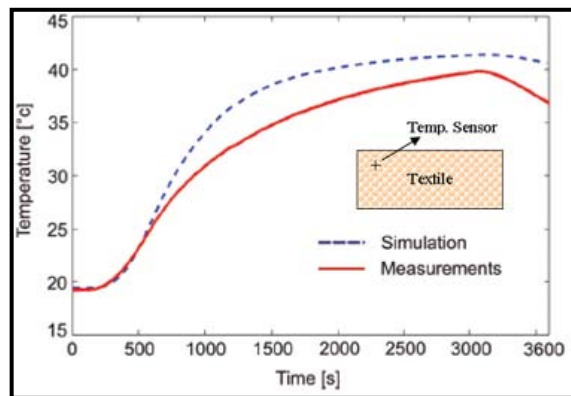
Figure 2.13. Simulation & experimental results of the study [12]

In addition, the textile used in the tests has folds and the geometry is not uniform as in the simulation and the air flow was not simulated yet. In one way, the difference between simulation and measurements can be reduced by using a smaller thermocouple that has less surface area.
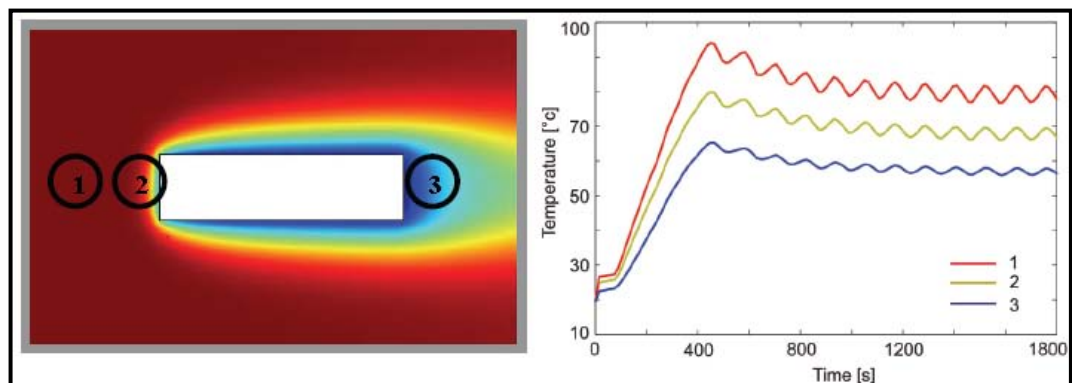


Figure 2.14. Distribution of the temperature for the air domain model [12]
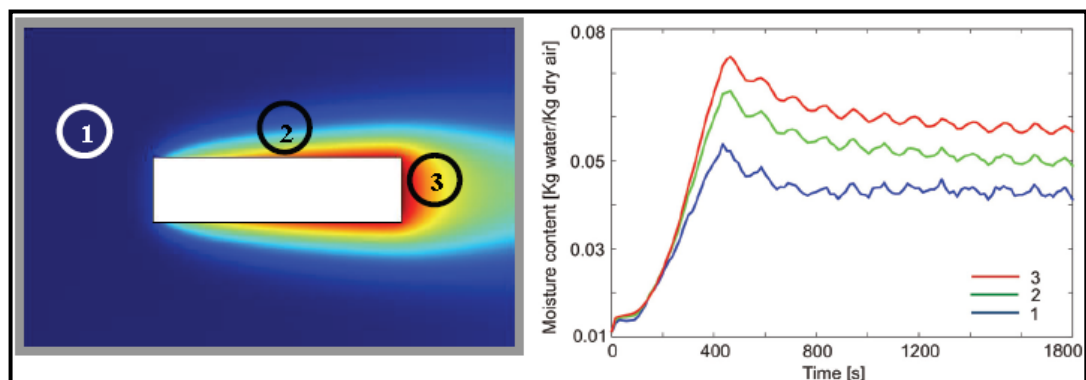


Figure 2.15. Distribution of the moisture content for the air domain model [12]

Sharp curves are due to large integration steps. Simulation results show strong tendency to enhancement by decreasing the integration step. Temperature and moisture content graphs are in good agreement with ideal drying curves.

## 2.7. MODELING OF SPECIFIC MOISTURE EXTRACTION RATE AND LEAKAGE RATIO IN A CONDENSING TUMBLE DRYER

The aim of this study is to use a design of experiments in order to create a statistical model over the condensing tumble dryer. The model will be used to find the best settings for the power supply to the heater, the internal airflow and the external airflow in order to reach a high specific moisture extraction rate (SMER) and a low leakage ratio.
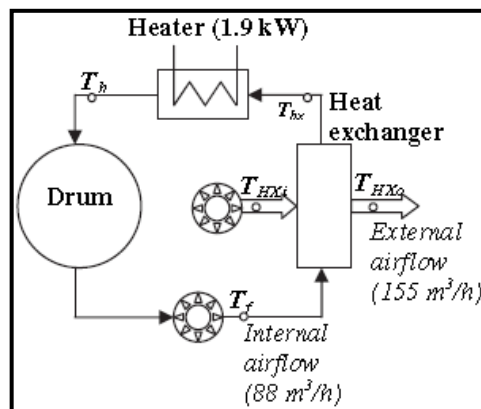


Figure 2.16. Schematics of the condenser dryer in the study [13]

The power supply to the heater, the internal and the external airflows were studied as factors affecting the performance of the dryer.

$$SMER = \frac{m_{Wi} - m_{Wo}}{Q_{total}}$$

(2.3)

The SMER in Equation 2.3 shows the ratio between the amount of evaporated water and the total energy supply. A high SMER would indicate an efficient drying process with low energy losses.

Tests performed in the condensing tumble dryer with varying values of power supply to the heater, internal airflow and external airflow. The measured values of SMER and leakage ratio are shown in Table 2.1.

Table 2.1. DOE results of the study [13]

| Experiment Number | Factors | | | Responses | |
|---|---|---|---|---|---|
| | $\dot{Q}_h$ (W) | $\dot{V}_I$ (m³/h) | $\dot{V}_E$ (m³/h) | $SMER$ (g/k) | $L_v$ (%) |
| 1 | 1355 | 66 | 72 | 0.259 | 50.1 |
| 2 | 1666 | 66 | 72 | 0.264 | 49.7 |
| 3 | 1329 | 88 | 72 | 0.257 | 56.3 |
| 4 | 1606 | 88 | 72 | 0.265 | 54.2 |
| 5 | 1381 | 66 | 155 | 0.241 | 29.3 |
| 6 | 1673 | 66 | 155 | 0.248 | 30.3 |
| 7 | 1401 | 88 | 155 | 0.241 | 35.8 |
| 8 | 1660 | 88 | 155 | 0.251 | 34.2 |
| 9 | 1381 | 77 | 113 | 0.253 | 38.8 |
| 10 | 1617 | 77 | 113 | 0.257 | 37.4 |
| 11 | 1500 | 66 | 113 | 0.249 | 32.1 |
| 12 | 1521 | 88 | 113 | 0.253 | 42.4 |
| 13 | 1578 | 77 | 72 | 0.264 | 46.4 |
| 14 | 1510 | 77 | 155 | 0.243 | 30.7 |
| 15 | 1442 | 77 | 113 | 0.251 | 38.0 |
| 16 | 1516 | 77 | 113 | 0.251 | 37.7 |
| 17 | 1529 | 77 | 113 | 0.251 | 38.1 |
| 18 | 1575 | 77 | 113 | 0.256 | 35.2 |
| 19 | 1523 | 77 | 113 | 0.252 | 36.2 |

In conclusion, a high power supply to the heater, a high internal airflow and a low external airflow give the highest SMER value. The leakage ratio is most affected by the external airflow. High moisture content leads to increased leakage.

# 3.  EXPERIMENTAL STUDY

## 3.1.  EXPERIMENTAL SETUP

The main aim of the experimental study is to investigate the mass transfer process between wet clothes and dry air inside the drum. Since the condenser dryer involves the complicate process of condensation in the condenser, it is easier to study the mass transfer process with the air-vented tumble dryer, which has no condenser. Typically, as mentioned before, an air-vented tumble dryer consists of fan, heater, drum, filter, and exhaust duct.

### 3.1.1.  Humidity Sensors and UDAQ System

In the present experiments, Sensiron SHT71 pin type relative humidity sensors shown in Figure 3.1 are utilized. These sensors measure the relative humidity and temperature simultaneously.
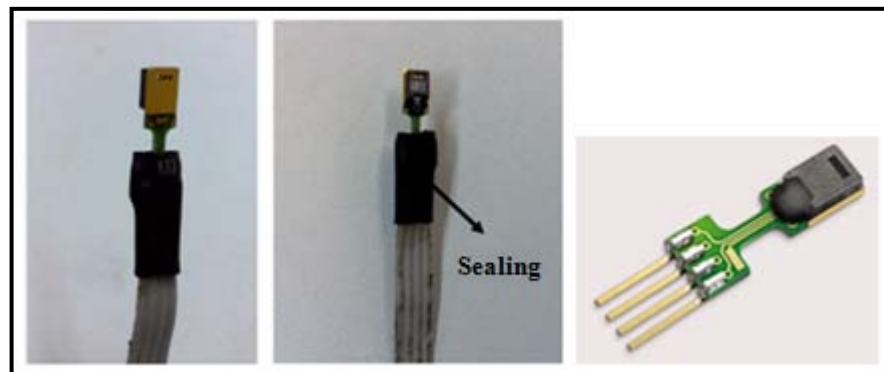


Figure 3.1. Relative humidity sensors

The sensors are characterized by its long-term stability and the cutting edge low energy consumption. A capacitive sensor element is used for measuring the relative humidity while, temperature is measured by a band-gap sensor. Sensors are coupled to a 14-bit analog to digital converter and a serial interface circuit. The part where the sensor is connected to the cable is sealed with hard plastic material in order to prevent the direct contact between water drops and the connecting part.

Accuracy limits for both relative humidity and temperature measurements are $\pm 3$ RH in percentage and $\pm 0.4$ °C respectively, which are given in Figure 3.2.
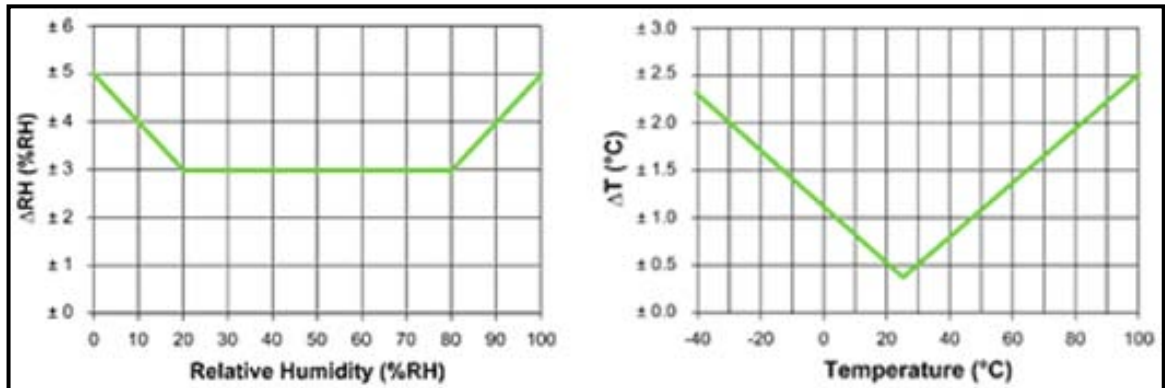


Figure 3.2.  Maximum accuracy limits of relative humidity & temperature for Sensiron SHT71 sensor [14]

Before starting the experiments, it has been decided to check whether humidity sensors are in good agreement with each other on temperature measurement. For this reason, a simple setup is developed. Series of humidity sensors and two thermocouples are isolated in a plastic bag with trapped air. They all submerged into hot water and water is forbidden to contact with the sensors in the plastic bag. Temperature of the air inside the plastic bag is measured by using both humidity sensors and thermocouples.

By experience, it is clear that the thermocouples give more accurate results than humidity sensors for temperature measurement. Thus, the consistency of the humidity sensors is checked by comparing measured temperature from both thermocouples and humidity sensors. The graphical representation of temperature measurement is shown in Figure 3.3. Humidity sensors that are employed for the experimental study on tumble dryer are selected in that manner.
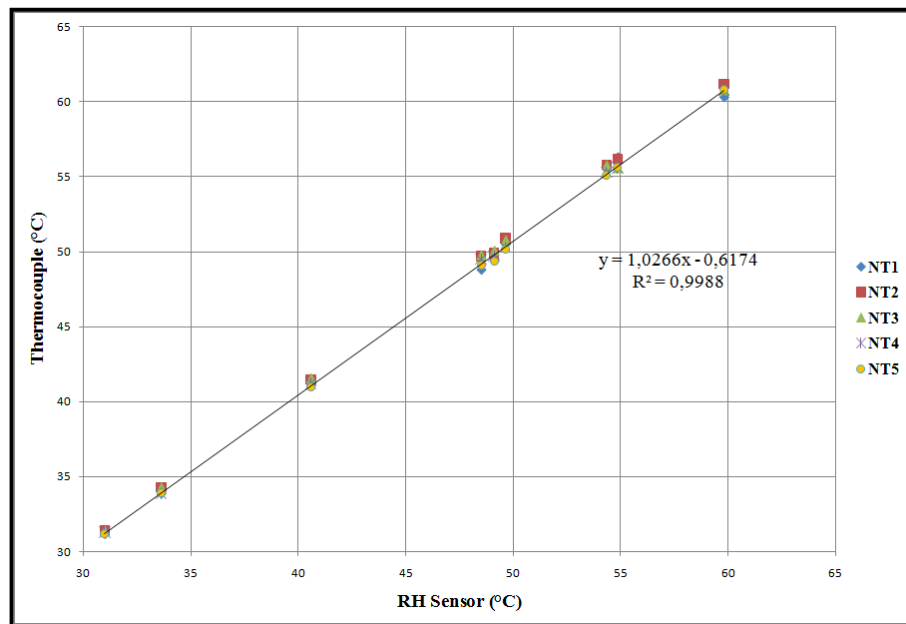
Figure 3.3. Relative humidity sensor calibration

The UDAQ measurement system for humidity sensor data transfer unit is shown in Figure 3.4. This system is developed in Arçelik A.Ş. with electrical circuitry and computer software. Humidity sensors are connected to the proper slots in order to be consistent with the naming in software. The system is connected to the computer and communicated via software. Since the system involves electrical circuitry, safety precautions should be taken. Thus, the system should be placed in a closed box during the measurement.
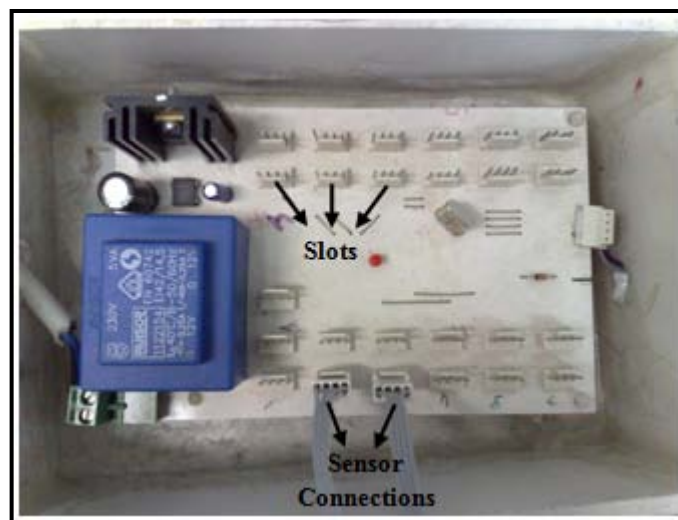


Figure 3.4. UDAQ system: hardware system for relative humidity sensor connection

### 3.1.2. Tumble Dryer

During this experimental study, both air-vented and air-condenser tumble dryers are used, which are given in Figure 3.5 schematically.
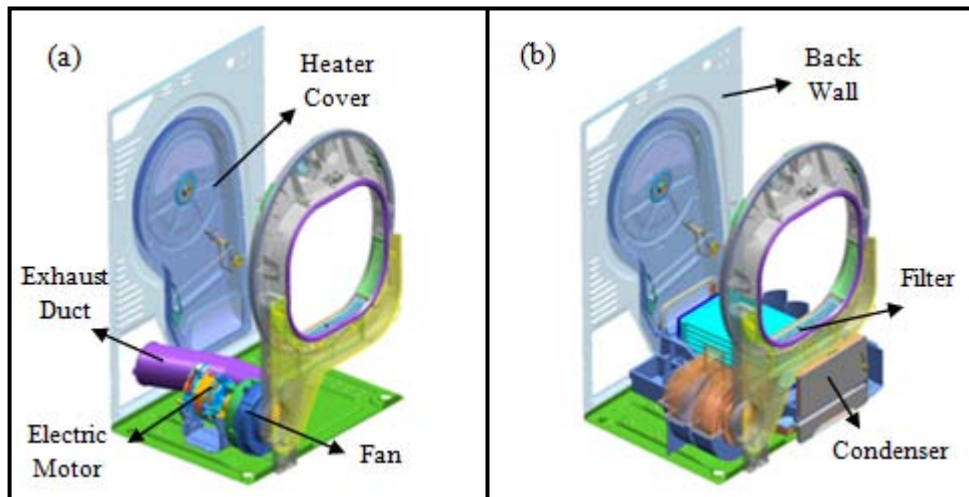


Figure 3.5. Schematics of the tumble dryers: a. air-vented dryer, b. air-condenser dryer

Since it is easier to investigate the mass transfer process without the complicate process of condensation, initial experimental study is carried out with air-vented tumble dryer. Then series of experiments are also conducted for air-condenser tumble dryer, which are used in comparing the results of the simulation model and the experimental data.

### 3.1.3. Data logger and Power Supply

All the sensors used in the present experimental setup need to be powered by electricity. Simply, power supply in Figure 3.6 (a) provides the electricity for the sensors. The desired electrical voltage or current for the sensors can also be altered by power supply. In addition, data logger in Figure 3.6 (b) contains channels on the socket, which are used for recording the output voltage or electrical current of the sensors. Later on, the output voltage or electrical current of the sensors are converted to desired data.
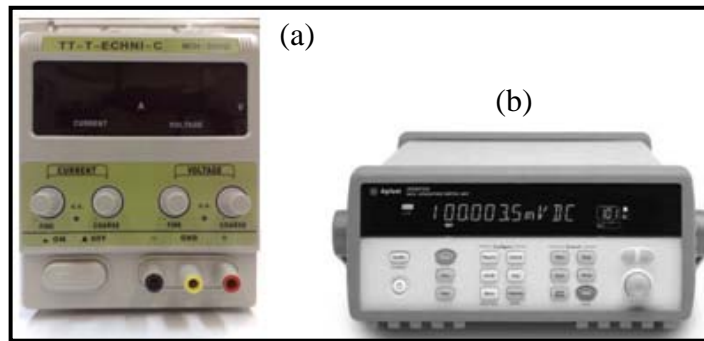
Figure 3.6. Power supply & data logger: a. power supply, b. data logger

The main aim of the data logger used in the present experiments is to record the output electrical current of the pressure transducer that is going to be explained in the next section.

### 3.1.4. Pressure Transducer and Annubar

Flow rate is also one of the most important parameter in the modeling of the drum. Hence, it is required to measure the flow rate of the drying process through the whole drying cycle. Pitot-tube is a useful system to measure the flow rate, but the probe of the pitot-tube is too narrow, which can be choked during drying due to the hot humid air at the exhaust duct. In addition, the requirement for the scanning of the flow area by hands contributes additional human error to the calculations in the pitot-tube system.

Annubar is an alternative system for pitot-tube, which is also used for measuring the flow rate. Annubar is a stationary measurement system where it is not required to scan the flow area by hands. Moreover, annubar system provides us to observe the change in flow rate during the entire drying process. Thus, the annubar system shown in Figure 3.7 is used in the present flow rate measurement. As it is shown in Figure 3.7, the annubar system is connected to the pressure transducer by two blue colored pipes. High-pressure and low-pressure connections should be fastened properly. In addition, the probes of the annubar system shown in Figure 3.7 (c) are wider than of the pitot-tube and thus they are much more resistive to the mentioned choking problem for the pitot-tube.
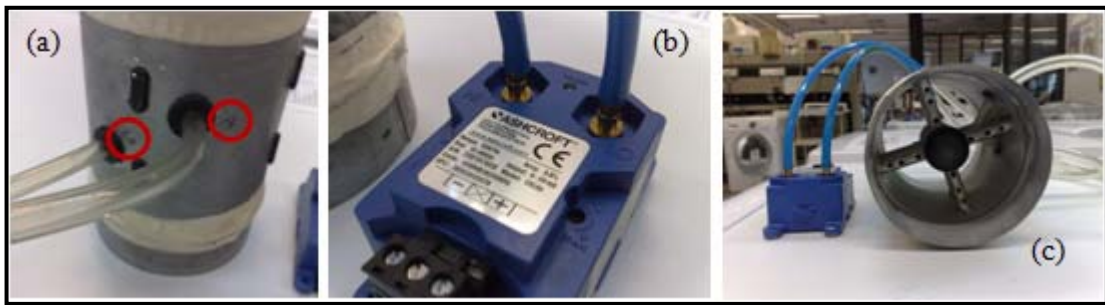
Figure 3.7. Flow rate measurement system using annubar: a. annubar, b. ASHCROFT pressure transducer (500 Pa), c. system connection

The ASHCROFT pressure transducer shown in Figure 3.7 (b) is limited up to 500 Pa in pressure. The output current range of pressure transducer varies between 4 mA and 20 mA. The output current range of the transducer is associated with the measured pressure. Thus, it is assumed that the transducer measures 500 Pa at 20 mA and 0 Pa at 4 mA. The function of the transducer is obtained by using the linearity, which is shown in Figure 3.8.

The coefficients of the line in the figure are entered to the software of the Agilent data logger program in order to convert the measured output current (A) into the pressure difference through the annubar. In addition, the pressure difference along the annubar is converted to flow rate (L/s) by using the calibration table, which was performed earlier at wind tunnel for the annubar system.
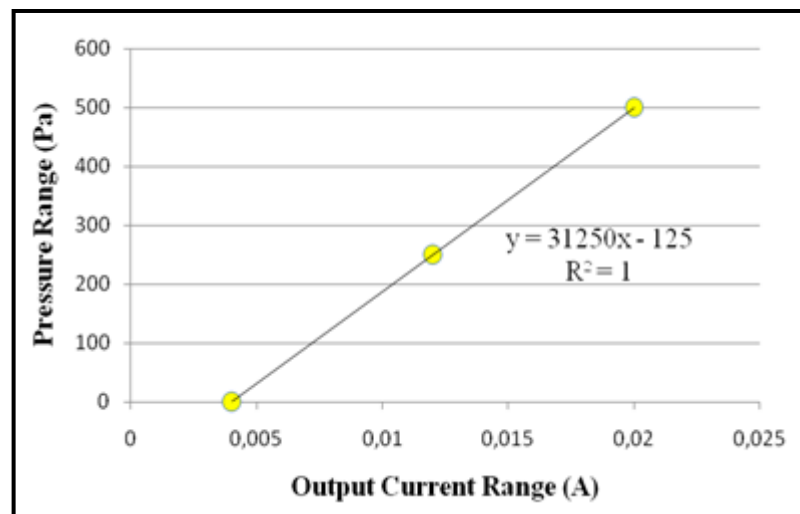


Figure 3.8. Pressure transducer function

The schematic illustration of the annubar system is given in Figure 3.9. It is shown that the annubar system is installed to the exhaust duct horizontally where air flows internally. The direction of the air flow through the exhaust duct is shown by red arrows.
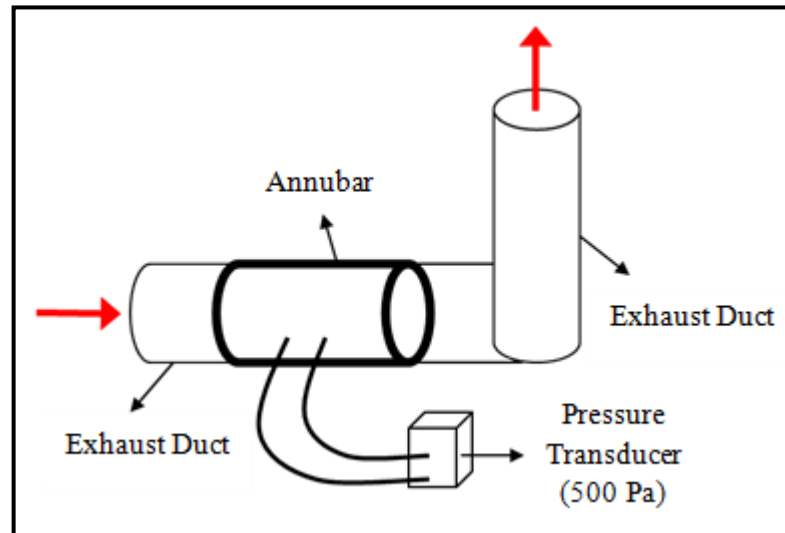


Figure 3.9. Schematic illustration of the annubar connection through the duct

In summary, data logger records the output current of the pressure transducer as air passes through the annubar that is installed horizontally at the exhaust duct of an air-vented tumble dryer. The output current of the pressure transducer is converted into flow rate by using the mentioned relationship between the parameters. Thus, the flow rate of the air-vented tumble dryer is determined.

**3.1.5.   Additional Electric Motor and Frequency Converter Unit**

Flow rate is one of the significant parameters, which affects the mass transfer process in tumble dryers. An additional electric motor is installed to the air-vented tumble dryer in order to investigate the effect of flow rate in more detail.

Additional electric motor with the frequency converter unit as shown in Figure 3.10 is connected to the fan. The frequency of the fan and thus the flow rate is controlled by a frequency converter.
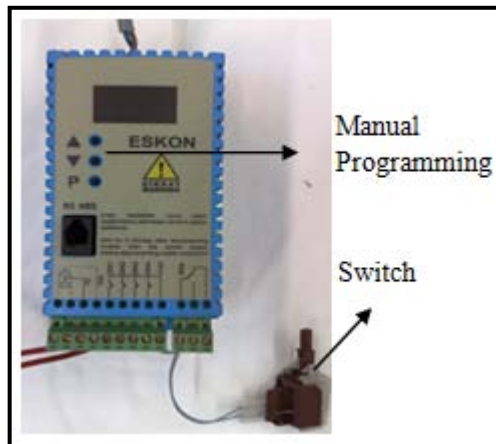
Figure 3.10. Frequency converter unit

An additional electric motor is installed under the drum to drive the fan while the existing motor is used just to rotate the drum at the constant frequency of 50 Hz. The speed of the additional motor can be changed using the frequency converter, and thus the fan speed can be adjusted to render a desired flow rate. Locations of the existing and additional motor are shown in Figure 3.11.
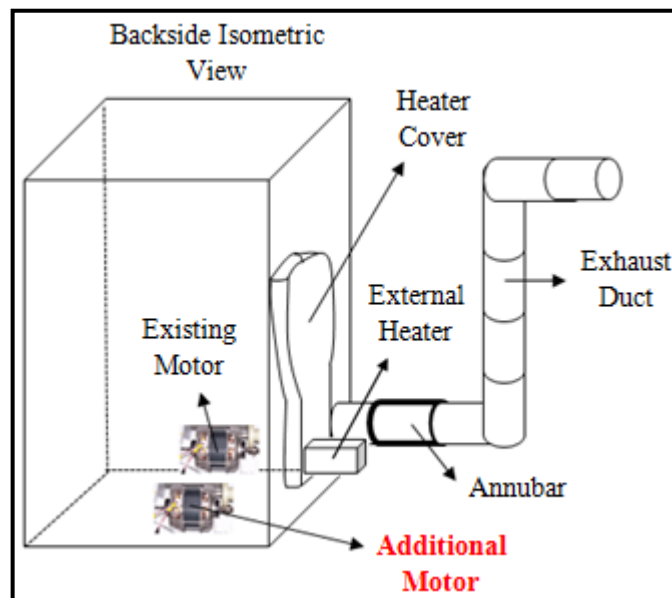


Figure 3.11. Schematic illustration of the motor placement

### 3.1.6.  Data Collecting System (VTS)

The data collecting system (VTS) shown in Figure 3.12 provides the information of the voltage and current applied to the tumble dryer and thus the total electric power used in the test. It is controlled by the software, which allows a user to select the stations and observe the measurement. Thermocouples can also be connected to this system for the temperature measurement. Energy consumption and temperatures at different locations can therefore, be monitored graphically by the VTS system during the entire drying process.



Figure 3.12. Data collecting system (VTS)

### 3.1.7.  External Heater

Under the drum of a tumble dryer, there is a dead space. The air in the dead space is warm due to heat transfer from the drum. This air tends to be inhaled into the inlet area of the heater. The average inlet air temperature can be up to 30 °C, and it is not easy to control. Therefore, a modification is made to isolate the dead space from the heater inlet. As a result, the fresh room air (nearly at 23 °C) enters the system, and the modification necessitates an additional heater. Some early study was conducted without the modification while the modification was made later to investigate the inlet temperature effect.

An additional helical heater unit is installed for the purpose of increasing the drum exit temperature. It is located upstream of the existing heater at the backside of the tumble dryer. As shown in Figure 3.13, the helical heater is wrapped to the mineral wool, placed in a shelf and then installed on the heater cover at the backside of the tumble dryer.
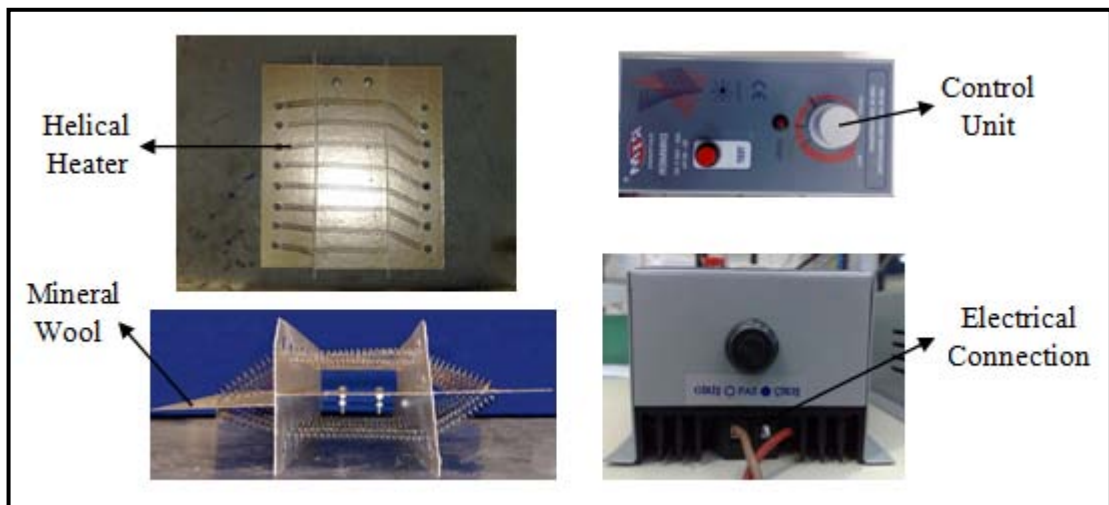
Figure 3.13. External heater and control unit

The external heater has a 1000 W maximum heater power limit. It is controlled externally by a rheostat mechanism in order to alter the heater power. Therefore, the effect of different inlet temperature on mass transfer during the drying process is desired to be investigated by the external heater power control. The location of the external heater unit at the backside of the tumble dryer is shown schematically in Figure 3.11 and Figure 3.14. In summary, the external heater unit located at the upstream of the existing heater on heater cover preheats the air temperature before passing through the existing heater.
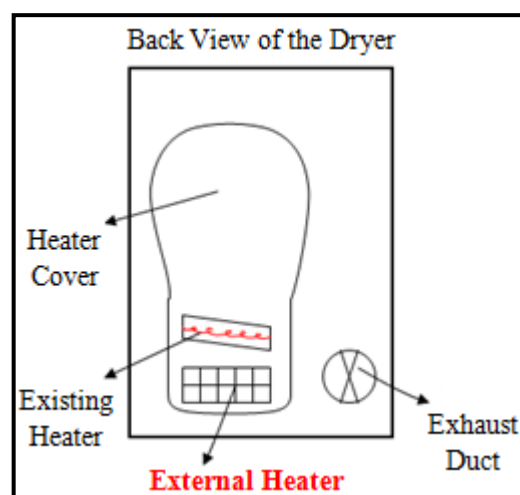


Figure 3.14. Schematic illustration of the external heater

### 3.1.8. Placements of Sensors

In this experimental study, both relative humidity and temperature are measured by humidity sensors. Humidity sensors are installed at the inlet and outlet of the drum.

After passing through the heater, air temperature just before entering the drum is not uniform. Therefore, it is very difficult to measure the average temperature of air at the drum inlet. It was attempted to measure temperatures at various locations at the drum inlet and the meaningful average temperature at the drum inlet could not be measured. Therefore, a humidity sensor is placed at the upstream of the heater. In addition, the drum inlet temperature is calculated by adding enthalpy through the heater. Thus in the present report, the drum inlet temperature is designated as the heater-enthalpy-compensated temperature measured upstream of the heater.

The location of the humidity sensors at the drum inlet is shown on the left-hand side of the Figure 3.15. Due to the radiation heat transfer, temperature of air increases significantly if the sensor is too close to the heater. In order to eliminate the effects of radiation heat transfer, humidity sensors are mounted just under the spur on the heater cover, specified by red circles on Figure 3.15.



Figure 3.15. Relative humidity sensor location at the drum inlet

Relative humidity sensor at the drum outlet is installed in a free space, where filter is placed. The humidity sensor is fixed under the filter by squeezing with the filter frame as shown in Figure 3.16.
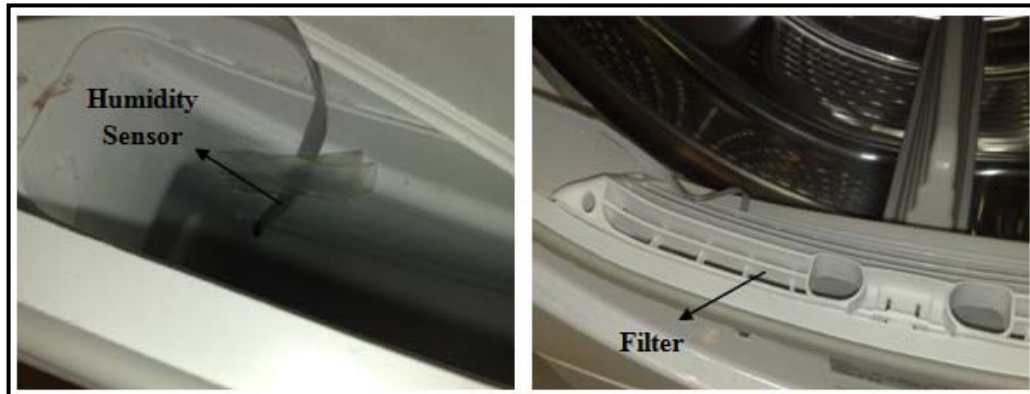


Figure 3.16. Relative humidity sensor location at the drum outlet

The proper inlet and outlet sensor locations are shown schematically in Figure 3.17, which are indicated by yellow dots. Blue and red arrows in the figure also represent the direction of preheated and post-heated air flows in an air-vented tumble dryer.
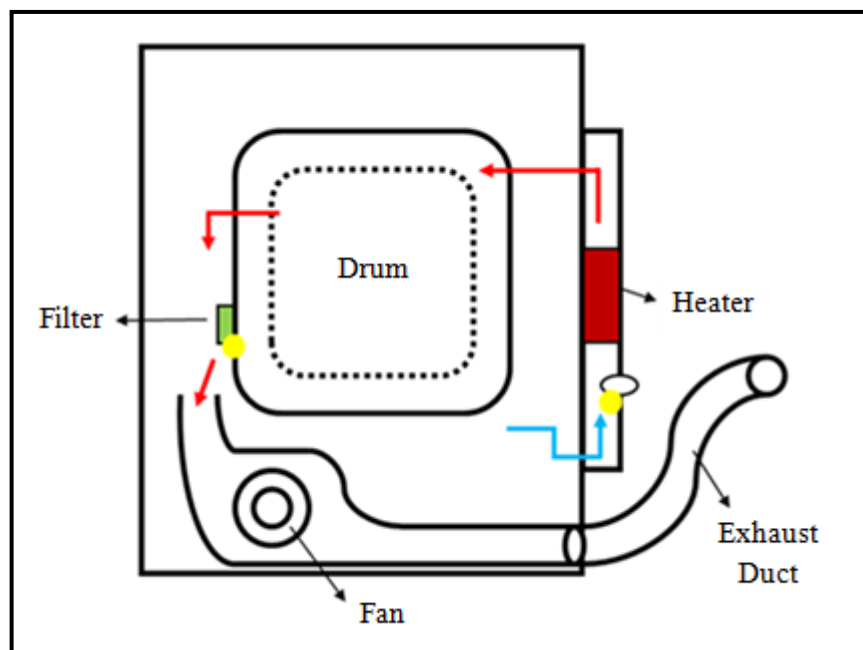


Figure 3.17. Schematics of the sensor locations: indicated by yellow dots

In summary, warm trapped air under the drum enters the heater by the fan. At the same time, fresh air also enters the heater through the grids on the backside of the dryer. The temperature of the fresh air increases before entering the drum while passing through the heater. Hot dry air encounters the wet clothes at the drum and mass transfer process takes place. Drying process continues at a nearly constant drum exit temperature while water exists sufficiently at the surface of the clothes. Temperature rapidly increases at drum exit when the clothes are almost dried.

## 3.2. DATA CALCULATION PROCEDURE

According to the main aim of the project, relative humidity and temperature at the drum inlet and outlet are measured. For the beginning, this approach is sufficient to investigate the mass transfer process in the drum for an air-vented tumble dryer. Parameters such as flow rate, fan speed are going to be investigated later on.

Flowchart of the data calculation procedure is given in Figure 3.18. Variables inside the green box are the measured variables, which are temperature and relative humidity at the inlet and the exit of the drum.
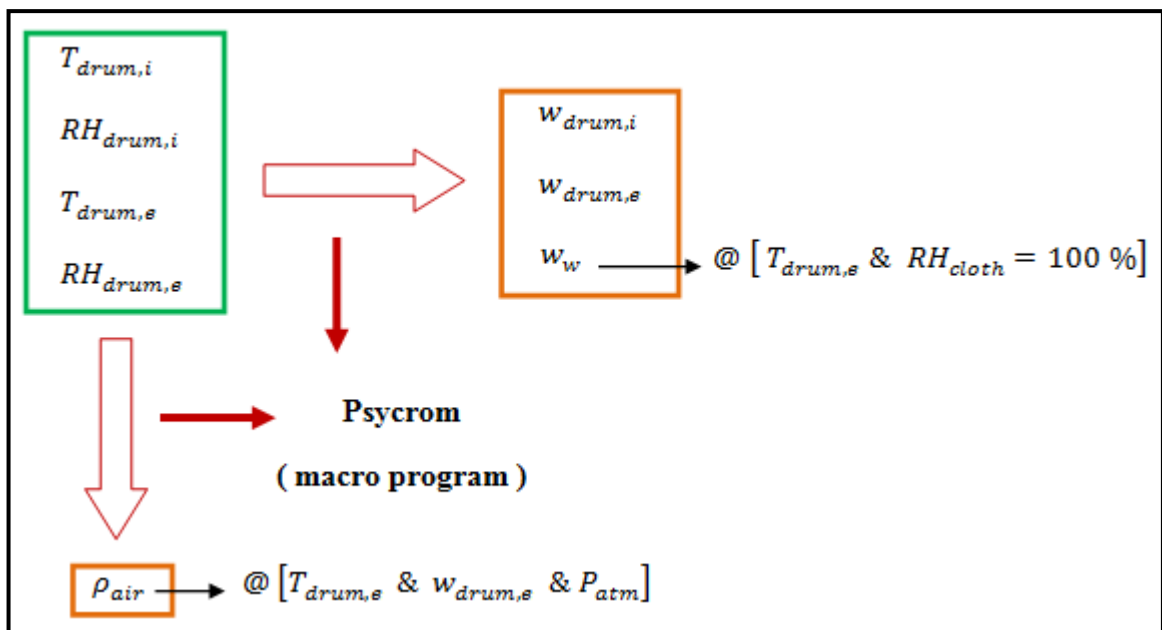


Figure 3.18. Flowchart of the experimental data calculation

The variables inside the orange box are the main calculated variables, which are density of air and the specific humidity values at the drum inlet, exit and the surface of the clothes. The other variables involved in the experimental data calculation depend on these main variables and they are going to be explained in detail.

Psycrom program mentioned in Figure 3.18 is an Excel Visual Basic (VBA) macro program written in Arçelik A.Ş. that performs the calculation steps as on psychrometric chart in thermodynamics. The relative humidity at the surface of the clothes is estimated as 100 per cent. This estimation is reasonable until the transient shutdown period of the drying process, because laundry inside the drum is almost wet.

Towards the end of the drying process, surface temperature of the clothes inside the drum increases and the relative humidity at the surface of the clothes starts to decrease where the assumption about the relative humidity at the surface of the clothes fails.

### 3.2.1. Specific Humidity Calculation

In the literature, specific humidity of water vapor is calculated by the Equation 3.1 below. This is the ratio of water vapor to the dry air.

$$w = \frac{m_v}{m_a} \tag{3.1}$$

Specific humidity can also expressed as:

$$w = \frac{m_v}{m_a} = \frac{P_v V/(R_v T)}{P_a V/(R_a T)} = \frac{P_v/R_v}{P_a/R_a} = 0.622 \frac{P_v}{P_a} \tag{3.2}$$

Total pressure is expressed as the sum of partial pressures of air and water vapor, shown in Equation 3.3.

$$P = P_a + P_v \tag{3.3}$$

By rearranging Equation 3.2, specific humidity can be modified in such a way:

$$w = \frac{0.622 P_v}{P - P_a}$$

(3.4)

The macro program calculates the specific humidity. Temperature, relative humidity and atmospheric pressure are entered as input parameters. Program turns back the specific humidity as output parameter. Since it is complicated to measure the temperature exactly at the surface of the clothes, temperature at the drum exit is used for calculating the specific humidity at the surface of the clothes.

### 3.2.2. Density Calculation

Density of the dry air is determined by the same way using the macro program. Similarly, temperature, specific humidity and atmospheric pressure are entered as input parameters. Program returns density of air as output parameter.

Density of the air is multiplied by the estimated volumetric flow rate of the tumble dryer in order to obtain the mass flow rate. In addition, before starting the experiment and at the end of the experiment, clothes are weighed. That process assists us to observe the amount of water that is dried or remained wet at the end of the experiment. For a perfectly insulated system that consists of 6 kg of laundry with 60 per cent initial humidity, 3600 grams of water is expected to be dried at the end of the experiment. When there is a difference about the total amount of water, the mass flow rate of the air is modified according to the ratio between total amount of water and the amount of water experienced at the end of the experiment that is given in Equation 3.5.

$$\frac{total\ amount\ of\ water}{the\ amount\ of\ water\ at\ the\ end\ of\ the\ experiment}$$

(3.5)

The mass flow rate of the air is modified by multiplying the density with the ratio given in Equation 3.5. The amount of water that is expected to be dried is calculated by the cumulative integration of the evaporation rate.

The explained calculation process of the amount of water to be dried is shown in Figure 3.19. Red line is for the 6 kg dry clothes with estimated volumetric flow rate. Blue line in the figure is for the modified volumetric flow rate. When we examine the figure, we can see that the total amount of water is slightly lower than 3600 grams and thus, the density of dry air is modified by the explained method.
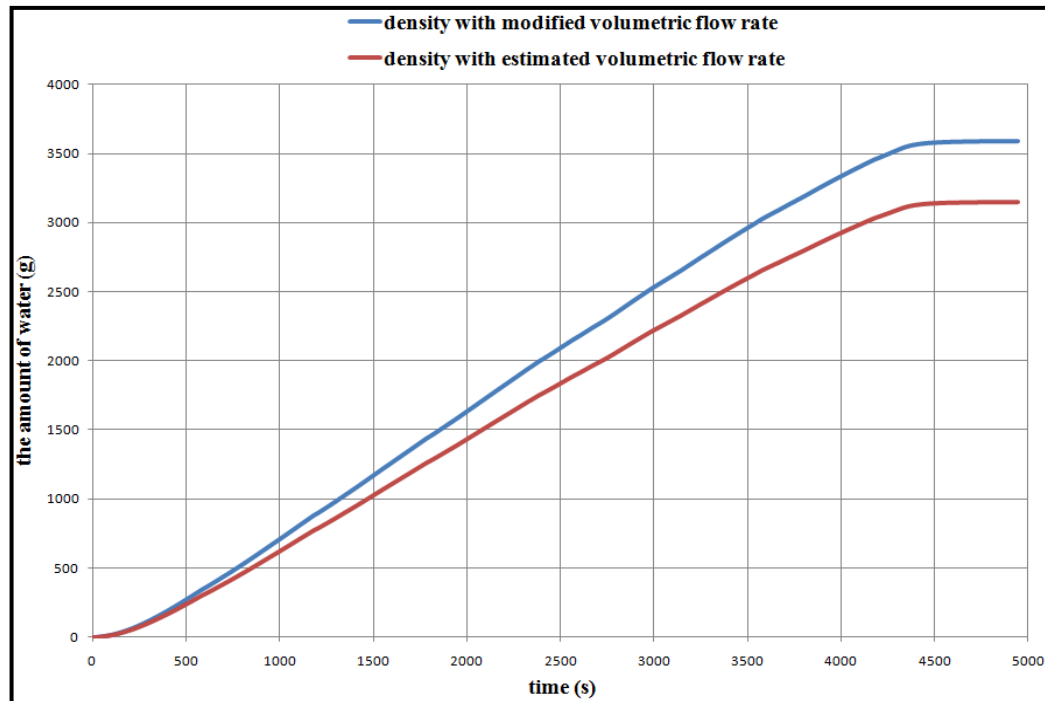


Figure 3.19. The amount of expected water to be dried: (for 6 kg of laundry with 60 per cent initial humidity)

In summary, the Psycrom macro program calculates density of the air. The mass flow rate of the tumble dryer is determined by the multiplication of the density of air and the estimated volumetric flow rate of the tumble dryer. When there is a difference about the amount of water experienced at the end of the experiment, density of the air is modified as mentioned.

### 3.2.3. Evaporation Rate Calculation

Evaporation rate is calculated by the difference between the specific humidity at drum inlet and exit. Formulation for the evaporation rate is given in Equation 3.6:

$$\dot{m}_v = \dot{m}_{air}\left(w_{drum,e} - w_{drum,i}\right) \tag{3.6}$$

The parameter $\dot{m}_{air}$ in the above equation represents the mass flow rate of the air. Evaporation rate is one of the most significant parameter in determining the total mass transfer coefficient of drying process.

### 3.2.4. Calculation for the Amount of Remaining Water

Total amount of water to be dried at the surface of the clothes can be calculated by the multiplication of the initial mass of the clothes with the initial moisture content. The amount of remaining water at the surface of the clothes is the difference between total amount of water and the existing amount of water at the surface of the clothes.

The amount of remaining water at the surface of the clothes can be determined by the formula given in Equation 3.7.

$$m_{w,remaining} = m_{w,total} - m_{w,existing} \tag{3.7}$$

### 3.2.5. Total Mass Transfer Coefficient Calculation

For the experimental study, total mass transfer coefficient represents the ratio of the amount of water across the drum to the amount of water at the surface of the clothes. Total mass transfer coefficient is calculated as follows:

$$(hA)_m = \frac{\dot{m}_v}{\rho_{air}\left(w_{cloth} - w_{drum,e}\right)} \tag{3.8}$$

$$(hA)_m = \frac{\dot{m}_{air}\left(w_{drum,e} - w_{drum,i}\right)}{\rho_{air}\left(w_{cloth} - w_{drum,e}\right)} \tag{3.9}$$

Total mass transfer coefficient is the multiplication of mass transfer coefficient and area. Thus, it is named as total mass transfer coefficient. It should be noted that the temperature at the surface of the clothes cannot measured directly and assumed equal to the temperature at the drum exit $(T_w = T_2)$ during the experimental study. Hence, the Equation 4.41 in the modeling yields to the Equation 3.8. Theoretical background and determination of the mass transfer coefficient will be covered in the simulation modeling section.

## 3.3. EXPERIMENTAL RESULTS

### 3.3.1. Initial Study

In the beginning of the experimental study, the mass transfer inside the drum of an air-vented tumble dryer is investigated with few experiments in order to understand the physics of the process. Therefore, series of experiments are conducted by changing the weight of the clothes and the initial moisture content. Parameters that are involved in the initial experimental study are given in Table 3.1.

Table 3.1. Initial study experiment matrix

| | The Amount of Load | | | | | |
|---|---|---|---|---|---|---|
| %RH | 3 kg | 4 kg | 5 kg | 6 kg | 7 kg | 8 kg |
| 40 | | * | | | | * |
| 50 | | * | | | | * |
| 60 | * | * | * | * | * | * |

During the initial experimental work, only the effects of moisture content and the weight of the clothes are investigated. Hence, heater algorithm and heater power are set constant in order to eliminate the effects originate from these parameters. Heater power level is set as 2500 W in order to dry 8 kg of load. Before fixing the algorithm of the heater and the heater power, couples of experiments are conducted. Dryness and the moisture content of the clothes are observed at the end of the experiments and proper parameters are rearranged.

If we examine Figure 3.20, we can realize from the light blue line that the maximum heater power level is about 2500 W. During the drying process, tumble rotates clockwise for a specific period then stops for 4-5 seconds and rotates counter-clockwise for 4-5 seconds. In addition, the heater is shutdown when tumble stops. Thus, the rapid falls at the heater power in Figure 3.20 are due to the explained working mechanism of the tumble dryer. Moreover, we can realize that the heater is shutdown and cooling phase of the drying process is achieved nearly after 85 minutes.
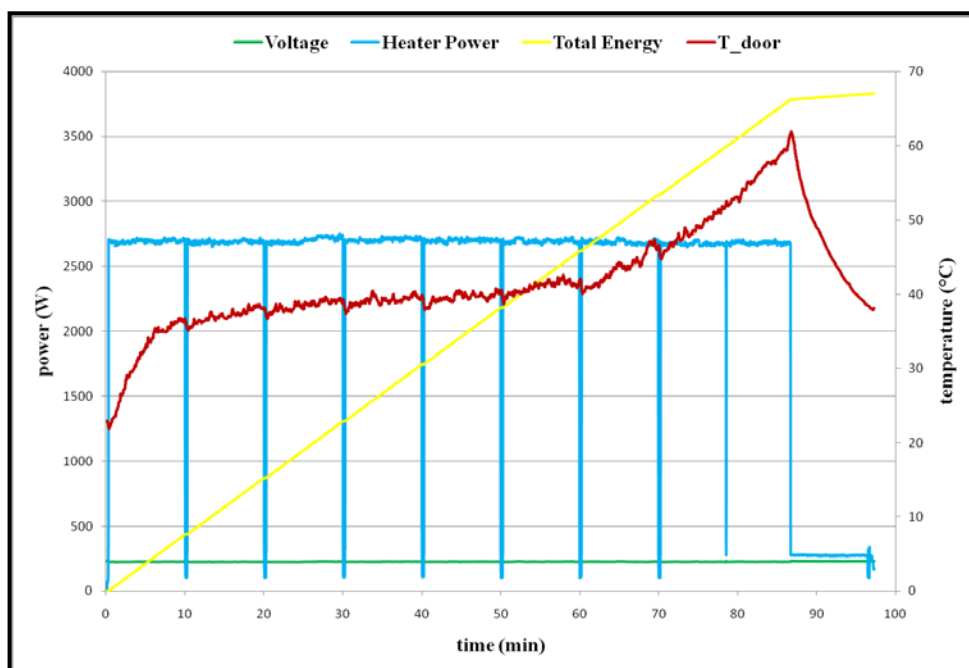


Figure 3.20. Heater algorithm of the tumble dryer for initial study: (with 2500 W heater)

Generally, heater of a tumble dryer consists of two sections with different power levels. For example, a 2500 W heater includes 1600 W and 900 W heaters. In order to supply the required heater power for drying, sometimes only the heater with higher power level is shut down and the heater with lower power level is remained working. In the arranged algorithm of the air-vented tumble dryer, both sections of the heater are operating together to provide 2500 W power level. After 85 minutes, cooling period of the algorithm is achieved where both sections of the heater are shut down and the fan operates to cool down the temperature at the surface of the clothes. In addition, rapid temperature increase in drum outlet is also a useful indicative of when the cooling period is achieved.

Temperature and relative humidity profiles at drum inlet and outlet are shown in Figure 3.21. It is found that the temperature at the exit of the drum increases up to a point and then reaches steady state. In addition, as clothes inside the drum start to dry, temperature at the surface of the clothes increases again, thus the temperature at the drum exit also increases nearly after 4500 seconds. Relative humidity at the drum exit starts to decrease significantly in the mean time. Thus, we can realize whether clothes are dried or not, just by monitoring the temperature increase at the drum exit after the steady state.
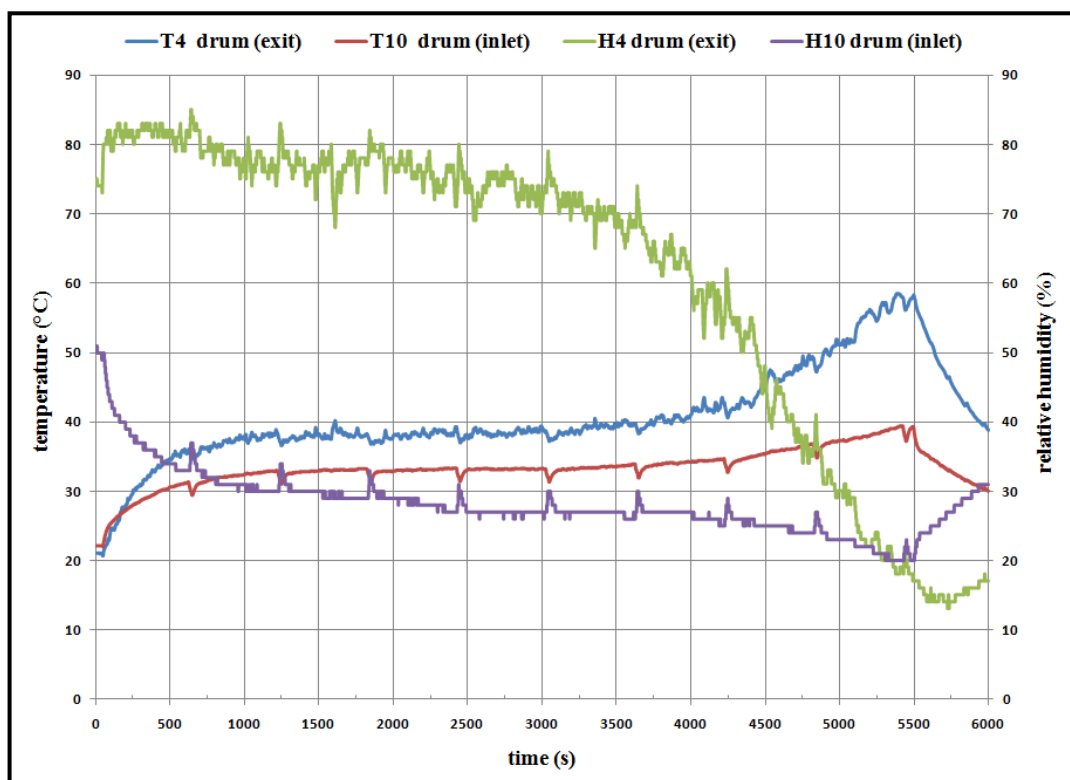


Figure 3.21. Temperature & relative humidity profiles for air-vented tumble dryer

In Figure 3.22, the specific humidity data at the drum inlet, at the drum exit and at the surface of the clothes are plotted with respect to time for 4 kg and 8 kg of load. It is found that the specific humidity at the drum inlet does not change, because the temperature at the inlet remains almost the same during the drying. However, specific humidity at drum exit changes with respect to the temperature at the drum exit. In addition, specific humidity at drum outlet for air-vented tumble dryer increases up to a certain point and then reaches steady state.
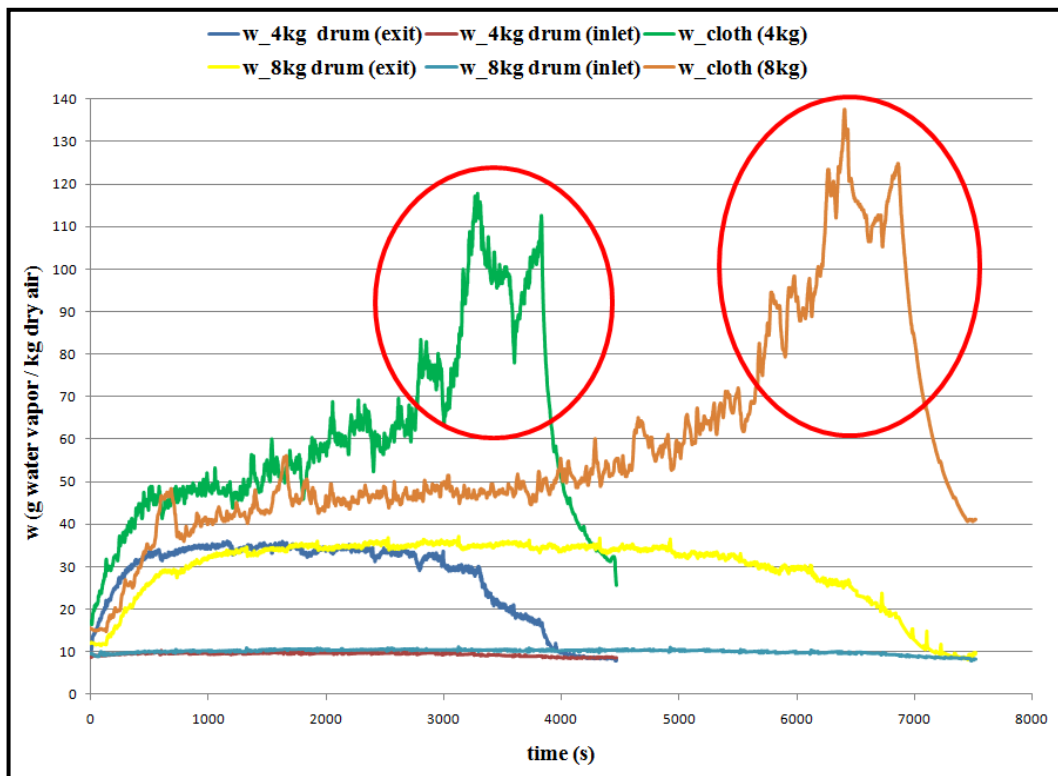
Figure 3.22. Specific humidity profile for air-vented tumble dryer: (for both 4 kg and 8 kg of load weight, at the drum inlet, at the drum exit and at the surface of the clothes)

Moreover, when we examine the specific humidity data at the surface of the clothes, we can easily see that the specific humidity increases up to steady state similarly at drum exit. However, as clothes start to dry an undesired overshoot is observed, which is shown with red circles in Figure 3.22. The overshoot at specific humidity data results from the previous assumption about relative humidity (RH=100 per cent) at the surface of the clothes. Relative humidity at the surface of the clothes decreases as clothes start to dry, but it is assumed as 100 per cent during the entire drying process. This problem will be handled in the following study.

The remaining water at the surface of the clothes is plotted in Figure 3.23 with respect to time for 3 kg of load to 8 kg of load. The amount of water at the surface of the clothes decreases in time as clothes dry.
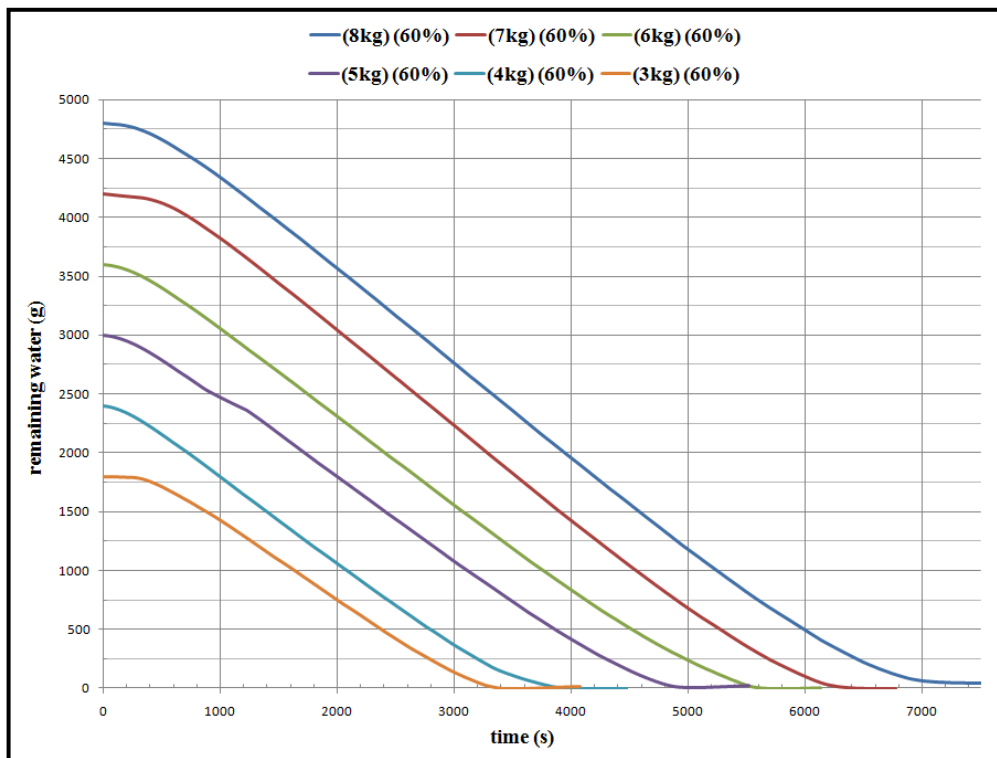
Figure 3.23. The profile of the remaining water at the surface of the clothes

The total mass transfer coefficient profile of the drying process is shown in Figure 3.24 for an air-vented tumble dryer. The profiles are determined for 3kg of load to 8 kg of load by setting the initial moisture content constant at 60 per cent. For an initial intuition, it can be stated that the total mass transfer coefficient data is accumulated at 6-7 and 8 kg of load. Similarly, the total mass transfer coefficient data is also accumulated at 3 and 4 kg of load. In addition, the data for 5 kg of load seems to be lie down in the middle of two accumulated data. Moreover, humidity sensors sometimes fail and read incorrect data when water drops contact with the surface of the measuring edge. Thus, the discrepancy at the beginning of the data for 3 kg of load is due to the direct contact of water drops with the humidity sensor.

The characteristic of the total mass transfer coefficient data is similar for all amounts of load in Figure 3.24. For a short period, nearly for 100 seconds the total mass transfer coefficient data stands at very low values. After that, makes a peak and then starts to fall down as clothes start to dry.
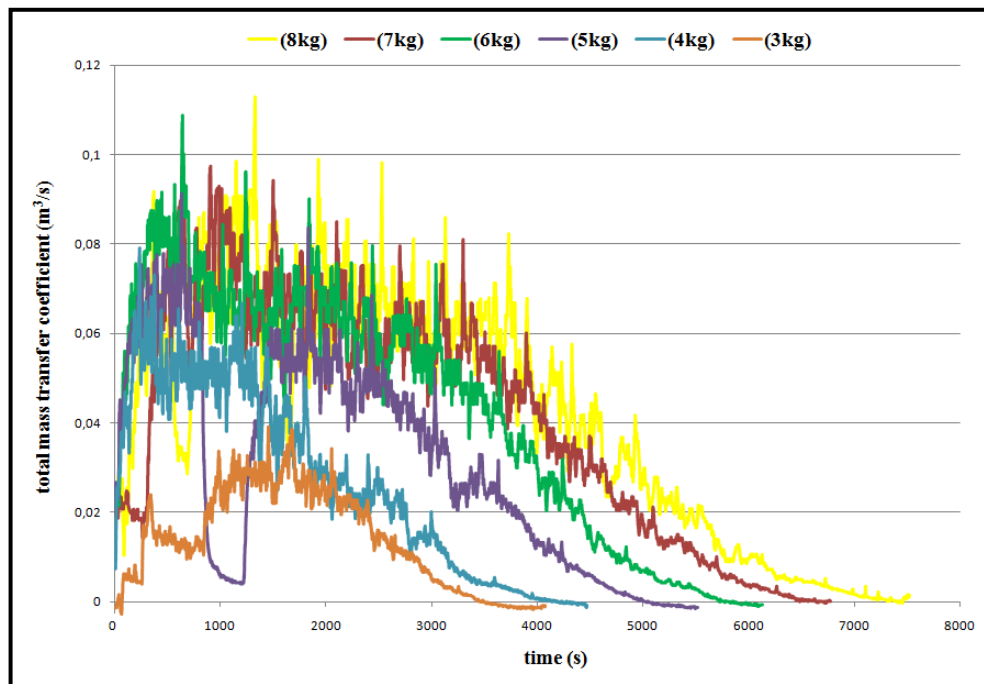
Figure 3.24. Total mass transfer coefficient profile for the air-vented tumble dryer: (for 3 kg to 8 kg of load weight at 60 per cent)

It has been anticipated that the total mass transfer coefficient at the surface of the clothes could be dependent on the amount of remaining water at the surface of the clothes. Hence, the total mass transfer coefficient data is plotted with respect to the amount of remaining water at the surface of the clothes in Figure 3.25 and Figure 3.26.

In Figure 3.25, initial moisture content of the clothes is fixed at 60 per cent and the weight of the load is changed. Similarly, the load weight is fixed at 4 kg and 8 kg in Figure 3.26. However, initial moisture content of the clothes is changed from 40 per cent to 60 per cent. It is found that the total mass transfer coefficient depends on the amount of remaining water at the surface of the clothes according to the following figures.

In summary, graphical results so far state that the characteristics of the total mass transfer coefficient do not change significantly under variable initial moisture content of the clothes or variable load weight. When we examine both graphs, we can realize that the total mass transfer coefficient traces the same path for different conditions. This inference is a massive event for initial experimental study. From now on, the other factors, which affect the total mass transfer coefficient, are going to be investigated.
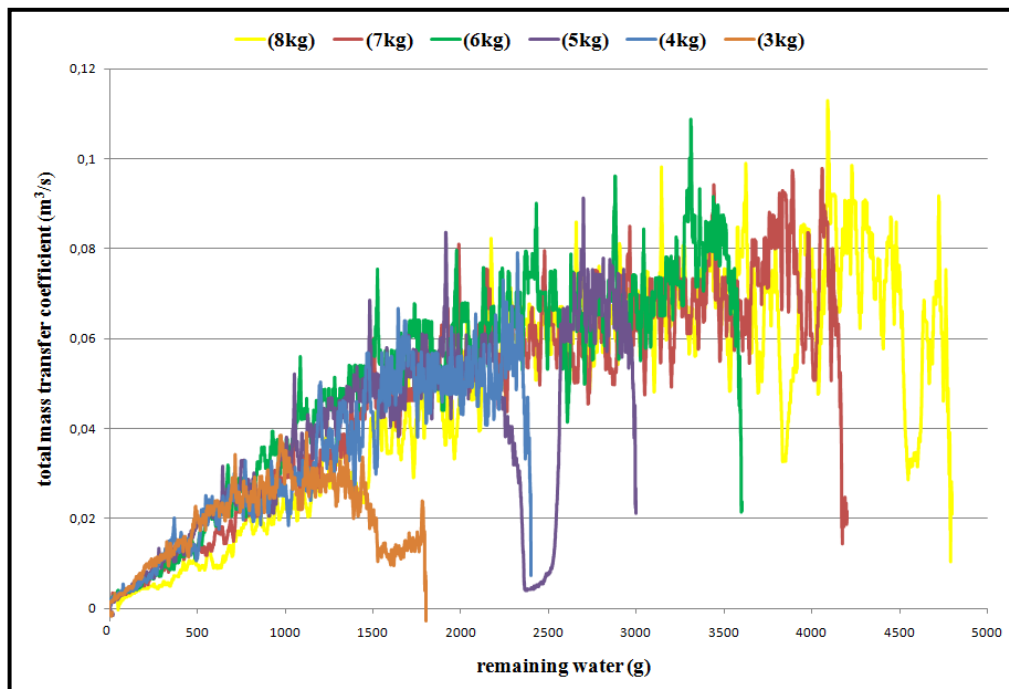
Figure 3.25. Total mass transfer coefficient with respect to the remaining water: (variable load weight and constant initial moisture content at 60 per cent)
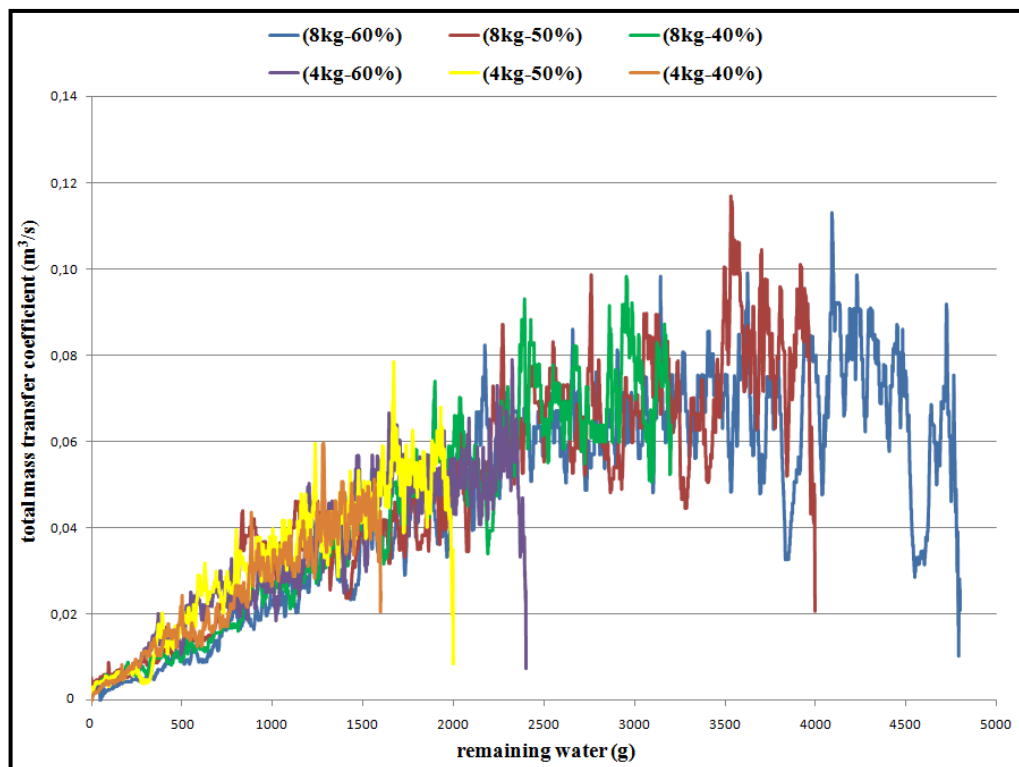


Figure 3.26. Total mass transfer coefficient with respect to the remaining water: (variable moisture content, constant load weight at 4 kg and 8 kg)

### 3.3.2. Variable Fan Speed

In order to investigate the effects of air flow rate, an extra motor is installed under the drum and driven externally by frequency converter as mentioned. Thus, the frequency of the fan in an air-vented tumble dryer is altered. In addition, the existing motor drives the tumble of the air-vented dryer at 50 Hz.

Distribution of the total mass transfer coefficient for variable fan frequency with respect to the remaining water is shown in Figure 3.27. In the following figure, all other parameters except the frequency of the fan are remained constant. In addition, frequency of the fan is altered from 40 Hz to 70 Hz. It is found that the change in the fan frequency, thus the flow rate has a minor effect on the total mass transfer coefficient.
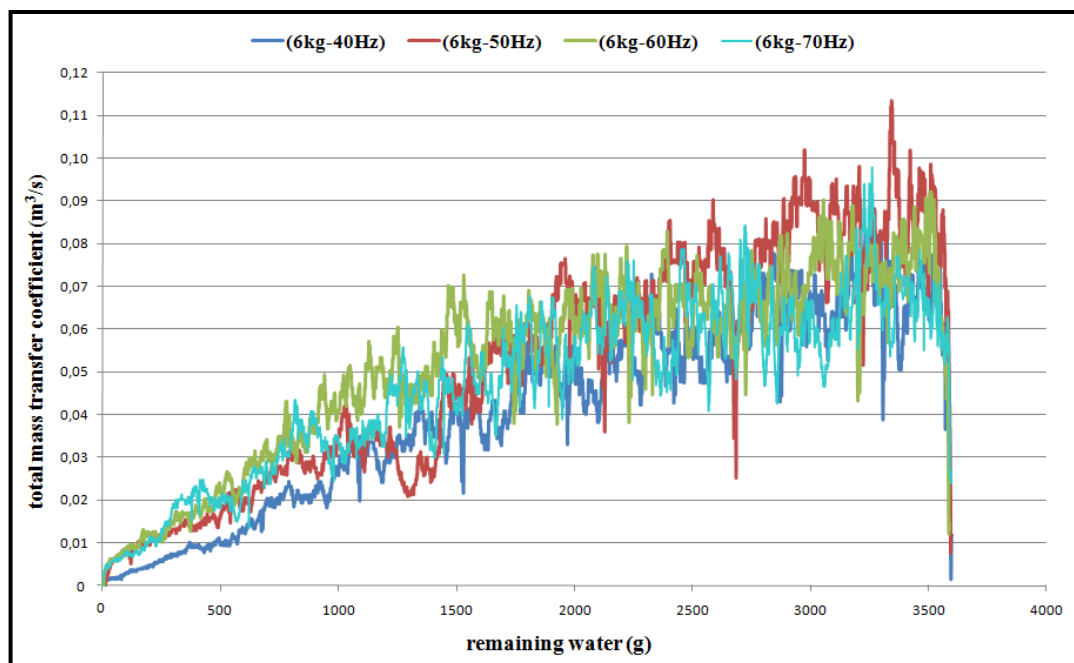


Figure 3.27. Total mass transfer coefficient with respect to remaining water: (variable fan frequency, constant load weight and initial moisture content at 6 kg and 60 per cent)

In Figure 3.28, the distribution of temperature at the drum exit is shown with respect to the variable frequency of the fan. As the frequency of the fan decreases, flow rate also decreases and thus, the temperature at the drum exit increases respectively. Temperature at the drum exit changes nearly about 5 °C at steady state in between 40 Hz and 70 Hz.
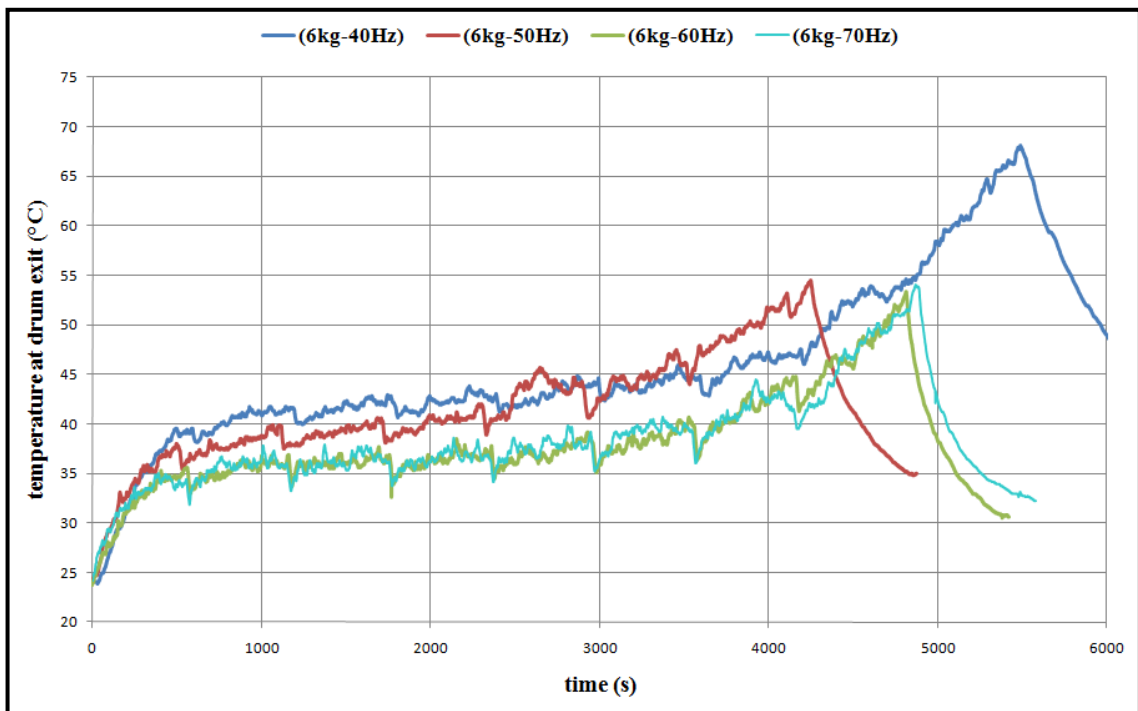
Figure 3.28. Effect of the fan speed on the temperature at the drum exit

### 3.3.3. Flow Rate Measurement

Flow rate is one of the significant parameter that is involved in determining the total mass transfer coefficient. Hence, flow rate of the air-vented tumble dryer is studied. For that reason, the mentioned annubar system is installed at the exhaust duct that enables us to measure the flow rate of the air-vented tumble dryer during the entire drying process.

Flow rate is measured for variable loads and variable fan frequencies. In addition initial moisture content of the clothes is fixed at 60 per cent. The experimental data for 3 kg and 6 kg of load at 40-50-60-70 Hz are shown in Figure 3.29. Graphical results show that the weight of the clothes does not affect the flow rate significantly. However, the effect of load weight on flow rate will be investigated in more detail. Moreover, the flow rate of the air-vented tumble dryer increases as expected when the frequency of the fan is decreased.
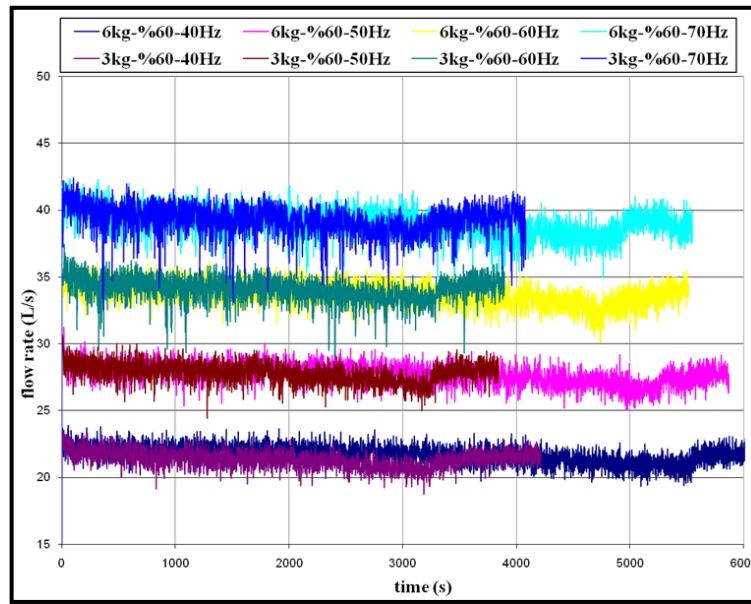
Figure 3.29. Flow rate measurement for 3-6 kg of load weight: (frequency from 40 Hz up to 70 Hz, constant initial moisture content at 60 per cent)

It has been figured out that the exhaust duct has a significant role on flow rate. Thus, the flow rate is measured without load from 30 Hz to 70 Hz by increasing the frequency of the fan by 5 Hz in each step and the average flow rate is calculated. The graphical result of the measurement process is shown in Figure 3.30. It is found that there is a significant difference between when the exhaust duct is connected or not.
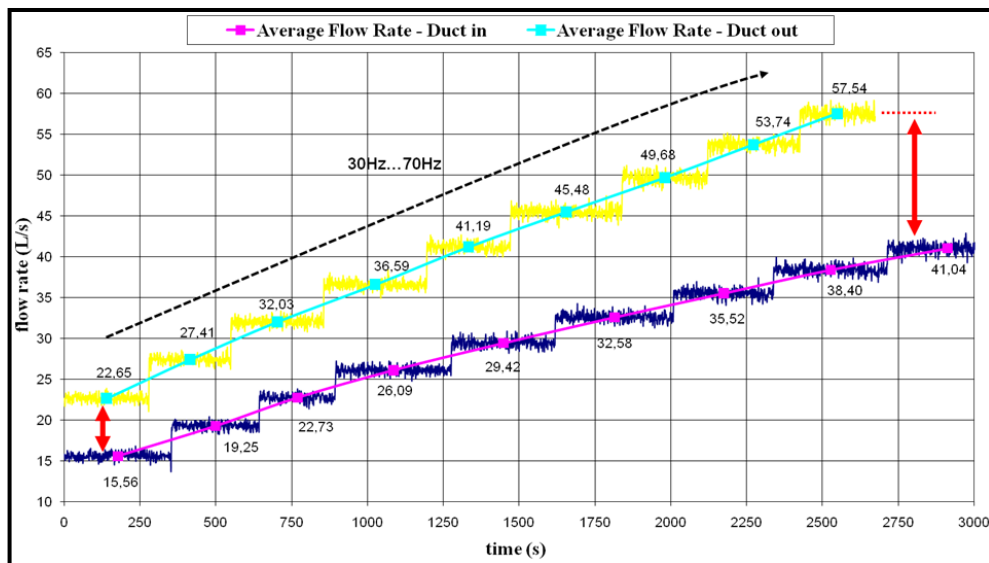


Figure 3.30. Effect of the exhaust duct connection on flow rate measurement

The average numerical values of the explained measurement are given in Table 3.2. The difference in the average values of flow rate increases as the frequency of the fan increases due to the increase in mass flow rate. In addition, the maximum difference in the average values of the flow rate is achieved at 70 Hz where the difference nearly reaches up to 16.5 L/s. As a result, it can be stated that there is a significant amount of pressure loss at the exhaust duct for an air-vented tumble dryer.

Table 3.2. The average values of the flow rate measurement when the exhaust duct is connected or not

| | | Duct in | Duct out | Difference |
|---|---|---|---|---|
| **Fan (Hz)** | 30 | 15.56 | 22.65 | 7.09 |
| | 35 | 19.25 | 27.41 | 8.16 |
| | 40 | 22.73 | 32.03 | 9.30 |
| | 45 | 26.09 | 36.59 | 10.50 |
| | 50 | 29.42 | 41.19 | 11.78 |
| | 55 | 32.58 | 45.48 | 12.90 |
| | 60 | 38.40 | 49.68 | 14.17 |
| | 65 | 35.52 | 53.74 | 15.34 |
| | 70 | 41.04 | 57.54 | 16.50 |

The effect of load weight on the flow rate is investigated in more detail. Thus, the flow rate is measured at 40-50-60-70 Hz for 3 kg, 6 kg and 8 kg of loads in order to emphasize the effect of the weight of the clothes. Temperature at the drum exit can achieve very high values at frequencies lower than 40 Hz, which can either damage the clothes inside the drum or dangerous for the heater of the tumble dryer. Thus, the experiments at frequencies lower than 40 Hz are conducted only for 0 kg of load weight.

The average values of the flow rate at mentioned load weights and the difference between the unloaded conditions are given in Table 3.3. It is found that for both 3 kg, 6 kg and 8 kg of load, the difference in the average values of the flow rate generally increases as the frequency of the fan increases. In addition, the effect of the load weight can be realized by examining the difference values of different load conditions at the same frequency.

Table 3.3. The effect of the weight of the clothes on flow rate measurement

| | | Flow Rate at Various Load Weights (L/s) | | | | | | | | | |
|---|---|---|---|---|---|---|---|---|---|---|---|
| | | **0 kg** | **3 kg** | **Diff.** | **4 kg** | **5 kg** | **6 kg** | **Diff.** | **7 kg** | **8 kg** | **Diff.** |
| **Fan (Hz)** | 30 | 15.56 | | | | | | | | | |
| | 35 | 19.25 | | | | | | | | | |
| | 40 | 22.73 | 21.36 | 1.37 | | | 21.73 | 1.00 | | 20.54 | 2.19 |
| | 45 | 26.09 | | | | | | | | | |
| | 50 | 29.42 | 27.83 | 1.59 | 27.91 | 27.84 | 27.74 | 1.67 | 27.27 | 26.79 | 2.62 |
| | 55 | 32.58 | | | | | | | | | |
| | 60 | 35.52 | 33.88 | 1.64 | | | 33.77 | 1.74 | | 32.83 | 2.69 |
| | 65 | 38.40 | | | | | | | | | |
| | 70 | 41.04 | 39.24 | 1.80 | | | 39.06 | 1.98 | | 38.24 | 2.80 |

The average values of the flow rate data is plotted with respect to the load weight in Figure 3.31. It is found that up to 6 kg, there is not significant change in the flow rate but there is nearly about 1 L/s decrease in flow rate around 8 kg. In addition, the volume of the clothes increases as clothes start to dry and the active flow area inside the drum decreases respectively. Thus, the decrease in flow rate after 6 kg may be due to the change in the volume of the clothes in the drum.
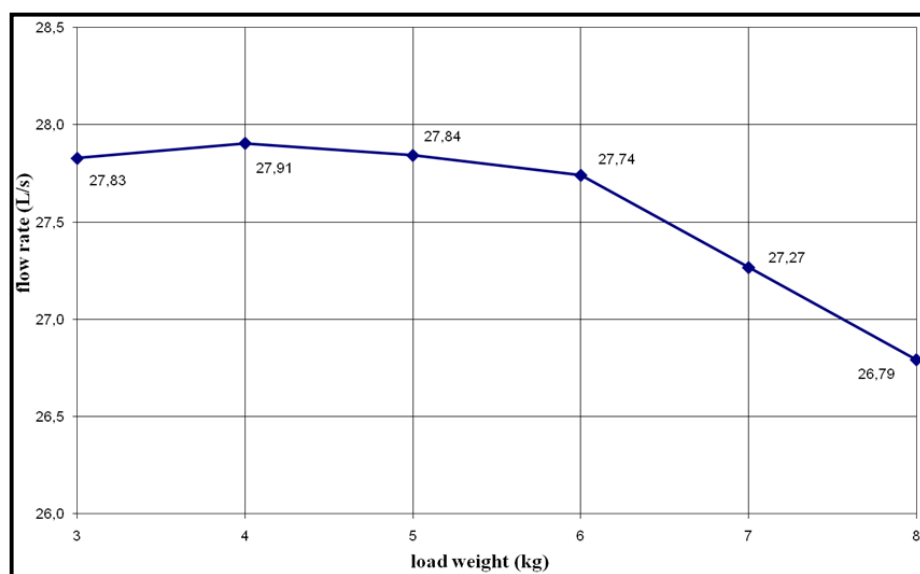


Figure 3.31. Graphical representation of the effect of load weight on the flow rate at 50 Hz

Distribution of the flow rate at different sections of the drying process is also investigated as a part of the experimental study. Four sections; after 300 seconds of drying, at steady state, before cooling and at the cooling period are investigated in Figure 3.32 and Figure 3.33.
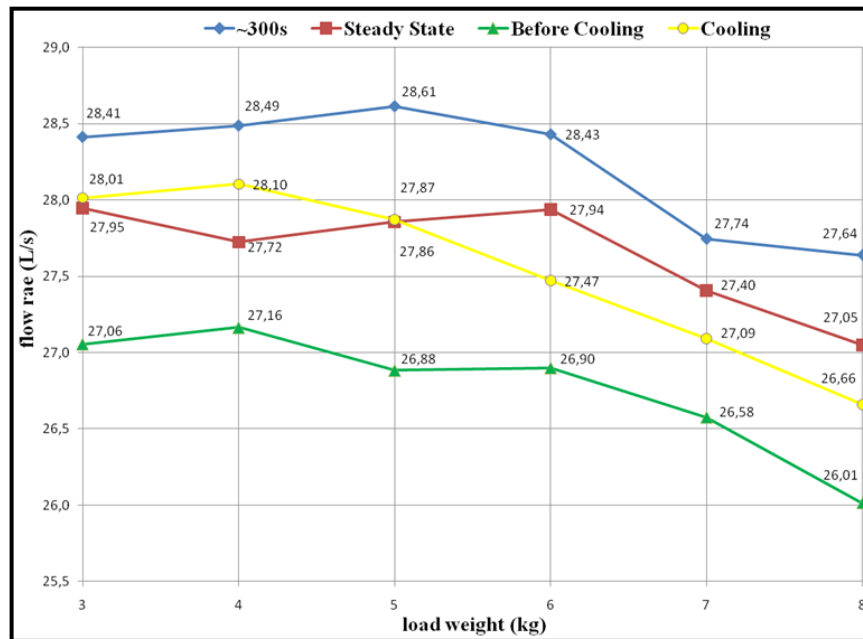


Figure 3.32. Distribution of flow rate on different sections of the drying process with respect to the load weight: (~300 s, steady state, before cooling, cooling sections)
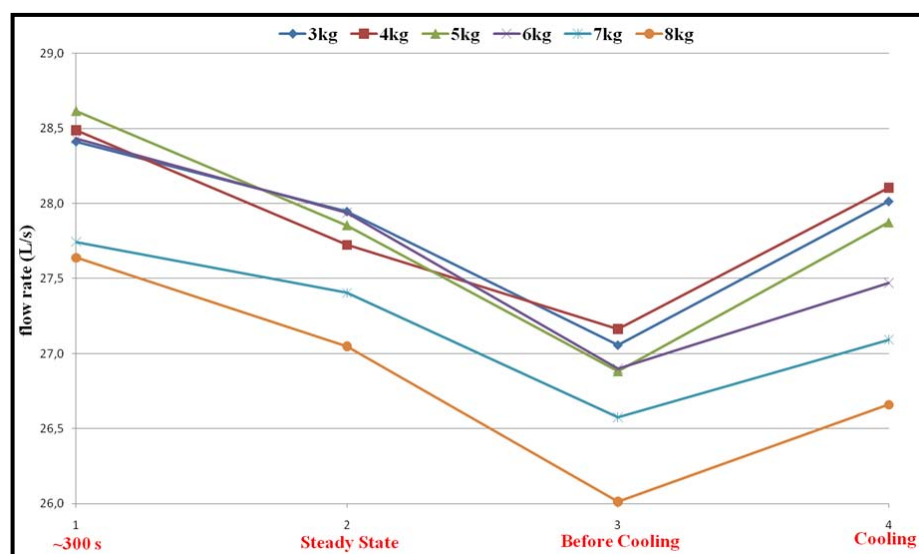


Figure 3.33. Distribution of flow rate on the load weight with respect to the different sections of the drying process: (3 kg to 8 kg of load weight)

In general, it can be stated that the flow rate decreases from 3 kg to 8 kg for all sections of drying process. However, flow rate started to increase at cooling section. This behavior is valid for all amounts of load weight. The decrease in the flow rate is reasonable due to the increase in the volume of the clothes as clothes dry.

In the beginning of the drying process, clothes are wet and stick to the corners of the drum. As clothes started to dry clothes became widen, the volume of the clothes increase, and they occupy much more space inside the drum. Hence, the flow rate of the tumble dryer is decreased. However, this effect is not eligible anymore at the cooling period. Fresh cool air may contribute an increment on the flow rate. The average values of the flow rate at different sections of drying for 50 Hz frequency are given in Table 3.4. There is not a significant amount of change in the average values of the flow rate, but the general effect of the flow rate on the drying process can be observed.

Table 3.4. The average values of flow rate for various sections of drying

| | | Flow Rate of Various Sections (L/s) at 50 Hz | | | |
|---|---|---|---|---|---|
| | | ~ 300 s | Steady State | Before Cooling | Cooling |
| **Load Weight (kg)** | 3 | 28.41 | 27.95 | 27.06 | 28.01 |
| | 4 | 28.49 | 27.72 | 27.16 | 28.10 |
| | 5 | 28.61 | 27.86 | 26.88 | 27.87 |
| | 6 | 28.43 | 27.94 | 26.90 | 27.47 |
| | 7 | 27.74 | 27.40 | 26.58 | 27.09 |
| | 8 | 27.64 | 27.05 | 26.01 | 26.66 |

### 3.3.4. Condenser Tumble Dryer

In order to investigate the mass transfer process in the drum for different types of tumble dryers, experiments are also conducted for air-condenser tumble dryer. In addition, the simulation program will be constructed for air-condenser tumble dryer, so that the experimental data will be used in the verification of the simulation model. Moreover, the situation in the air-condenser dryer is concerned, whether the total mass transfer coefficient depends on the amount of remaining water at the surface of the clothes or not.

Humidity sensors that are involved at the experiments of air-condenser tumble dryer are placed on the same locations as air-vented tumble dryer. Briefly, drum inlet sensor is placed on the heater cover at the upstream of the heater and the drum outlet sensor is fixed at the free space under the filter frame. Temperature and relative humidity profiles at the drum inlet and exit for air-condenser tumble dryer are shown in Figure 3.34.

The characteristics of the temperature and relative humidity at drum outlet are similar with air-vented tumble dryer results. However, relative humidity reaches higher values and remains nearly constant for a long period. Temperature at drum outlet is also significantly higher for air-condenser tumble dryer than of the air-vented tumble dryer.

In addition, relative humidity at the drum inlet condition for air-condenser dryer is completely different from the air-vented tumble dryer due to the condensation process along the condenser. Moreover, temperature at the drum inlet is significantly higher for air-condenser tumble dryer.
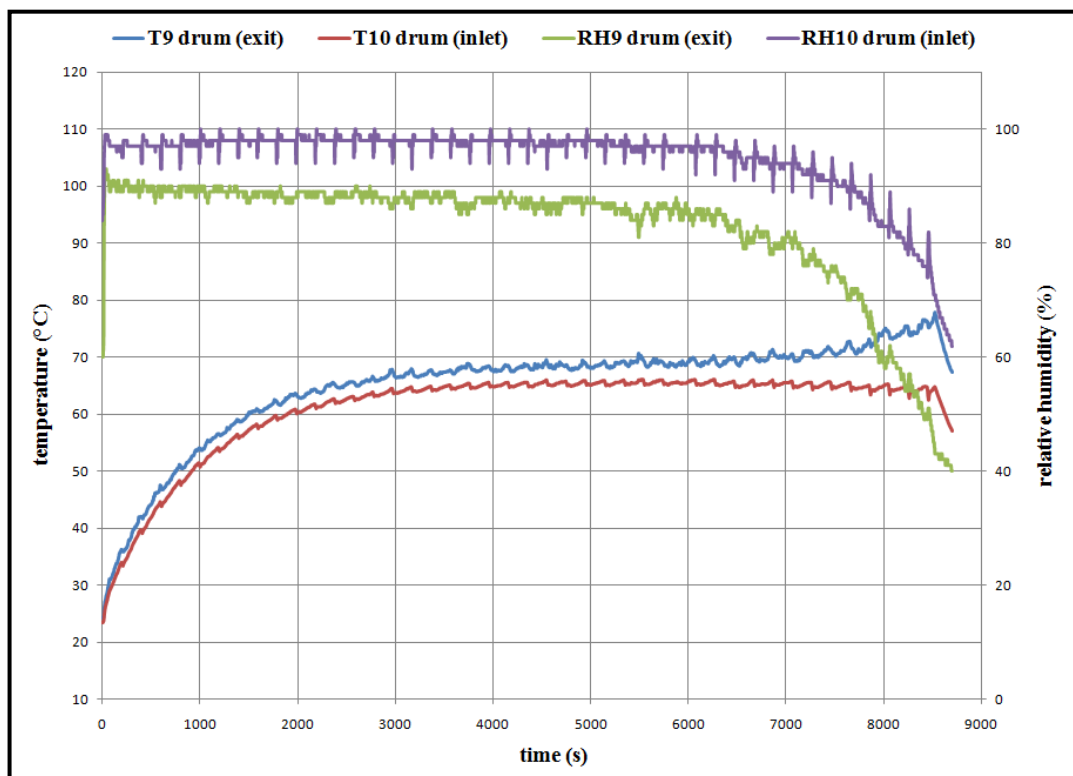


Figure 3.34. Temperature & relative humidity profiles of the air-condenser tumble dryer

The total mass transfer coefficient with respect to the amount of remaining water for air-condenser dryer at constant initial moisture content with variable load weight is plotted in Figure 3.35. Similarly, the total mass transfer coefficient for air-condenser dryer is also depends on the amount of remaining water at the surface of the clothes. The red boxes indicate the initial jump in the data at the beginning of the experiment. The initial jump may result from the high evaporation rate at the beginning of the experiments. Since the clothes are wet, evaporation occurs faster than any other section of the drying process. In addition, the difference between the total mass transfer coefficient of heating transient and steady state is quite higher for air-condenser tumble dryer than of air-vented tumble dryer.
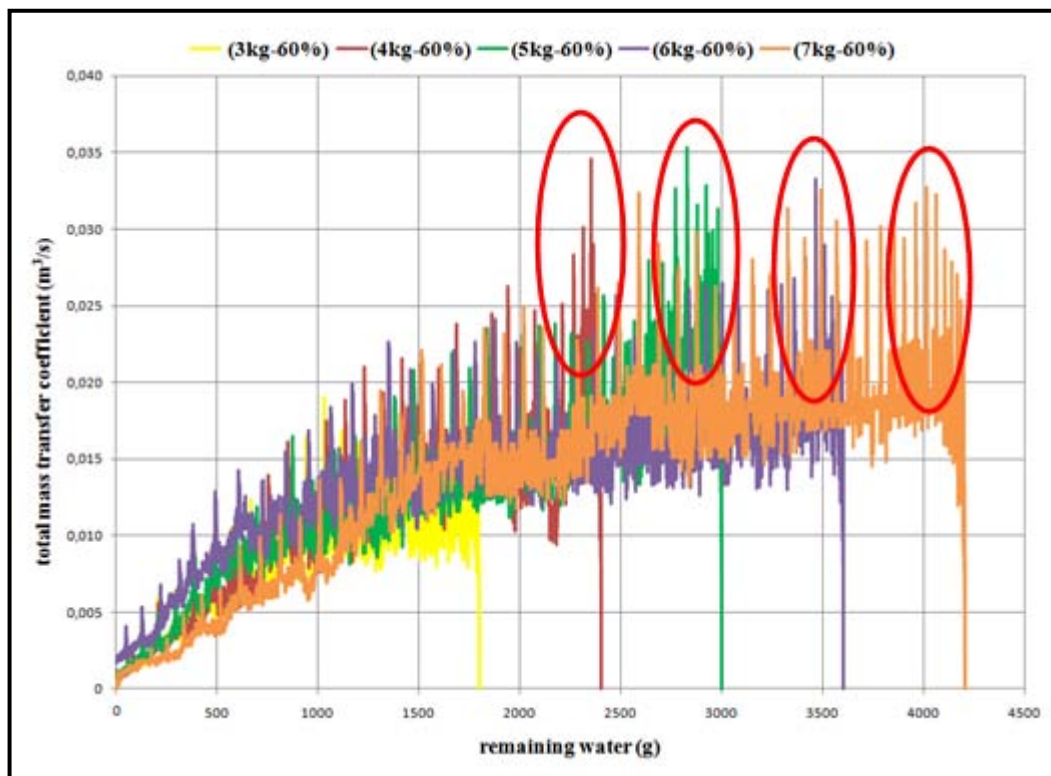


Figure 3.35. Total mass transfer coefficient with respect to the remaining water for air-condenser tumble dryer (variable load, constant initial moisture content)

Distribution of the total mass transfer coefficient for both air-vented and air-condenser tumble dryers are given in Figure 3.36. The characteristic of the total mass transfer coefficient is similar for both types of tumble dryers. However, the difference between the initial and the final value at the end of the experiments is higher for air-vented tumble dryer.

Moreover, the total mass transfer coefficient at steady state for air-vented tumble dryer is nearly six times higher than of the air-condenser tumble dryer. This is an expected result because in an air-condenser tumble dryer, water is extracted by condensation via heat exchanger. However, water is extracted from clothes directly by the evaporation through the drum in air-vented tumble dryers.
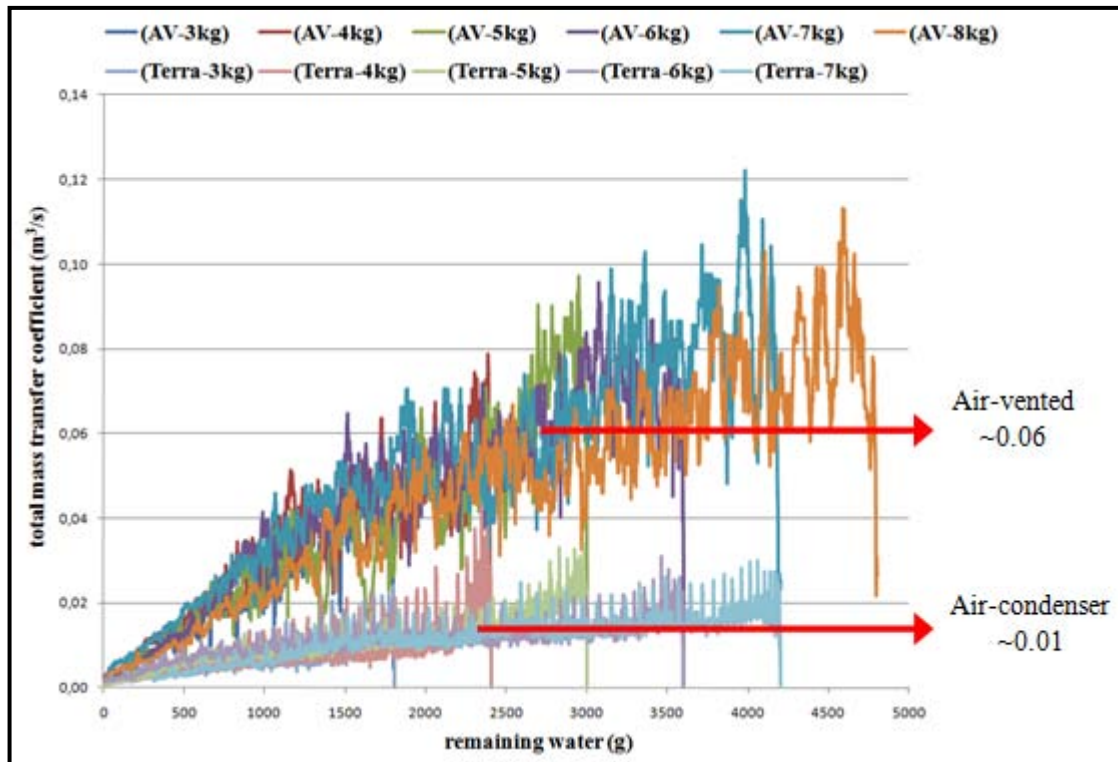


Figure 3.36. Comparison of the total mass transfer coefficient for tumble dryers

### 3.3.5. Mechanical Movement of the Clothes

In the drying literature, load in a tumble dryer consists of bed sheets, towels and pillowcases according to the standards. Sometimes long bed sheets could accumulate at the inside surface of the drum and may remain wet. This condition affects the evaporation process inside the drum and thus, the total mass transfer coefficient respectively. In order to investigate the effect of the load distribution inside the drum, experiments are carried out for load consisting of only towels and only long bed sheets.

In Figure 3.37, it is found that the temperature at the drum exit for load consists of only the bed sheet is nearly 5 °C higher than of the load consists of only the towels. In this situation, it is expected that the evaporation process for bed sheet load should be faster than the towels. However, we should take into consideration that the bed sheets are accumulated at the inside surface of the drum.

In addition, the characteristic of the temperature profile for load consisting of only the towels is uniform than of the load consisting of only the bed sheets.
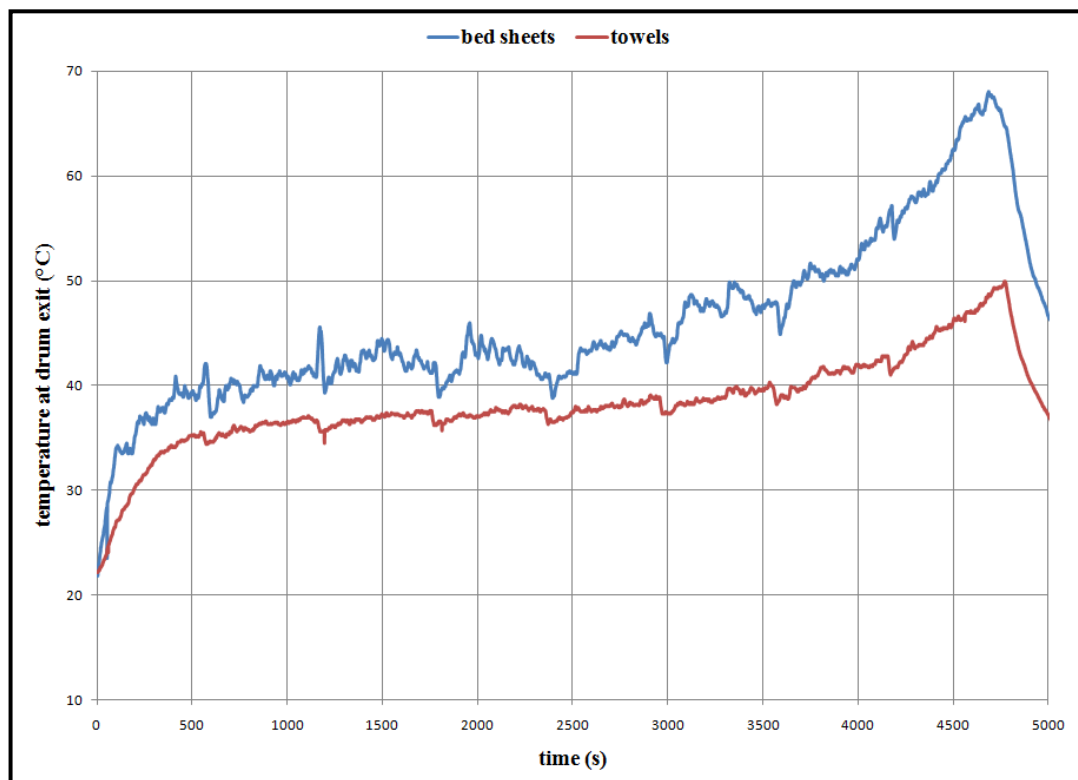


Figure 3.37. Temperature profile at the drum exit: (towels-bed sheets)

The graph of the total mass transfer coefficient with respect to the amount of remaining water at the surface of the clothes for bed sheets and towels is given in Figure 3.38. It is found that the total mass transfer coefficient is higher for the load consisting of only the towels. According to the mentioned graph, evaporation process for towels accrues faster than of the bed sheets. Long bed sheets may flocculated inside the drum and remain wet. This is one of the factors, which affects the drying process.
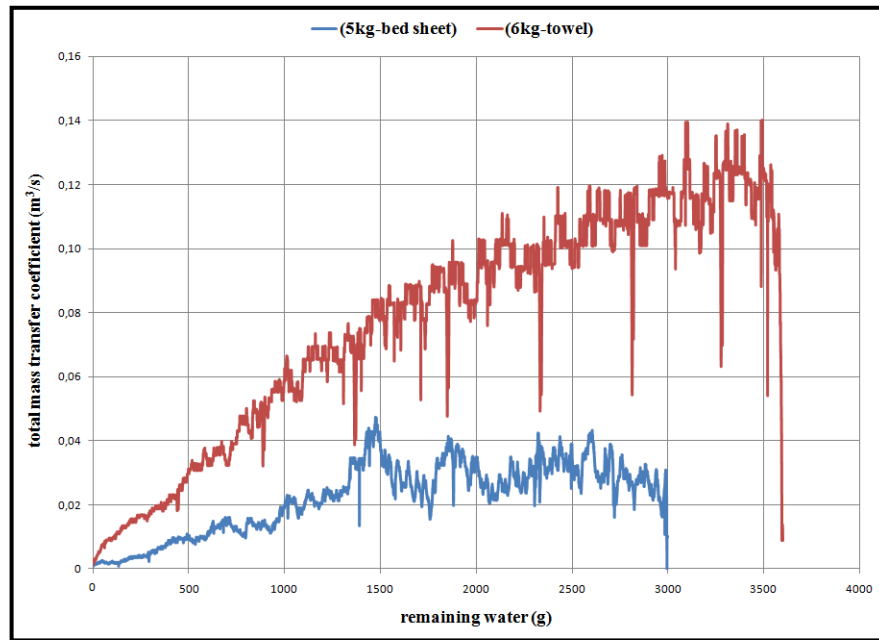
Figure 3.38. Total mass transfer coefficient with respect to the remaining water: (towels-bed sheets)

### 3.3.6. Textile Type

Effect of textile type is also shortly investigated during the experimental study. One set of experiment is conducted for synthetic and cotton type textile. Experiments are conducted for 4 kg and 8 kg of load with synthetic and cotton type textile separately. In addition, we have to take into consideration that the surface area of the test specimen for the synthetic textile is much smaller than of the test specimen for cotton type textile. In the end, the total mass transfer coefficients are plotted.

It is clear that the synthetic type textile has tendency to release water from the surface of the clothes. Therefore, it is expected to obtain a higher evaporation rate for synthetic type textile. In Figure 3.39, we can examine that the total mass transfer coefficient for synthetic type textile is significantly higher than of the cotton type textile. This implication indicates that the evaporation rate should be higher for the synthetic type textile. When we examine Figure 3.40, it is found that the evaporation rate for synthetic type textile is significantly higher than of the cotton type textile. Indeed, this topic should be investigated alone as future work, which is not the main subject of this project.
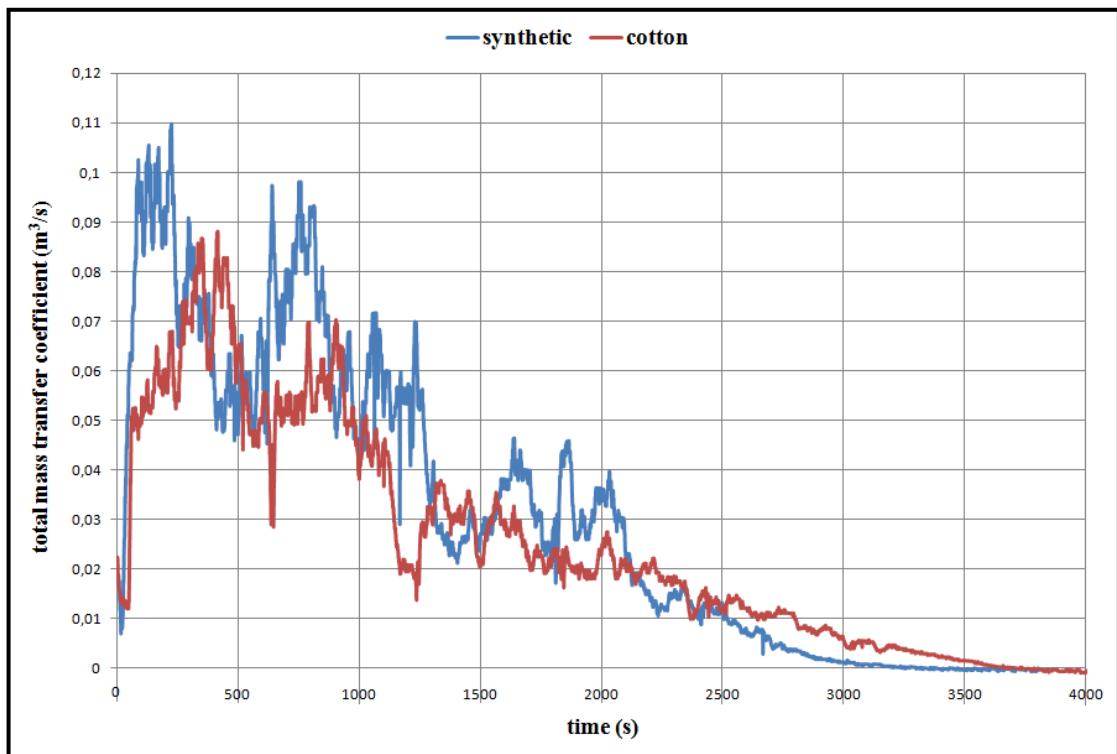
Figure 3.39. Total mass transfer coefficient with respect to time: (synthetic-cotton)
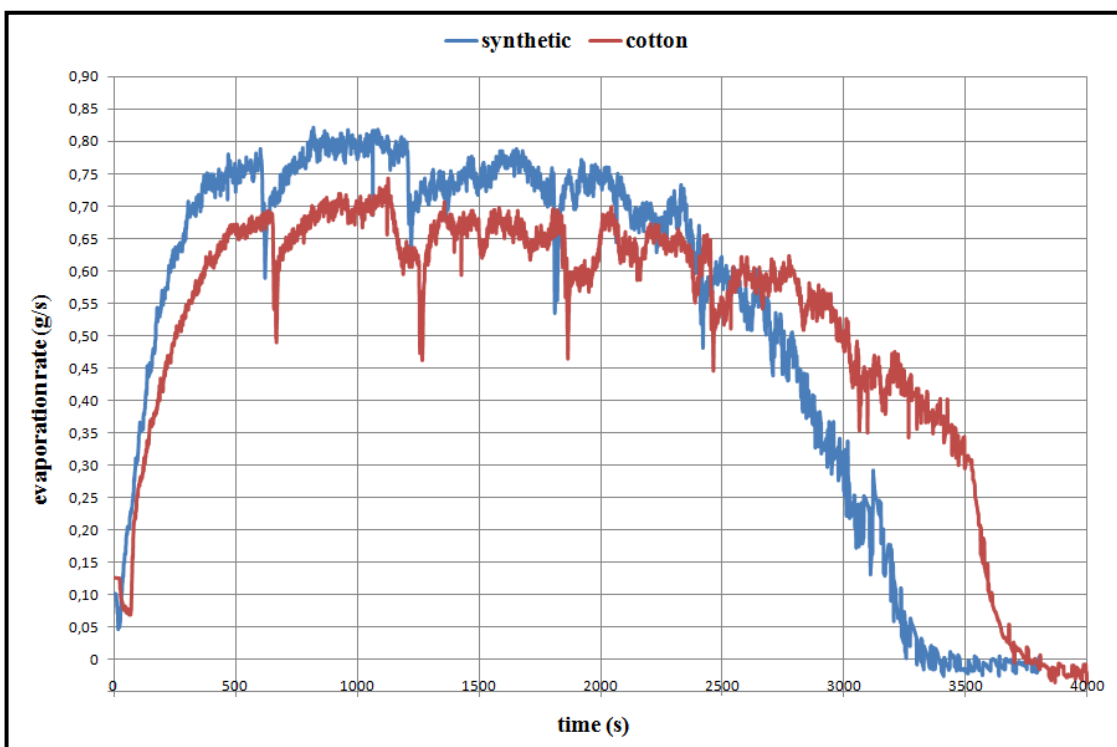


Figure 3.40. Evaporation rate with respect to time: (synthetic-cotton)

### 3.3.7. Design of Experiment (DOE)

Design of experiment (DOE) is a structured, organized method that is used for determining the relationship between the different factors affecting a process and the output of that process. A design of experiment (DOE) is formed for air-vented tumble dryer after conducting series of experiments with different parameters that are involved in the drying process in order to investigate mass transfer process in more detail.

DOE involves designing set of experiments, in which all relevant factors are varied systematically. Analyzed results of these experiments help us to identify optimal conditions, the factors that influence the results and those that do not, as well as other details such as the existence of interactions. Factors that are involved in design of experiment are given in Table 3.5 with minimum and maximum numerical values.

Table 3.5. Factors of the DOE

| Factors | Min. Value | Max. Value |
|---|---|---|
| Weight of the Clothes (kg) | 3 | 7 |
| Flow Rate (L/s) | 22.5 | 35.5 |
| Existing Heater (W) | 1500 | 2500 |
| External Heater (W) | 100 | 500 |
| Initial Moisture Content (%) | 40 | 60 |

In order to minimize the time spent for the present experiments, a fractional factorial design was preferred instead of using a full factorial design. Full factorial design includes measurements at all combinations of the experimental factor levels while a factorial design consists of a carefully selected subset (fraction) of the experimental runs of a full factorial design.

The two-level of factorial design is constructed by choosing minimum and maximum quantitative values. Since a two-level full factorial design of experiment has been chosen for the five factors mentioned above, the DOE would require 32 test runs ($2^5$).

Instead of executing such a large test program, a design of ¼ fraction has been chosen with three replications to obtain information about the main effects and low-order interactions. Moreover, one center point is added to the test runs in order to examine the change in the total mass transfer coefficient between the maximum and minimum levels of the quantitative factors. Consequently, a DOE with 25 test runs is formed as represented in Table 3.6.

Table 3.6. DOE experiment matrix

| Std Order | Run Order | Weight of Clothes (kg) | Initial Moisture Content (%) | Flow Rate (Hz) | External Heater (W) | Existing Heater (W) |
|---|---|---|---|---|---|---|
| 1 | 1 | 3 | 40 | 40 | 500 | 2500 |
| 2 | 2 | 7 | 40 | 40 | 100 | 1500 |
| 3 | 3 | 3 | 60 | 40 | 100 | 2500 |
| 4 | 4 | 7 | 60 | 40 | 500 | 1500 |
| 5 | 5 | 3 | 40 | 60 | 500 | 1500 |
| 6 | 6 | 7 | 40 | 60 | 100 | 2500 |
| 7 | 7 | 3 | 60 | 60 | 100 | 1500 |
| 8 | 8 | 7 | 60 | 60 | 500 | 2500 |
| 9 | 9 | 3 | 40 | 40 | 500 | 2500 |
| 10 | 10 | 7 | 40 | 40 | 100 | 1500 |
| 11 | 11 | 3 | 60 | 40 | 100 | 2500 |
| 12 | 12 | 7 | 60 | 40 | 500 | 1500 |
| 13 | 13 | 3 | 40 | 60 | 500 | 1500 |
| 14 | 14 | 7 | 40 | 60 | 100 | 2500 |
| 15 | 15 | 3 | 60 | 60 | 100 | 1500 |
| 16 | 16 | 7 | 60 | 60 | 500 | 2500 |
| 17 | 17 | 3 | 40 | 40 | 500 | 2500 |
| 18 | 18 | 7 | 40 | 40 | 100 | 1500 |
| 19 | 19 | 3 | 60 | 40 | 100 | 2500 |
| 20 | 20 | 7 | 60 | 40 | 500 | 1500 |
| 21 | 21 | 3 | 40 | 60 | 500 | 1500 |
| 22 | 22 | 7 | 40 | 60 | 100 | 2500 |
| 23 | 23 | 3 | 60 | 60 | 100 | 1500 |
| 24 | 24 | 7 | 60 | 60 | 500 | 2500 |
| 25 | 25 | 5 | 50 | 50 | 300 | 2000 |

The values of the factors in Table 3.6 are determined by the experimental studies, which were performed earlier. In addition, some of the factors such as heater power are limited up to certain values in order not to damage textile during the drying process. In this DOE study, the output result is the effect of factors on the total mass transfer coefficient.

Total mass transfer coefficient is investigated at three sections. First section includes only the transient region for a short period at the beginning of the experiment. Second section is the steady state region where the total mass transfer coefficient is assumed almost constant. Third section is for the entire drying process including the start transient and the cooling period of the drying process. The factors and some of their interactions that affect the total mass transfer coefficient at steady state section are shown on the column labeled as "Term" in Table 3.7.

Table 3.7. Experimental data analysis via Minitab for the total mass transfer coefficient at steady state

| Factorial Fit: $(hA)_{m_{ss}}$ versus load weight, moisture content, flow rate, external heater, existing heater | | | | | |
|---|---|---|---|---|---|
| **Term** | **Effect** | **Coeff** | **SE Coeff** | **T** | **P** |
| Constant | | 0.043619 | 0.00096 | 45.42 | 0.000 |
| load weight | 0.031672 | 0.015836 | 0.00096 | 16.49 | 0.000 |
| **moisture content** | 0.002851 | 0.001425 | 0.00096 | 1.48 | **0.157** |
| flow rate | 0.006713 | 0.003356 | 0.00096 | 3.49 | 0.003 |
| **external Heater** | -0.003589 | -0.001794 | 0.00096 | -1.87 | **0.080** |
| existing Heater | 0.007536 | 0.003768 | 0.00096 | 3.92 | 0.001 |
| moisture content*flow rate | -0.004215 | -0.002108 | 0.00096 | -2.19 | 0.043 |
| moisture content*existing heater | -0.005373 | -0.002686 | 0.00096 | -2.80 | 0.013 |
| Ct Pt (Center Point) | -0.004602 | 0.004802 | -0.96 | 0.352 | |
| | | | | | |
| **R-Sq** | **95.22%** | | | | |
| **R-Sq (adj)** | **92.83%** | | | | |

Since terms have the values of P's lower than 0.05, the null hypothesis is rejected, meaning that the factors and their interactions listed take significant role on determining the output. Three-way interactions are eliminated in the beginning of the analysis. Moisture content and external heater parameters, which were highlighted in Table 3.7, are also eliminated due to P values higher than 0.05. In addition, remaining two-way interactions are eliminated. In the end, we came up with three main effects; load weight, flow rate and the existing heater parameters. Same method is followed for the analysis of the other sections of the total mass transfer coefficient at transient and overall period.

Another output of the analysis to be considered is the R-square adjusted value shown in Table 3.7. The parameter R-sq (adj) is a mathematical term that states how much of the total variation on the output can be explained by the selected factors. In example, according to the analysis, the factors and their interactions are responsible for 92.83 per cent of the change on the total mass transfer coefficient at steady state.

The induced main effects for the total mass transfer coefficient at steady state are plotted in Figure 3.41. Red dots in the figure represent the center point data for the analysis. It can be understood that the center point has an effect on the analysis or not by examining the following figure. Since from the linearity of the main effects plot, it is found that the center point has no effect on the analysis.
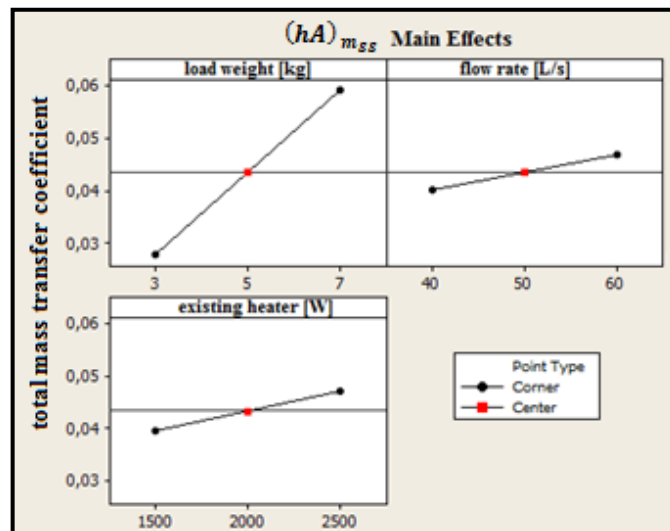


Figure 3.41. Main effects plot for the total mass transfer coefficient at steady state

Moreover, the induced main effects plot for the total mass transfer coefficient at transient and overall period of the drying process are shown in Figure 3.42 and Figure 3.43 respectively. In the end, it can be stated that the center point is not effective on the total mass transfer coefficient for both transient and overall periods.
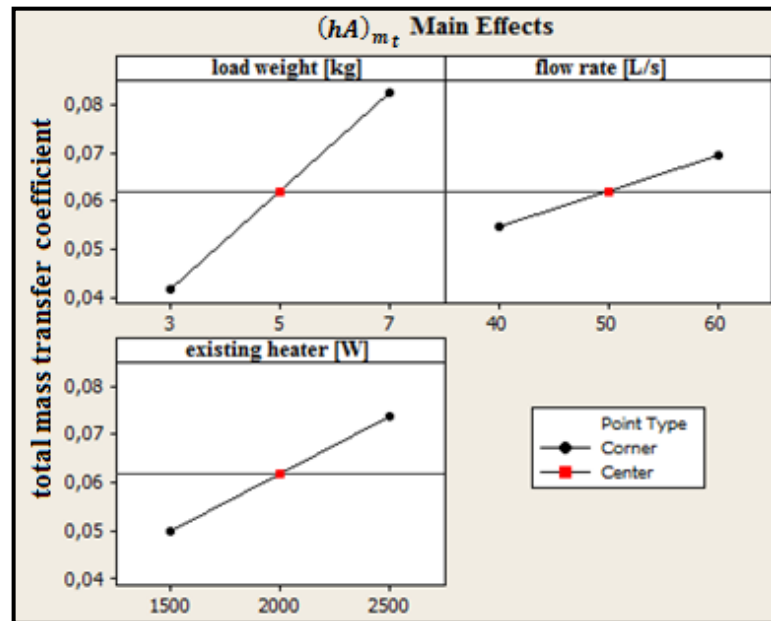


Figure 3.42. Main effects plot for the total mass transfer coefficient at transient period
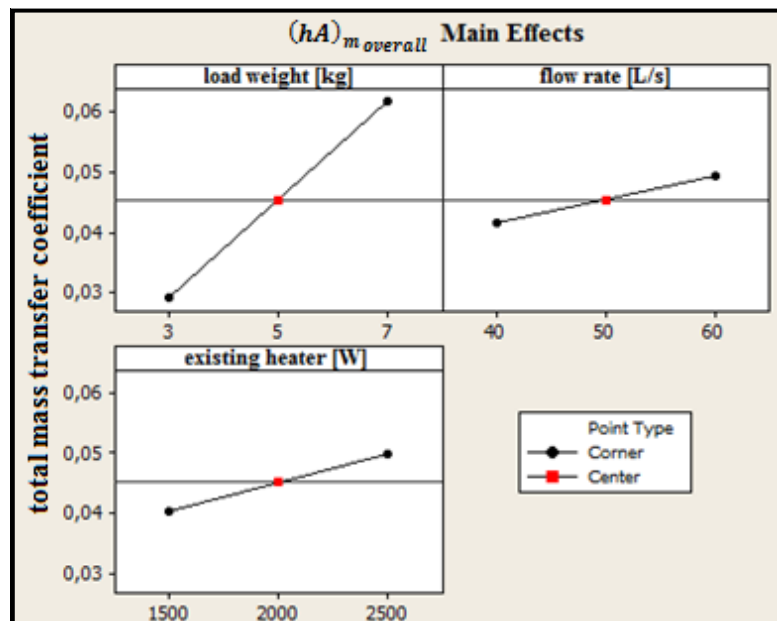


Figure 3.43. Main effects plot for the total mass transfer coefficient at overall period

After examining the effects of the factors individually, the ratio of the effect for each factor is investigated. For beginning, the sum of square values of the factors is examined. The sum of square values of the factors is calculated by Minitab. Ratio of each effect is determined via dividing the sum of square of a factor by the total sum of squares. The ratio of the effect for each factor is an indicative of whether a change on the factor may cause a significant change on the output of the analysis or not.

The ratio of factor effects on the total mass transfer coefficient at steady state is shown in Figure 3.44. The most effective factor on the total mass transfer coefficient is found to be the load weight. In addition, the amount of remaining water at the surface of the clothes is calculated by using load weight and the initial moisture content of the load as mentioned. Thus, the parameter labeled as load weight in the analysis could be treated as the amount of remaining water at the surface of the clothes.
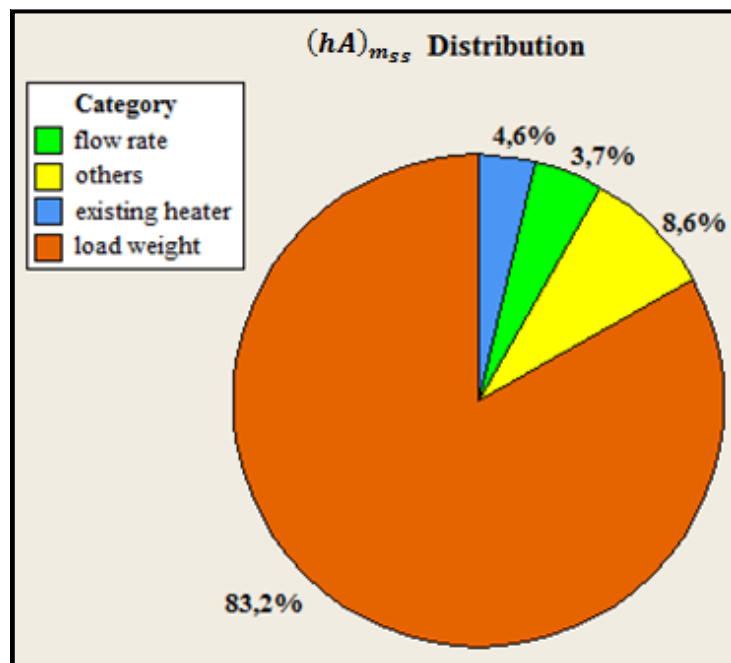


Figure 3.44. Pie chart representation of the factors on the total mass transfer coefficient: (at steady state region of the drying process)

Pie chart representation of the factors on the total mass transfer coefficient for the transient and the overall period of the drying process are given in Figure 3.45 and Figure 3.46 respectively by applying the same method.
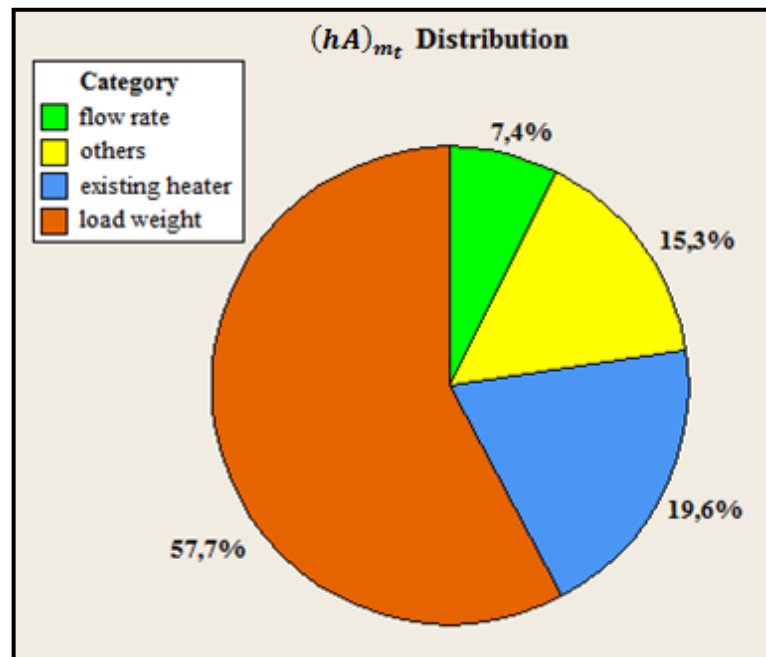
Figure 3.45. Pie chart representation of the factors on the total mass transfer coefficient: (at transient region of the drying process)
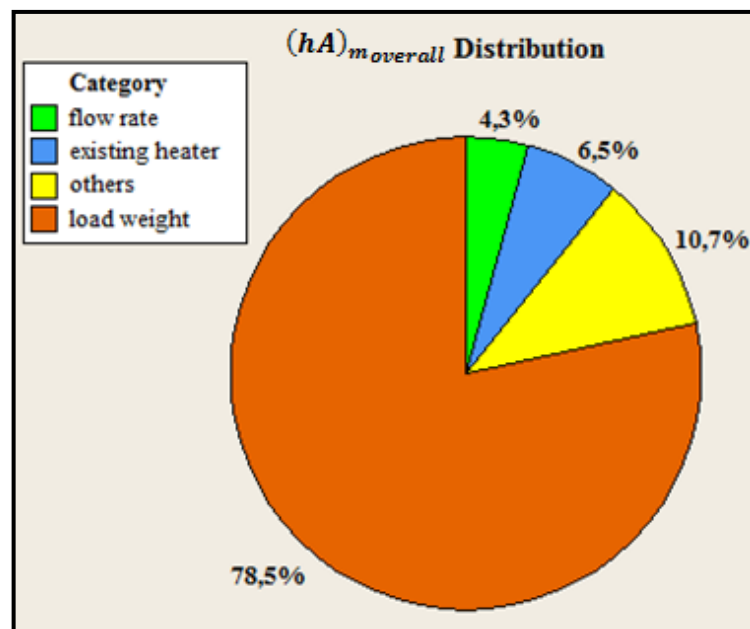


Figure 3.46. Pie chart representation of the factors on the total mass transfer coefficient: (at overall drying process)

Consequently, the amount of remaining water at the surface of the clothes is the most effective parameter on the total mass transfer coefficient for the all three sections. However, the sum of the other main factor effects is close to the effect of remaining water at the surface f the clothes at the transient section. In addition, flow rate is found to be the least effective parameter on the total mass transfer coefficient for the all three sections.

Moreover, the existing heater parameter has a minor effect at steady state when it is compared to the amount of remaining water at the surface of the clothes. However, in the transient section it has a significant role on the total mass transfer coefficient. In addition, the factor labeled as "others" includes the sum of all the minor effects of eliminated parameters and interaction of the main parameters.

# 4. SIMULATION MODELING

The main aim of this project is to investigate the transient operation of heat and mass transfer between wet clothes and dry air in tumble dryers. In addition, a simulation model of the transient drying process will be constructed. Experimental study is explained so far, from now on, a mathematical model of an air-condenser tumble dryer is going to be generated in this section by using the conservation of energy and mass. Hence, the main components of an air-condenser tumble dryer such as fan, heater, drum and condenser will be covered in detail.

In the beginning, general information about the drying process and modeling will be expressed. Then the modeling of main components will be explained individually. All the input and output parameters that are involved at the simulation model will also be stated.

## 4.1. PHASES OF DRYING PROCESS

Generally, temperature profile at the drum exit of a tumble dryer is investigated at three phases, which are shown in Figure 4.1. Temperature at drum exit is also named as "the door temperature" in tumble dryer literature.
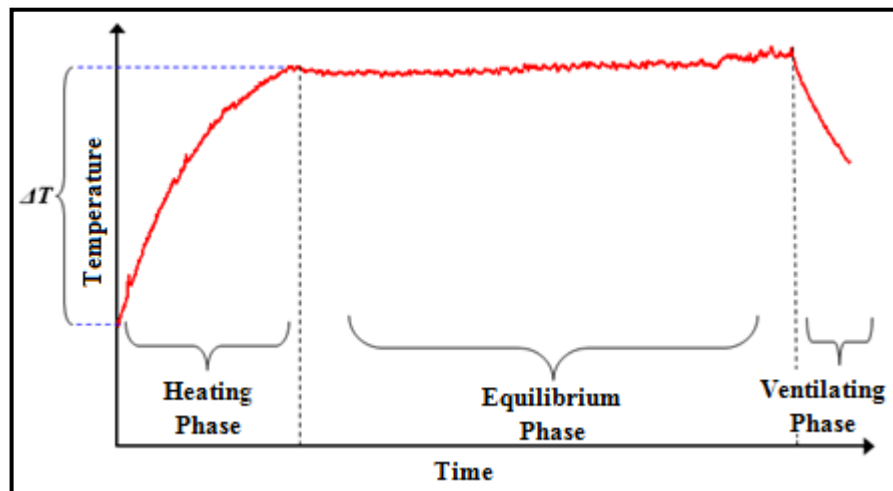


Figure 4.1. Phases of the drying period [3]: a. heating phase, b. equilibrium (steady state) phase, c. ventilating (cooling) phase

The first phase of drying process is the heating phase, where temperature at the drum exit increases rapidly in time until it reaches steady state. In this section, cold wet clothes are heated significantly and at the end of the heating phase, temperature at the surface of the clothes is increased to a sufficient level where evaporation with higher rate is achieved.

The door temperature is almost constant or increases very slowly in the equilibrium phase of drying process, which is also named as the steady state. Thus, the second phase is called the equilibrium phase. Moisture at the surface of the clothes is extracted by the mass transfer process between hot dry air and wet clothes during the equilibrium phase. At the end of the steady state, the door temperature slightly increases, which indicates that the clothes in the drum are dried sufficiently.

Third and the last phase of the drying process is the ventilating phase, which is also known as "cooling phase". After the steady state phase, surface temperature of the clothes is hot and makes it uncomfortable to unload the dryer. In this section, heater is shut down and dry air is blown from cooling fan in condenser dryers to cool down the surface temperature of the clothes. The cooling phase could seem as waste of energy, but it is preferred by most of the customers for comfort.

## 4.2. NEWTON'S METHOD

In numerical analysis, Newton's method, which is also known as the Newton-Raphson method, named after Isaac Newton and Joseph Raphson is employed. Newton's method is a root-finding algorithm that uses the first few terms of the Taylor series of a function. This method is perhaps the best-known method for finding successively better approximations to the roots of a real-valued function.

In addition, Newton's method can often converge remarkably quickly, especially if the iteration begins sufficiently close to the desired root. Unfortunately, when iteration begins far from the desired root, Newton's method can easily lead an unwary user astray with little warning. Thus, good implementations of the method embed it in a routine that also detects and perhaps overcomes possible convergence failures.

Suppose we have given a function $f(x)$ and its derivative $f'(x)$ and we begin to solve the root by an initial guess, $x_0$. The first approximation is given as below:

$$x_1 = x_0 - \frac{f(x_0)}{f'(x_0)} \tag{4.1}$$

If we would like to continue approximating the solution, general form is given as:

$$x_{n+1} = x_n - \frac{f(x_n)}{f'(x_n)} \tag{4.2}$$

In Figure 4.2, schematic representation of the method is expressed to understand the physics of the method better. The idea of Newton's method is as follows: one starts with an initial guess, which is reasonably close to the true root. Then its tangent line (slope) approximates the function and one computes the x-intercept of this tangent line. The x-intercept will typically be a better approximation to the function's root than the original guess, and the method can be iterated.
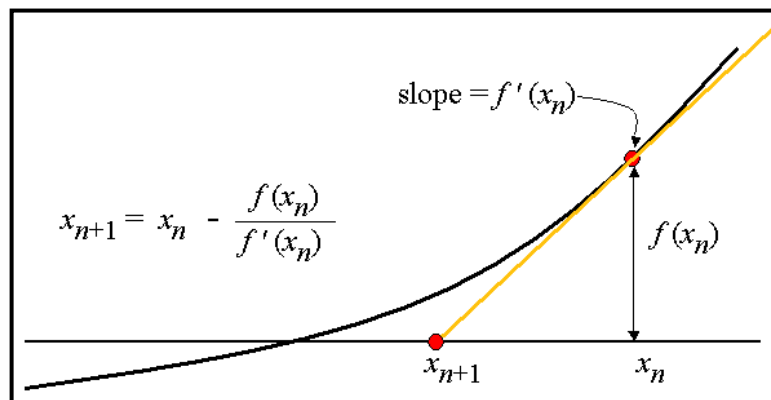


Figure 4.2. Schematics of the Newton's method: (root finding process)

Newton's method is a very useful and simple tool to use when the initial guess is valid. Thus, the Newton's method is utilized when it is required to find the root of an equation during the modeling. Newton's method yields to reasonable results most of the time.

## 4.3. AIR PROPERTIES

Air is the main fluid flowing inside the tumble dryer. Specific humidity of the air increases at the evaporation process from the surface of the clothes and at the condensation process inside the heat exchanger where water drops are formed. Thus, thermo-physical properties of the air are required during the entire drying process.

### 4.3.1. Vapor Pressure Correlation of Air

The most commonly used vapor pressure correlations in the literature are given by Wexler and afterwards Sonntag updated these formulations to ITS's-90 [15]. Huang also published an updated version of Wexler´s equation. Wagner & Pruss presented new formulations for vapor pressure above water and ice, respectively [16].

Sonntag formulation for calculating the vapor pressure is expressed in Equation 4.3. In addition, the constant coefficients of the formulation are given in Table 4.1.

$$P_s = exp\left(\sum_{i=1}^{4} a_i T^{i-2} + a_7 ln(T)\right) \tag{4.3}$$

Table 4.1. Coefficients for the Sonntag vapor pressure correlation [16]

| Coefficients | Above Water | Above Ice |
|---|---|---|
| $a_1$ | -6.097E+03 | -6.026E+03 |
| $a_2$ | 2.124E+01 | 2.933E+01 |
| $a_3$ | -2.711E-02 | 1.061E-02 |
| $a_4$ | 1.674E-05 | -1.320E-05 |
| $a_7$ | 2.434 | -4.938E-01 |
| Standard Uncertainty | $< \pm 0.005$ % RH | $< \pm 0.5$ % RH |

Vapor pressure is expressed as $P_s$ (saturation pressure), and calculated by the given formulation with the coefficients given above. Partial differential of vapor pressure with respect to temperature $(\partial P_s/\partial T)$ is also calculated in the program.

Moreover, a subroutine is generated for calculating the vapor pressure at given temperature by using Equation 4.3 in the simulation program. The subroutine receives temperature as input value and turns back vapor pressure as output parameter. Moreover, the partial differential of vapor pressure with respect to temperature $(\partial P_s / \partial T)$ is calculated by applying the same approach in determining the vapor pressure.

### 4.3.2. Viscosity, Conductivity and Prandtl Number

Dynamic viscosity, thermal conductivity and Prandtl number for air are calculated by the following formulation. Additionally, it should be noted that the temperatures are taken in Kelvin during the calculations [7].

$$\mu = 9.213E - 07 + T(6.9326E - 08 + T(-3.62E - 11)) \tag{4.4}$$

$$k = -1.945E - 04 + T(9.861E - 05 + T(-3.500E - 08)) \tag{4.5}$$

$$Pr = 0.837 + T(-6.1E - 04 + T(6.0E - 07)) \tag{4.6}$$

### 4.3.3. Enthalpy Calculation

Enthalpy of the air is determined separately for three phases of air, which are the fluid phase, the gaseous phase and the phase between gas and liquid [7].

$$h_f = 0.6446687 + T(4.16485 + T(0.00019215847)) \tag{4.7}$$

$$h_g = 2500.895 + T(1.834738 + T(-0.0003184265 + T(-0.0000031198158 + T(-0.000000024703951)))) \tag{4.8}$$

$$h_{fg} = h_g - h_f \tag{4.9}$$

Another subroutine is also formed for the enthalpy calculation in the FORTRAN simulation program. Since they all depend on the temperature, the temperature is received as input. In addition, partial differentials of enthalpy with respect to temperature $\left(\partial h_f/\partial T\ ,\ \partial h_g/\partial T\ ,\ \partial h_{fg}/\partial T\right)$ are determined similarly.

Moreover, one useful subroutine was formed, which receives the enthalpy as input parameter and turns back the temperature value as output by applying the Newton's Method to the proper formulation.

$$h = Cp_{air}T + wh_g \qquad (4.10)$$

When enthalpy is known and it is desired to determine the temperature, Equation 4.10 is equaled to zero then the below partial differentials are determined with respect to temperature.

$$f = Cp_{air}T + wh_g - h \qquad (4.11)$$

$$\frac{\partial f}{\partial T} = Cp_{air} + w\frac{\partial h_g}{\partial T} \qquad (4.12)$$

Function and its derivative are determined, now Newton's method is applicable in determining the temperature by including the initial guess as in Equation 4.13.

$$T = T_0 - \frac{f(T)}{\partial f/\partial T} \qquad (4.13)$$

## 4.4. FAN MODEL

Mass flow rate of air is one of the most important parameter that has to be taken into account in the modeling of fan. In addition, the air leakage is modeled and included in the model. For the beginning, air pressure is determined in order to calculate density of air.

Vapor pressure is determined by the multiplication of relative humidity with the saturation pressure at given temperature as in Equation 4.14. Saturation pressure is determined by the mentioned subroutine.

$$P_v = \phi_{drum} P_s \qquad (4.14)$$

Atmospheric air can be treated as ideal-gas mixture. In addition, atmospheric air pressure is the sum of partial pressure of dry air $(P_{air})$ and that of water vapor $(P_v)$ specified in Equation 4.15. Since the vapor pressure and the atmospheric air pressure are known, pressure of dry air can be determined.

$$P_0 = P_{air} + P_v \qquad (4.15)$$

Density of dry air is calculated according to the Equation 4.16. Temperature at drum should be taken in Kelvin.

$$\rho_{air} = \frac{P_{air}}{RT_{drum}} \qquad (4.16)$$

The schematic representation of the air leakage in fan is given in Figure 4.3. Mass flow rate of air at the fan inlet and exit are specified including the mass flow rate of air leakage through the fan.
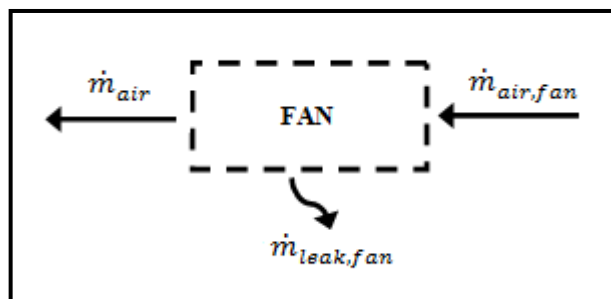


Figure 4.3. Control volume of the fan leakage

The rate of air leakage through the fan is determined by the leakage ratio, which was investigated experimentally exclusive of this project.

Moreover, the parameters that are involved in the modeling of the fan in Figure 4.3 are expressed as follows:

$$\dot{m}_{air,fan} = FR_p \rho_{air} \tag{4.17}$$

$$\dot{m}_{leak,fan} = \frac{\dot{m}_v R_{fan}}{w_{drum}} \tag{4.18}$$

$$\dot{m}_{air} = \dot{m}_{air,fan} - \dot{m}_{leak,fan} \tag{4.19}$$

## 4.5. HEATER MODEL

Another significant component of a tumble dryer is the heater where it is used for heating up the dry air to a sufficient level. Specific humidity of the air remains unchanged through the heater, thus, $w_{cond} = w_{heat}$ . In the beginning of the heater model, temperature and the specific enthalpy at heater are determined.

$$h_{heat} = Cp_{air}T_{heat} + w_{cond}h_g \tag{4.20}$$

$$\frac{\partial h_{heat}}{\partial T_{heat}} = Cp_{air} + w_{cond}\frac{\partial h_g}{\partial T_{heat}} \tag{4.21}$$

Heat generation and heat loss at the heater are given in Equation 4.22 and Equation 4.23. Mean temperature between the heater and the condenser is also expressed in Equation 4.24.

$$Q_{heater} = hA_{heater}(T_{heater} - T_m) \tag{4.22}$$

$$Q_{L,heater} = hA_{loss,heater}(T_{heat} - T_\infty) \tag{4.23}$$

$$T_m = \frac{1}{2}(T_{heat} + T_{cond}) \tag{4.24}$$

Schematic illustration of the flow mechanism in an air-condenser tumble dryer is shown in Figure 4.4 in order to follow the notation of the inlet and outlet easily during the modeling. Locations of the components in the figure are shown in side section view. The flow direction of the air is also specified with red colored arrows. In summary, humid air flows across the channels of the condenser before passing through the heater in condenser tumble dryers.
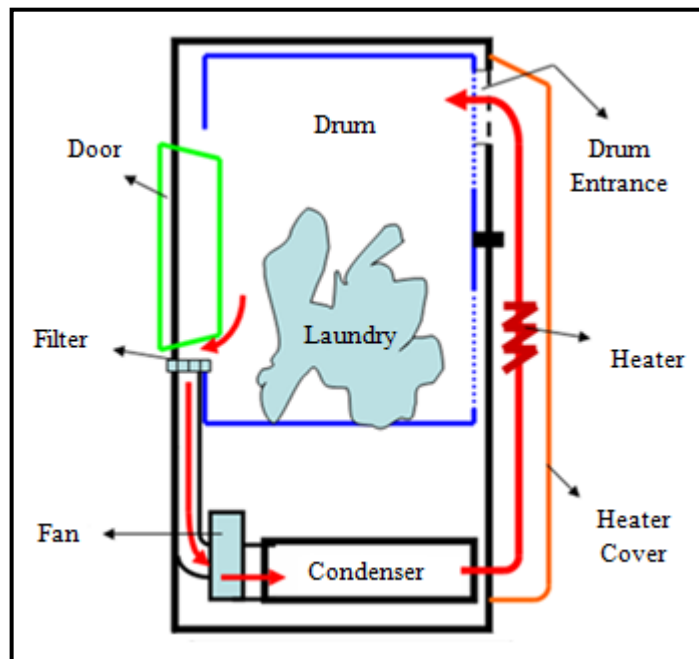


Figure 4.4. Schematic illustration of an air-condenser tumble dryer

For next step, temperature at the heater is solved numerically by the Newton's method applied on the flow equation in Equation 4.25. The general time dependent equation for the heater is expressed in Equation 4.26.

$$Q_{heater} = \dot{m}_{air}(h_{heat} - h_{cond}) + Q_{L,heater} \tag{4.25}$$

$$\dot{Q}_H(t) = mc\frac{dT_m}{dt} + Q_{heater} \tag{4.26}$$

If we integrate Equation 4.26 with respect to the heater temperature, we came up with the Equation 4.27. In the end, heat generation is obtained including the heat losses. Temperature at the heater is also determined. In summary, there are two main equations in the model, the Equation 4.25 for heater to determine the heat generation and the Equation 4.26 for the flow to determine the temperature at heater.

$$T_{heater,2} = T_{heater,1} + \frac{\Delta t}{mc}\left(\dot{Q}_H(t) - Q_{heater}\right) \tag{4.27}$$

## 4.6. DRUM MODEL

One of the most important components of a tumble dryer is the drum or in other words, tumble. Complex mass transfer process happens inside the drum. Thus, heat and mass transfer processes involved in the drum are investigated in two separate control volumes. One control volume is for the laundry and water at the surface of clothes. Additionally, the other control volume is for the drum and the air inside the drum. Schematics of the mass transfer across the drum are shown in Figure 4.5.
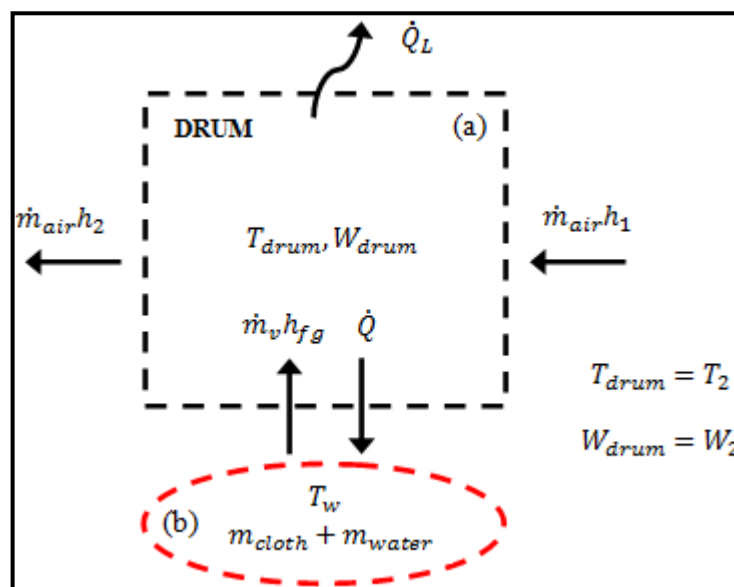


Figure 4.5. Control volume of the mass transfer across the drum: a. control volume of drum and air inside, b. control volume of laundry and water at the surface of the clothes

### 4.6.1. Control Volume for Clothes and the Water at the Surface of the Clothes

The schematic representation of control volume between clothes in the drum and the water at the surface of the clothes is shown in Figure 4.6. For next step, energy and mass conservation are applied on the specified control volume.
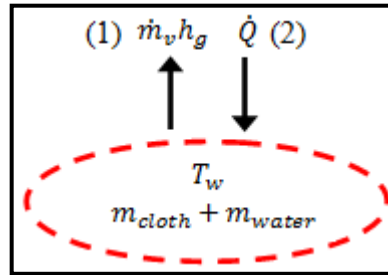


Figure 4.6. Control volume of the laundry and the water at the surface of the clothes: 1. energy from evaporation of water, 2. heat transfer between laundry and drum

Energy balance for the control volume results:

$$\dot{Q}_{CV} + \sum \dot{m}_i \left( h_i + \frac{V_i^2}{2} + gz_i \right)$$

$$=$$ \hfill (4.28)

$$\frac{d}{dt}\left[ m \left( u + \frac{V^2}{2} + gz \right) \right]_{CV} + \sum \dot{m}_e \left( h_e + \frac{V_e^2}{2} + gz_e \right) + \dot{W}_{CV}$$

Since kinetic and potential terms are neglected, heat transfer rate for the control volume can be expressed as:

$$\dot{Q}_{CV} = \frac{d}{dt}(mu)_{CV} + \dot{m}_e h_e \hspace{2cm} (4.29)$$

Total mass of the control volume in Equation 4.29 can be modified as the sum of water at the surface of the clothes and the clothes itself. Thus, the Equation 4.30 is obtained as:

$$\dot{Q}_{CV} = \frac{d}{dt}(m_c u_c + m_w u_w)_{CV} + \dot{m}_e h_e \tag{4.30}$$

When we impose the distributive property of the differentiation on Equation 4.30:

$$\dot{Q}_{CV} = m_c \frac{du_c}{dt} + m_w \frac{du_w}{dt} + u_w \frac{dm_w}{dt} + u_c \frac{dm_c}{dt} + \dot{m}_v h_g \tag{4.31}$$

Since the mass of clothes is conserved and the mass of water is expressed as follows:

$$\frac{dm_w}{dt} = -\dot{m}_v \tag{4.32}$$

$$\frac{dm_c}{dt} = 0 \tag{4.33}$$

$$\dot{Q}_{CV} = m_c Cv_c \frac{dT_w}{dt} + m_w Cv_w \frac{dT_w}{dt} - \dot{m}_v u_w + \dot{m}_v h_g \tag{4.34}$$

Internal energy of water at the surface of clothes can be estimated as the enthalpy of liquid phase itself, as expressed in Equation 4.35.

$$u_w \approx h_f \tag{4.35}$$

Therefore, Equation 4.34 yields to Equation 4.36 given below:

$$\dot{Q}_{CV} = (m_c Cv_c + m_w Cv_w)\frac{dT_w}{dt} + \dot{m}_v(h_g - h_f) \tag{4.36}$$

$$\dot{Q}_{CV} = (m_c C_c + m_w C_w)\frac{dT_w}{dt} + \dot{m}_v h_{fg}(T_w) \tag{4.37}$$

After proper rearrangements on the Equation 4.36, heat transfer rate of the control volume can be reduced into Equation 4.38 at steady state.

$$\dot{Q}_{CV} = \dot{m}_v h_{fg}(T_w) \tag{4.38}$$

In the end, from the conservation of energy in time dependent domain, balance equation is obtained as it is given in Equation 4.39. We should be aware of the assumption carried out on the internal energy of the water. In addition, in Figure 4.5, it is shown with $h_{fg}$ directly, but it is derived after the assumption.

$$(m_c C p_c + m_w C p_w) \frac{dT_w}{dt} = \dot{Q} - \dot{m}_v h_{fg} \tag{4.39}$$

Energy entering to the specified control volume, $\dot{Q}$ term in Figure 4.6 is clarified by Equation 4.40 as follows:

$$\dot{Q} = hA(T_{drum} - T_w) \tag{4.40}$$

Water evaporated from the surface of the clothes, $\dot{m}_v$ in the following control volume is expressed in Equation 4.41 as follows:

$$\dot{m}_v = (hA)_m \rho_{air} \left( w_w \frac{T_w}{T_2} - w_2 \right) \tag{4.41}$$

In order to determine the density of the dry air ($\rho_{air}$), first the pressure of the dry air is determined as given below:

$$P_a = \frac{0.622}{(0.622 + w_2)} P_0 \tag{4.42}$$

Then the density of the dry air is determined as in Equation 4.43. It should be noted that the temperature at drum exit is taken in Kelvin.

$$\rho_{air} = \frac{P_a}{R_a(T_2 + 273.15)} \tag{4.43}$$

Finally, the change in the water amount at the surface of the clothes with respect to time is expressed in Equation 4.44.

$$\frac{dm_w}{dt} = -\dot{m}_v \qquad (4.44)$$

The physical meaning of the minus sign in the following equation states that the amount of water at the surface of clothes is decreasing with respect to time.

### 4.6.2.  Theoretical Background of the Mass Transfer Coefficient

The mass transfer coefficient is expressed by $h_m$ in Equation 4.41. Mass transfer coefficient mainly depends on the amount of remaining water at the surface of the clothes inside the drum as mentioned. In addition, the experimental study driven at air-vented and air-condenser tumble dryers verify the mentioned inference. Moreover, the specific humidity at the surface of the clothes, which is involved in determining the mass transfer coefficient, is calculated by adhering to the assumption that the relative humidity at the surface of the clothes is 100 per cent.

There is a mass transfer associated with convection in that mass is transported from one place to another in flow systems such as in the tumble dryer. In general, the mass transfer coefficient is defined by Equation 4.45 similarly in heat transfer phenomenon.

$$\dot{m}_i = h_{m_i} A\left(C_{i_1} - C_{i_2}\right) \qquad (4.45)$$

In the above equation, $\dot{m}_i$ represents the diffusive mass flux of any component $i$, $C_i$ represents the concentrations through which the diffusion occurs and $h_{m_i}$ is for the mass transfer coefficient with cross sectional area $A$. In the experimental study, the total mass transfer coefficient is used which is expressed by $(hA)_m$.

Moreover, it can be stated that the heat, mass and momentum transfers have similarities according to the governing laws. For a laminar boundary layer, energy and momentum equations represented in Equation 4.46 and 4.47 have similar characteristics.

$$u\frac{\partial u}{\partial x} + v\frac{\partial u}{\partial y} = v\frac{\partial^2 u}{\partial y^2} \qquad (4.46)$$

$$u\frac{\partial T}{\partial x} + v\frac{\partial T}{\partial y} = \alpha\frac{\partial^2 T}{\partial y^2} \qquad (4.47)$$

Equation 4.46 is for the momentum equation at constant pressure. Equation 4.47 is for the incompressible flow involving low-velocity. The ratio of the two mentioned equations is the Prandtl number given in Equation 4.48.

$$Pr = \frac{v}{\alpha} = \frac{C_p\mu}{k} \qquad (4.48)$$

Prandtl number is the link between velocity and temperature field, thus, an important parameter for convection involved heat transfer. Same approach can be followed in order to define the diffusive mass transfer at the surface including the concentrations.

$$u\frac{\partial C_i}{\partial x} + v\frac{\partial C_i}{\partial y} = D\frac{\partial^2 C_i}{\partial y^2} \qquad (4.49)$$

If we examine Equation 4.46, Equation 4.47 and Equation 4.49, we can realize that the three equations are in similar forms. Concentration and velocity profiles will have the same shape if the ratio $v/D = 1$. This dimensionless ratio is named as Schmidt number in the literature, which is expressed in Equation 4.50.

$$Sc = \frac{v}{D} = \frac{\mu}{\rho D} \qquad (4.50)$$

Schmidt number is a significant parameter, where both convection and mass transfer involved during a process likewise in clothes drying. Thus, it is a useful parameter to indicate the relation between the viscous diffusion rate and the mass diffusion rate.

The role of Schmidt number is similar to the Prandtl number in convection heat transfer. Likewise, Prandtl number indicates the relation between the viscous diffusion rate and the thermal diffusion rate. In addition, the functional dependence of the heat transfer coefficient in convectional heat transfer and the functional dependence of the mass transfer coefficient in convectional mass transfer are given below.

$$\frac{hx}{k} = f(\text{Re}, \text{Pr}) \tag{4.51}$$

$$\frac{h_D x}{D} = f(\text{Re}, \text{Sc}) \tag{4.52}$$

Concentration and temperature profiles are similar when the ratio $\alpha/D = 1$, which also means $\alpha = D$. Lewis number given in Equation 4.53 is the ratio of thermal diffusivity to the mass diffusivity, which is used to characterize fluid flows where heat and mass transfer involved simultaneously by convection.

$$Le = \frac{\alpha}{D} = \frac{Sc}{Pr} \tag{4.53}$$

Finally, Sherwood number is expressed in Equation 4.54, which represents the ratio between the convective heat transfer coefficient and the diffusive mass transfer coefficient.

$$Sh = \frac{kx}{D} \tag{4.54}$$

In summary, the relationship between heat and mass transfer is clarified in the theoretical background of the mass transfer coefficient. Dimensionless parameters are introduced, which are involved in relating the heat and mass transfer. In addition, similarities found on the characteristics of the diffusive mass transfer equation, momentum equation and the convectional heat transfer equation are mentioned.

### 4.6.3. Control Volume for Drum and Air inside the Drum

Control volume for the air inside the drum and the drum itself is shown schematically by the black dashed line in Figure 4.7 given below.
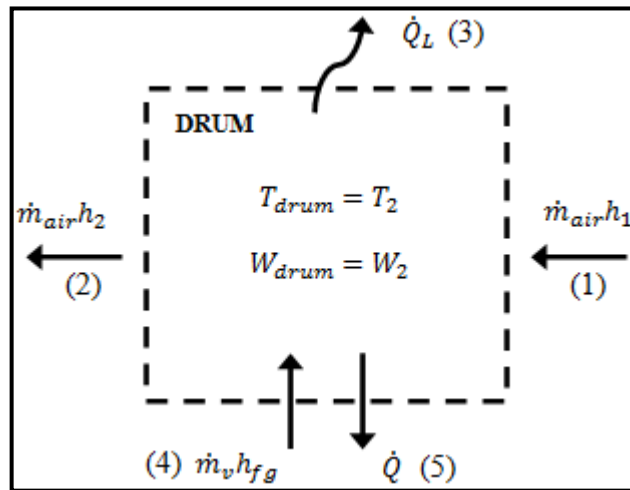


Figure 4.7. Control volume for the drum and the air inside: 1. air inlet, 2. air outlet, 3. heat loss from drum, 4. energy from evaporation of water, 5. heat transfer between laundry and drum

First, the heat loss from the drum control volume can be expressed as:

$$\dot{Q}_L = (hA)_L (T_2 - T_\infty) \tag{4.55}$$

Conservation of mass for the dry air inside the drum can be written as:

$$\frac{dm_{air}}{dt} = \dot{m}_{a1} - \dot{m}_{a2} \tag{4.56}$$

Similarly, the conservation of the mass for water vapor is as follows:

$$\frac{dm_v}{dt} = \frac{d}{dt}(w_2 m_{air}) \tag{4.57}$$

By applying partial differentiation to the Equation 4.57:

$$\frac{dm_v}{dt} = m_{air}\frac{dw_2}{dt} + w_2\frac{dm_{air}}{dt} \tag{4.58}$$

If we plug Equation 4.56 into Equation 4.58, Equation 4.58 yields to the Equation 4.59 given below:

$$\frac{dm_v}{dt} = m_{air}\frac{dw_2}{dt} + w_2(\dot{m}_{a1} - \dot{m}_{a2}) \tag{4.59}$$

In addition, mass of water vapor at the control volume can be expressed as:

$$\frac{dm_v}{dt} = w_1\dot{m}_{a1} - w_2\dot{m}_{a2} + \dot{m}_v \tag{4.60}$$

By using the relationship between Equation 4.59 and Equation 4.60:

$$m_{air}\frac{dw_2}{dt} = \dot{m}_{a1}(w_1 - w_2) + \dot{m}_v \tag{4.61}$$

The conservation of energy for the control volume can be expressed as:

$$\frac{d}{dt}(m_{air}h_2) = \dot{m}_{a1}h_1 - \dot{m}_{a2}h_2 + \dot{m}_vh_g - \dot{Q} - \dot{Q}_L \tag{4.62}$$

By applying the partial differentiation to the term on the right hand side of Equation 4.62, the following equations are determined:

$$\frac{d}{dt}(m_{air}h_2) = \frac{dm_{air}}{dt}h_2 + m_{air}\frac{dh_2}{dt} \tag{4.63}$$

$$\frac{dm_{air}}{dt}h_2 + m_{air}\frac{dh_2}{dt} = (\dot{m}_{a1} - \dot{m}_{a2})h_2 + m_{air}\frac{dh_2}{dt} \tag{4.64}$$

By using the relation between Equation 4.62 and Equation 4.64, we obtain:

$$m_{air} \frac{dh_2}{dt} = \dot{m}_{a1}(h_{a1} - h_{a2}) + \dot{m}_v h_g - \dot{Q} - \dot{Q}_L \qquad (4.65)$$

There also air leakage exists inside the drum that has to be taken into consideration as mentioned. Air leakage can be classified in two parts, air entering the drum control volume and air leaving the drum control volume. Air leakage is shown schematically in Figure 4.8.
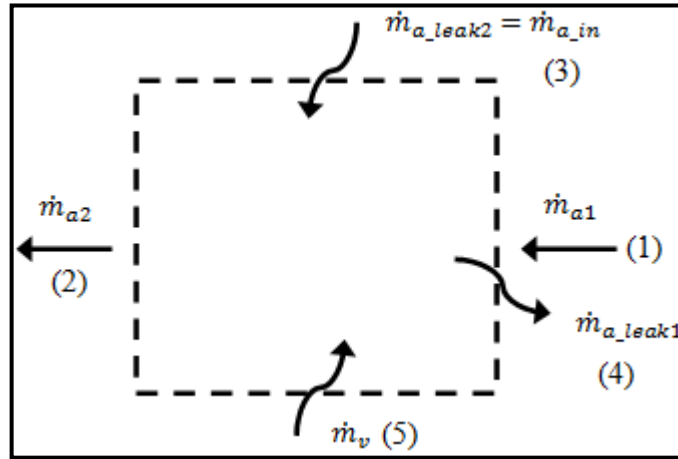


Figure 4.8. Control volume of the air leakage inside the drum: 1. drum air inlet, 2. drum air outlet, 3. air leakage entering drum, 4. air leakage leaving drum, 5. hot vapor entering drum

The conservation of mass for the dry air in the figure is expressed as:

$$\frac{dm_{air}}{dt} = \dot{m}_{a1} - \dot{m}_{a2} - \dot{m}_{a\_leak1} + \dot{m}_{a\_in} \qquad (4.66)$$

Similarly, the conservation of mass for the water vapor is as follows:

$$\frac{dm_v}{dt} = w_1 \dot{m}_{a1} - w_2 \dot{m}_{a2} + w_\infty \dot{m}_{a\_in} + \dot{m}_v \qquad (4.67)$$

The conservation of energy for the control volume can be written as:

$$\frac{d}{dt}(m_{air}h_2) = \dot{m}_{a1}h_1 - \dot{m}_{a2}h_2 - \dot{m}_{a\_leak1}h_1 + \dot{m}_{a\_leak2}h_\infty + \dot{m}_v h_g - \dot{Q} - \dot{Q}_L \quad (4.68)$$

Mass of air and water vapor are assumed unchanged during the process. Thus, they are equated to zero as expressed below:

$$\frac{dm_{air}}{dt} \approx 0 \quad (4.69)$$

$$\frac{dm_v}{dt} \approx 0 \quad (4.70)$$

By using the Equations given in 4.69 and 4.70, Equations 4.66, 4.67 and 4.68 yield to the Equations 4.71, 4.72 and 4.73 respectively.

$$\dot{m}_{a\_in} = \dot{m}_{a2} - \left(\dot{m}_{a1} - \dot{m}_{a\_leak1}\right) \quad (4.71)$$

$$\dot{m}_{a2}w_2 = \left(\dot{m}_{a1} - \dot{m}_{a\_leak1}\right)w_1 + \dot{m}_{a\_in}w_\infty + \dot{m}_v \quad (4.72)$$

$$h_2 \frac{dm_{air}}{dt} + m_{air} \frac{dh_2}{dt}$$
$$= \quad (4.73)$$
$$\dot{m}_{a1}h_1 - \dot{m}_{a2}h_2 - \dot{m}_{a\_leak1}h_1 + \dot{m}_{a\_leak2}h_\infty + \dot{m}_v h_g - \dot{Q} - \dot{Q}_L$$

In the end, conservation of mass for dry air, conservation of mass for water vapor and conservation of energy are achieved including the air leakage. Moreover, partial differentiation is applied for the conservation of energy given in Equation 4.68.

In drum subroutine, there are four unknown parameters; $m_w$ , $w_2$ , $T_w$ and $T_2$ . These are temperature and specific humidity at drum exit, temperature at the surface of the clothes and the amount of remaining water at clothes' surface. The mass of remaining water ($m_w$) will be solved explicitly and the other three parameters ($w_2, T_w, T_2$) are going to be solved implicitly. Thus, three equations will be sufficient to solve three parameters.

The Equations 4.39, 4.72 and 4.73 are rearranged as Equations 4.74, 4.75 and 4.76 respectively. The modified forms of the equations are used to construct Jacobian matrix. The Jacobian matrix makes it possible to solve iteratively for the required unknown parameters by applying Newton's method.

$$f_1 = (m_c Cp_c + m_w Cp_w)(T_w - T_w^-) - \left(Q - \dot{m}_v h_{fg}\right)\Delta t = 0 \qquad (4.74)$$

$$f_2 = \dot{m}_{a2} w_2 - \left(\dot{m}_{a1} - \dot{m}_{a\_leak1}\right)w_1 - \dot{m}_{a\_in} w_\infty - \dot{m}_v = 0 \qquad (4.75)$$

$$
\begin{aligned}
f_3 = &+ m_{air}(h_2 - h_2^-) \\
&- \left[\left(\dot{m}_{a1} - \dot{m}_{a_{leak1}}\right)(h_1 - h_2)\right]\Delta t \\
&- \left[\dot{m}_{a_{in}}(h_\infty - h_2)\right]\Delta t \\
&- \left[\dot{m}_v h_g - Q - Q_L\right]\Delta t = 0
\end{aligned}
\qquad (4.76)
$$

Jacobian matrix is represented in Equation 4.77 given below:

$$J = \begin{bmatrix} \dfrac{\partial f_1}{\partial T_w} & \dfrac{\partial f_1}{\partial w_2} & \dfrac{\partial f_1}{\partial T_2} \\[2mm] \dfrac{\partial f_2}{\partial T_w} & \dfrac{\partial f_2}{\partial w_2} & \dfrac{\partial f_2}{\partial T_2} \\[2mm] \dfrac{\partial f_3}{\partial T_w} & \dfrac{\partial f_3}{\partial w_2} & \dfrac{\partial f_3}{\partial T_2} \end{bmatrix} \qquad (4.77)$$

As we can understand from the form of the Jacobian matrix, three partial differentials are required for each equation set. Totally nine partial differentials in Jacobian matrix are going to be determined.

$$\frac{\partial f_1}{\partial T_w} = +(m_c Cp_c + m_w Cp_w) + hA\Delta t$$

$$+ h_{fg}(hA)_m \rho_{air}\left[\frac{w_w}{(T_2+273.15)} + (T_w+273.15)\frac{\frac{\partial w_w}{\partial T_w}}{(T_2+273.15)}\right]\Delta t \tag{4.78}$$

$$\frac{\partial f_1}{\partial w_2} = -h_{fg}\left[(hA)_m\rho_{air} + (hA)_m w_2 \frac{(T_w+273.15)}{(T_2+273.15)} w_w \frac{\partial\rho_{air}}{\partial w_2}\right]\Delta t \tag{4.79}$$

$$\frac{\partial f_1}{\partial T_2} = -hA\Delta t - h_{fg}\left[(hA)_m\rho_{air}\frac{(T_w+273.15)}{(T_2+273.15)^2} w_w\right]\Delta t$$

$$- h_{fg}\left[(hA)_m w_2 \frac{(T_w+273.15)}{(T_2+273.15)} w_w \frac{\partial\rho_{air}}{\partial T_2}\right]\Delta t \tag{4.80}$$

$$\frac{\partial f_2}{\partial T_w} = -(hA)_m\rho_{air}\left[\frac{w_w}{(T_2+273.15)} + \frac{(T_w+237.15)}{(T_2+273.15)}\frac{\partial w_w}{\partial T_w}\right] \tag{4.81}$$

$$\frac{\partial f_2}{\partial w_2} = \dot{m}_{a2} + \left[(hA)_m\rho_{air} + (hA)_m w_2 \frac{(T_w+273.15)}{(T_2+273.15)} w_w \frac{\partial\rho_{air}}{\partial w_2}\right] \tag{4.82}$$

$$\frac{\partial f_2}{\partial T_2} = \left[(hA)_m\rho_{air}\frac{(T_w+273.15)}{(T_2+273.15)^2} w_w + (hA)_m w_2 \frac{(T_w+273.15)}{(T_2+273.15)} w_w \frac{\partial\rho_{air}}{\partial T_2}\right] \tag{4.83}$$

$$\frac{\partial f_3}{\partial T_w} = -h_g(hA)_m\rho_{air}\left[\frac{w_w}{(T_2+273.15)} + \frac{(T_w+273.15)}{(T_2+273.15)}\frac{\partial w_w}{\partial T_w}\right]\Delta t - hA\Delta t \tag{4.84}$$

$$\frac{\partial f_3}{\partial w_2} = + \frac{\partial m_{air}}{\partial w_2}(h_2 - h_2^-) + (m_{air} + \dot{m}_{a2}\Delta t)\frac{\partial h_2}{\partial w_2}$$

$$+ h_g\left[(hA)_m\rho_{air} + (hA)_m w_2 \frac{(T_w+273.15)}{(T_2+273.15)} w_w \frac{\partial\rho_{air}}{\partial w_2}\right]\Delta t \tag{4.85}$$

$$\frac{\partial f_3}{\partial T_2} = +\frac{\partial m_{air}}{\partial T_2}(h_2 - h_2^-) + (m_{air} + \dot{m}_{a2}\Delta t)\frac{\partial h_2}{\partial T_2} + [hA + (hA)_L]\Delta t$$

$$+ h_g\left[(hA)_m\rho_{air}\frac{(T_w + 273.15)}{(T_2 + 273.15)^2}w_w\right]\Delta t \tag{4.86}$$

$$+ h_g\left[(hA)_m w_2\frac{(T_w + 273.15)}{(T_2 + 273.15)}w_w\frac{\partial\rho_{air}}{\partial T_2}\right]\Delta t$$

Partial differentials in Jacobian matrix are determined and expressed from Equation 4.78 through the Equation 4.86. There are internal partial differentials in the determined equations from Equation 4.78 to the Equation 4.86. Internal partial differentials are also going to be determined according to the proper equations.

Partial differential $\partial w_w/\partial T_w$ is determined by applying differentiation to the general specific humidity equation in Equation 3.4.

$$\frac{\partial w_w}{\partial T_w} = 0.622\left[\frac{\frac{\partial P_s}{\partial T_w}}{(P_0 - P_s)} + \frac{P_{sat}\frac{\partial P_s}{\partial T_w}}{(P_0 - P_s)^2}\right] = 0.622\left[\frac{P_0\frac{\partial P_s}{\partial T_w}}{(P_0 - P_s)^2}\right] \tag{4.87}$$

Pressure of the dry air is determined in Equation 4.42. Partial differentials $\partial m_{air}/\partial w_2$ and $\partial m_{air}/\partial T_2$ are determined according to the Equation 4.42.

$$\frac{\partial m_{air}}{\partial w_2} = -\frac{0.622}{(0.622 + w_2)^2}\frac{P_0 V}{RT_2} = -\frac{m_{air}}{0.622 + w_2} \tag{4.88}$$

$$\frac{\partial m_{air}}{\partial T_2} = -\frac{0.622}{0.622 + w_2}\frac{P_0 V}{RT_2^2} = -\frac{m_{air}}{T_2} \tag{4.89}$$

Partial differential $\partial h_2/\partial w_2$ and $\partial h_2/\partial T_2$ are determined by applying differentiation to the Equation 4.90.

$$h_2 = Cp_{air}T_2 + w_2 h_{g2} \tag{4.90}$$

Partial differentials $\partial h_2/\partial w_2$ and $\partial h_2/\partial T_2$ are expressed in Equation 4.91 and Equation 4.92 respectively:

$$\frac{\partial h_2}{\partial w_2} = h_{g2} \tag{4.91}$$

$$\frac{\partial h_2}{\partial T_2} = Cp_{air} + w_2 \frac{\partial h_{g2}}{\partial T_2} \tag{4.92}$$

Partial differentials $\partial \rho_{air}/\partial T_2$ and $\partial \rho_{air}/\partial w_2$ are determined by applying differentiation to the Equation 4.43.

$$\frac{\partial \rho_{air}}{\partial T_2} = -\frac{P_a}{R_a(T_2 + 273.15)^2} \tag{4.93}$$

$$\frac{\partial \rho_{air}}{\partial w_2} = -\frac{P_a}{(0.622 + w_2)R_a(T_2 + 273.15)} \tag{4.94}$$

It should be noted that the differentials $\partial P_s/\partial T_w$ and $\partial h_{g2}/\partial T_2$ are determined by the subroutines written in the program.

Since all the required partial differentials both in Jacobian matrix and the internal ones are determined, solution set of the proper equations can be expressed. Solution set is given as follows:

$$\bar{X}_n = \begin{bmatrix} X_1 \\ X_2 \\ X_3 \end{bmatrix} = \begin{bmatrix} T_w \\ w_2 \\ T_2 \end{bmatrix} \tag{4.95}$$

$$F(\bar{X}_n) = \begin{bmatrix} f_1 \\ f_2 \\ f_3 \end{bmatrix} \tag{4.96}$$

The Newton's method expressed below is applied in order to determine the solution of the equations iteratively:

$$J(\bar{X}_n)\Delta\bar{X}_n = F(\bar{X}_n) \tag{4.97}$$

$$\Delta\bar{X}_n = \bar{X}_n - \bar{X}_{n+1} \tag{4.98}$$

$$X_{n+1} = X_n - \frac{f(X_n)}{\acute{f}(X_n)} \tag{4.99}$$

Equation 4.97 is solved until $\Delta\bar{X}_n$ becomes zero by performing a matrix operation shown below:

$$\begin{bmatrix} j_{11} & j_{12} & j_{13} \\ j_{21} & j_{22} & j_{23} \\ j_{31} & j_{32} & j_{33} \end{bmatrix}\begin{bmatrix} \Delta X_1 \\ \Delta X_2 \\ \Delta X_3 \end{bmatrix} = \begin{bmatrix} f_1 \\ f_2 \\ f_3 \end{bmatrix} \tag{4.100}$$

Finally, the roots of the solution set are determined as follows:

$$\Delta X_1 = \frac{j_{12}j_{23}f_3 - j_{12}j_{33}f_2 + j_{13}j_{32}f_2 - j_{13}j_{22}f_3 + j_{22}j_{33}f_1 - j_{32}j_{23}f_1}{j_{11}j_{22}j_{33} - j_{11}j_{32}j_{23} - j_{21}j_{12}j_{33} + j_{32}j_{21}j_{13} - j_{22}j_{31}j_{13} + j_{21}j_{12}j_{23}} \tag{4.101}$$

$$\Delta X_2 = \frac{j_{33}f_2 - j_{23}f_3 + (j_{23}j_{31} - j_{21}j_{33})\Delta X_1}{j_{22}j_{33} + j_{23}j_{32}} \tag{4.102}$$

$$\Delta X_3 = \frac{j_{11}f_3 - j_{31}f_1 + (j_{31}j_{12} - j_{32}j_{11})\Delta X_2}{j_{33}j_{11} + j_{31}j_{13}} \tag{4.103}$$

In the end, the required unknown parameters $w_2$, $T_w$ and $T_2$ are determined implicitly by matrix operation. Mentioned calculating scheme is continued until the convergence of the iteration is achieved. Thus, parameters that are involved in the Jacobian matrix are determined iteratively by using the Newton's method.

### 4.6.4. Water Activity Parameter

Another important parameter in the modeling of the drum is the water activity. One of the urgent problems that had been faced during the modeling is the decrease in relative humidity at the end of the equilibrium phase. Relative humidity at the surface of the clothes during the drying process is assumed 100 per cent as mentioned. However, as clothes start to dry, temperature at the surface of the clothes increases and relative humidity decreases respectively. Thus, the assumption about relative humidity at the surface of the clothes fails at that moment of drying. Therefore, the water activity parameter in Equation 4.104 [17-18] is introduced in order to change the relative humidity at the surface of the clothes by rearranging the vapor pressure.

$$a = 1 - \left[ \frac{\beta m\_c + \delta}{1 + \delta^{\gamma m\_c}} \right] \tag{4.104}$$

Generally, water activity parameter is used in food industry in order to specify different formations of bacterium on the surface of the foods at which moisture content interval. However, in this project, water activity parameter is used to change the vapor pressure as clothes start to dry. In addition, the water activity depends on the moisture content and the constant coefficients.

Since the water activity parameter is introduced, specific humidity calculation at the surface of the clothes is revisited. Thus, the general specific humidity in Equation 3.4 is modified as in Equation 4.105. Moreover, since the specific humidity at the surface of the clothes is modified, the partial differential $\partial w_w / \partial T_w$ in Equation 4.87 is redefined as in Equation 4.106.

$$w_w = 0.622 \frac{\alpha P_s}{P_0 - \alpha P_s} \tag{4.105}$$

$$\frac{\partial w_w}{\partial T_w} = 0.622 \left[ \frac{P_0 \frac{\partial P_s}{\partial T_w}}{(P_0 - a P_s)^2} \right] \tag{4.106}$$

Water activity was studied earlier and the constant parameters that are involved in determining the water activity were investigated experimentally in the literature. Thus, the water activity parameter with respect to moisture content for different textile type is shown in Figure 4.9 is used. The constant coefficients for various types of fabrics are also specified in the figure.
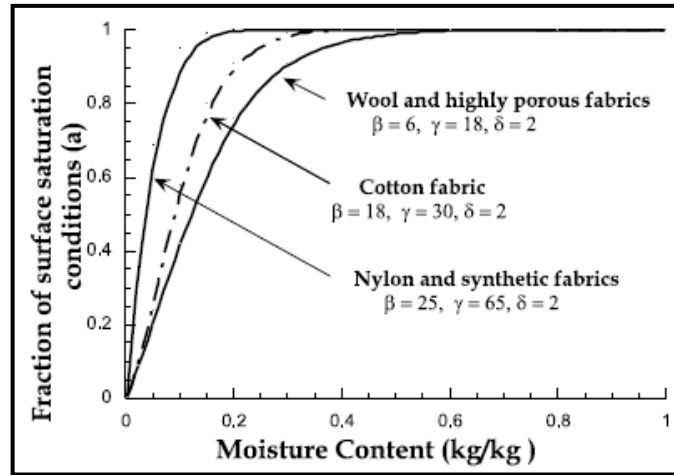


Figure 4.9. Water activity graphs for various types of fabrics [18]

In order to calculate the water activity parameter experimentally, the total mass transfer coefficient $\left((hA)_{m_0}\right)$ for air-condenser tumble dryer is assumed constant during the drying process. This assumption is almost valid for the entire drying process except first five minutes of the heating phase. The Equation 4.107 is determined by using the relations between Equation 3.6, Equation 3.8 and Equation 4.105 including the mentioned assumption.

$$\alpha = \frac{\left[\dfrac{P_0}{0.622}\dfrac{\dot{m}_v}{\rho_{air}(hA)_{m_0}}\right] + w_{drum,exit}}{P_s + \left[\dfrac{P_s}{0.622}\left(\dfrac{\dot{m}_v}{\rho_{air}(hA)_{m_0}} + w_{drum,exit}\right)\right]} \tag{4.107}$$

Thus, the water activity is calculated for both according to the experimental data by using Equation 4.107 and theoretically by using the Lambert relation given in Equation 4.104. The water activity parameter is plotted with respect to the moisture content similarly in the literature in Figure 4.10.
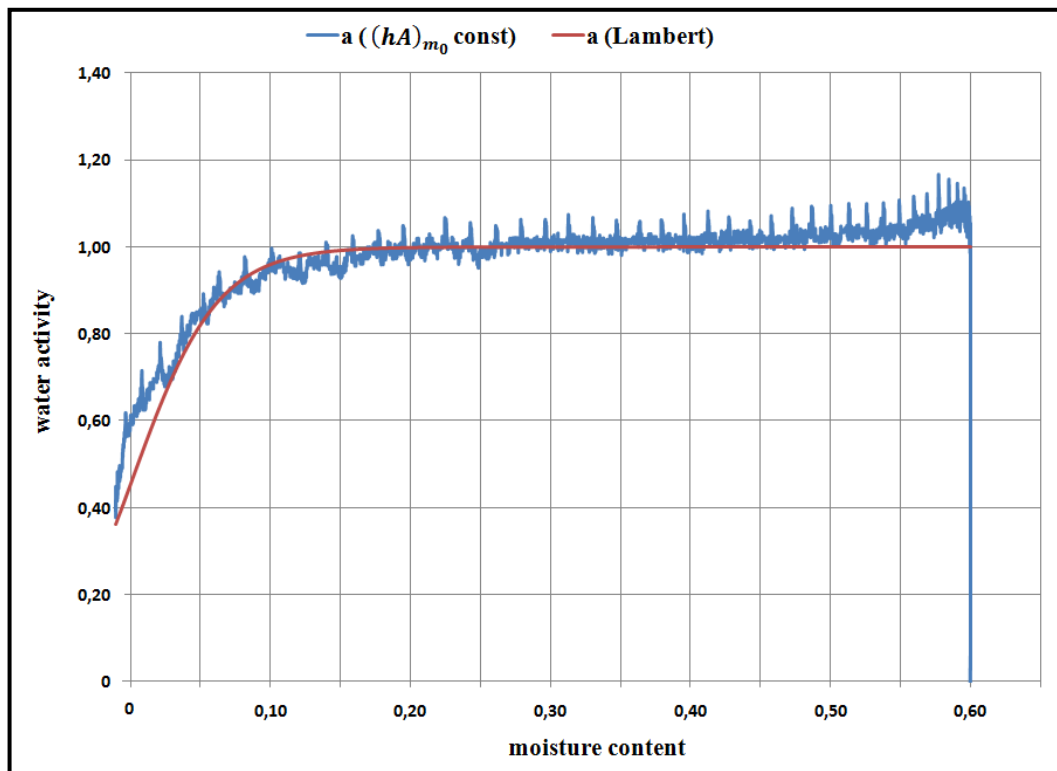
Figure 4.10. Water activity correlation

In Figure 4.10, the blue line represents the water activity parameter that is calculated experimentally by assuming the total mass transfer coefficient is constant. In addition, the red line in the following figure represents the water activity parameter, which is obtained by changing the constant coefficients of the Lambert equation in the literature. Thus, water activity parameter is determined, which is used at the end of the equilibrium phase of the drying process.

## 4.7. CONDENSER MODEL

Condenser is one of the most important components of a tumble dryer where water is extracted from humid air via condensation. Hot process air and cold cooling air flow across the channels of the condenser.

In general, heat exchangers are classified according to the direction of the flow inside. The two well-known types of heat exchangers are parallel-flow and counter-flow heat exchangers.

Schematics of the temperature distribution for parallel-flow and counter-flow heat exchangers are shown in Figure 4.11. The directions of the hot air and cold air are represented by red and blue colors respectively. In parallel-flow heat exchangers, both process air and cooling air are in the same direction. However, in counter-flow heat exchangers, process air and cooling are have the opposite directions.
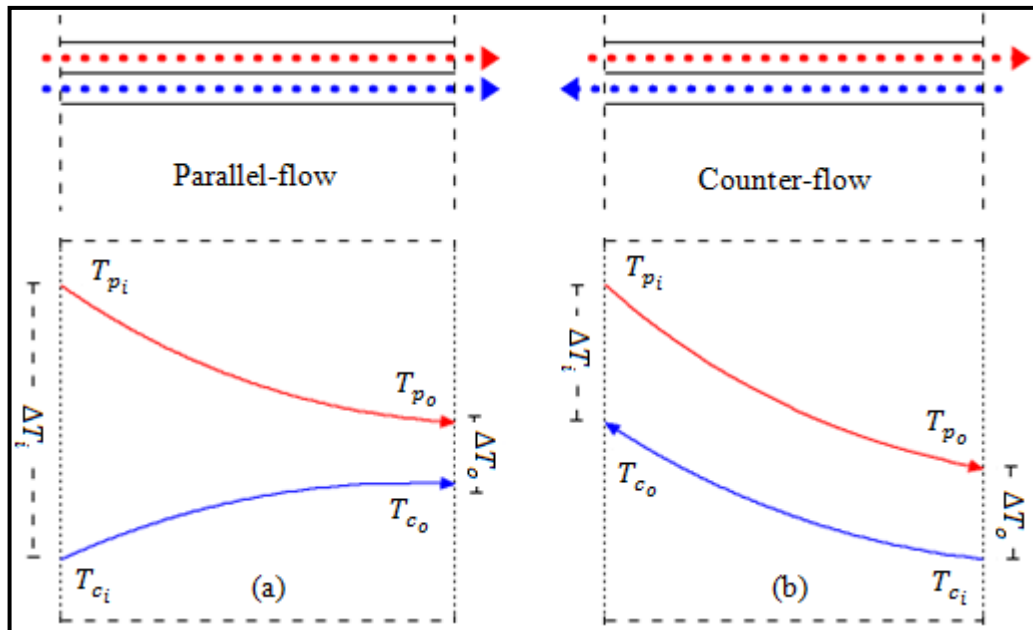


Figure 4.11. Temperature distribution of heat exchangers according to the flow direction:

a. parallel-flow, b. counter-flow

Temperature difference between the inlet and outlet for a parallel-flow heat exchanger is higher than of the counter-flow heat exchanger. It should be taken into consideration that the outlet temperature of the cooling air can be higher than the outlet temperature of the process air for a counter-flow heat exchanger.

Condenser in the study can be modeled by using two different methods, first method is the effectiveness NTU method and the second method is the logarithmic temperature difference method (LMTD). Both methods have advantages and disadvantages according to the situations. Each of the methods is going to be discussed separately.

### 4.7.1. Effectiveness-NTU Method

The Logarithmic Mean Temperature Difference (LMTD) method requires cumbersome iterative schemes to solve for outlet temperatures. Thus, NTU method is advantageous compared to the LMTD when only the inlet temperatures of the fluid are known. In such cases, an alternative approach effectiveness-NTU method is preferable.

In NTU method, maximum possible heat transfer rate $q_{max}$ should be determined in order to define the effectiveness of a heat exchanger. In counter flow heat exchangers, one of the fluids will face the maximum possible temperature difference.

Cold fluid is heated until the temperature of the fluid becomes equal to the inlet temperature of hot fluid. Similarly, hot fluid is cooled until the temperature of the fluid becomes equal to the inlet temperature of cold fluid. This situation depends on whether which fluid experiences the larger amount of temperature change.

For $C_c < C_h$ :

$$q_{max} = C_c\left(T_{h,i} - T_{c,i}\right) \tag{4.108}$$

For $C_h < C_c$ :

$$q_{max} = C_h\left(T_{h,i} - T_{c,i}\right) \tag{4.109}$$

When we generalized this approach, we came up with the following:

$$q_{max} = C_{min}\left(T_{h,i} - T_{c,i}\right) \tag{4.110}$$

Effectiveness ratio is defined as:

$$\varepsilon \equiv \frac{q}{q_{max}} \tag{4.111}$$

After proper rearrangements, effectiveness ratio can be redefined as:

$$\varepsilon = \frac{C_h(T_{h,i} - T_{h,o})}{C_{min}(T_{h,i} - T_{c,i})} = \frac{C_c(T_{c,o} - T_{c,i})}{C_{min}(T_{h,i} - T_{c,i})} \tag{4.112}$$

Effectiveness ratio is dimensionless and determined in the range of $0 \leq \varepsilon \leq 1$. When the effectiveness ratio and inlet temperatures are known, actual heat transfer rate is determined as follows:

$$q = \varepsilon C_{min}(T_{h,i} - T_{c,i}) \tag{4.113}$$

Effectiveness ratio is a function of $NTU$ and the ratio $C_{min}/C_{max}$ depending on the magnitudes of hot and cold fluid heat capacity rates. The parameter $NTU$ is also dimensionless and stands for the number of transfer units, which is widely used in heat exchanger analysis.

$$NTU = \frac{UA}{C_{min}} \tag{4.114}$$

In the literature, heat capacity ratio is expressed as:

$$C_r = \frac{C_{min}}{C_{max}} \tag{4.115}$$

Effectiveness for different types of heat exchangers such as parallel-flow, counter-flow and cross-flow are determined. The effectiveness of a heat exchanger is determined for a single unit then modified to the number of transfer units (NTU).

In the beginning of the condenser modeling, it is decided to use effectiveness-NTU method due to the advantage of the method. It is simpler to apply NTU method on the condenser model than of the LMTD method as mentioned.

There are two main problems encountered in the application of the effectiveness-NTU method. First problem was the root-finding problem shown in Figure 4.12. Second problem is about the convergence shown in Figure 4.13.



Figure 4.12. Graph of the root-finding problem
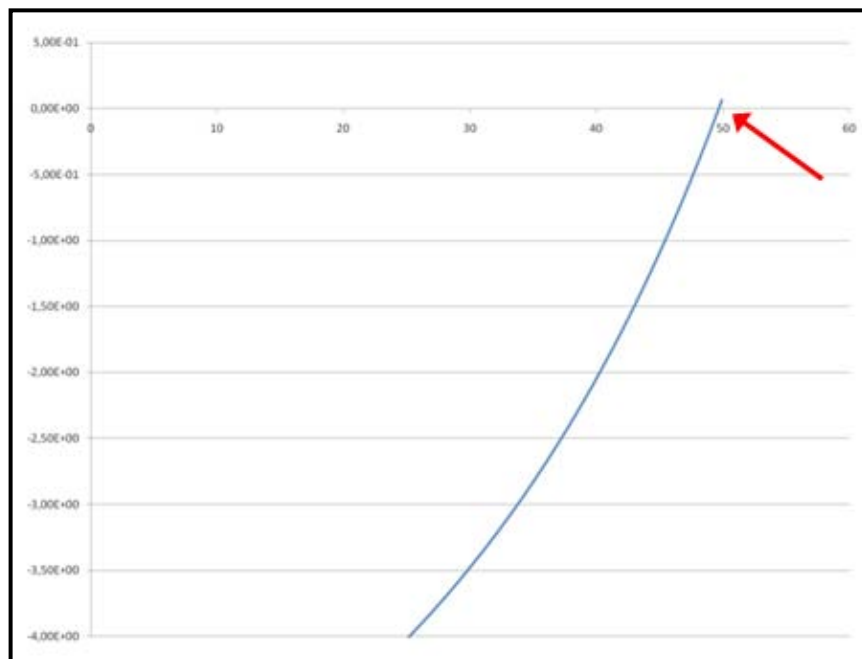


Figure 4.13. Graph of the convergence problem

Roots of the equations are solved iteratively by Newton's method. Sometimes slope of the equation does not fit the line and crosses at more than one location, which gives us a wrong solution. Thus, the linearity of the curve in Figure 4.12 is affected. Since the curve crosses the solution line at more than one location, there is more than one solution. One of the solutions is valid, but it is not easy to realize which one is the correct solution at complex equation sets.

The second problem is about the convergence. Sometimes, initial guess has to be chosen very close to the inlet temperature. Thus, it is found that the inlet and outlet temperatures are almost the same after much iteration under these conditions. This solution is not a reasonable since it is strongly dependent on the initial guess.

## 4.7.2.  Logarithmic Mean Temperature Difference Method (LMTD)

This method is very simple to use when the fluid inlet temperatures are known and outlet temperatures are specified or can be determined easily from the conservation of energy. If only the inlet temperatures are known, an iterative scheme has to be constructed. Total rate of heat transfer between hot and cold fluids and given below:

$$q = \dot{m}_h C_{p,h}\left(T_{h,i} - T_{h,o}\right) \tag{4.116}$$

$$q = \dot{m}_c C_{p,c}\left(T_{c,o} - T_{c,i}\right) \tag{4.117}$$

The temperature difference between hot and cold fluids is expressed by:

$$\Delta T = T_h - T_c \tag{4.118}$$

If we combine the equations, Equation 4.116 and Equation 4.117 with the Newton's law of cooling, we came up with the Equation 4.119 below:

$$q = UA\Delta T_{lm} \tag{4.119}$$

Counter-flow heat exchanger is used as condenser for the tumble dryer, which was simulated by the program. Hence, the logarithmic mean temperature difference for counter-flow is going to be determined.

If we apply differentiation to Equation 4.116, Equation 4.117 and Equation 4.118, we came up with the following equations respectively:

$$dq = -\dot{m}_h C_{p,h} dT_h = -C_h dT_h \tag{4.120}$$

$$dq = \dot{m}_c C_{p,c} dT_c = C_c dT_c \tag{4.121}$$

$$d(\Delta T) = dT_h - dT_c \tag{4.122}$$

Heat transfer across the surface area $dA$ can also be expressed as:

$$dq = U\Delta T dA \tag{4.123}$$

When we combine those equations and perform integration:

$$\int_1^2 \frac{d(\Delta T)}{\Delta T} = -U\left(\frac{1}{C_h} + \frac{1}{C_c}\right)\int_1^2 dA \tag{4.124}$$

$$ln\left(\frac{\Delta T_2}{\Delta T_1}\right) = -UA\left(\frac{1}{C_h} + \frac{1}{C_c}\right) \tag{4.125}$$

When we rearrange Equation 4.125 and substitute the terms $C_h$ and $C_c$ :

$$q = UA\frac{\Delta T_2 - \Delta T_1}{ln(\Delta T_2/\Delta T_1)} = UA\Delta T_{lm} \tag{4.126}$$

As a result, it has been clarified that how the general equation of heat transfer for LMTD method given in Equation 4.119.

For a counter flow heat exchanger, logarithmic mean temperature difference is expressed as follows:

$$\Delta T_{lm} = \frac{\Delta T_2 - \Delta T_1}{ln(\Delta T_2/\Delta T_1)} = \frac{\Delta T_1 - \Delta T_2}{ln(\Delta T_1/\Delta T_2)} \tag{4.127}$$

$$\Delta T_1 = T_{h,i} - T_{c,o}$$
$$\Delta T_2 = T_{h,o} - T_{c,i} \tag{4.128}$$

It should be noted that, at the same inlet and outlet temperatures, the log mean temperature difference for counter-flow exceeds than of parallel-flow, $\Delta T_{lm,CF} > \Delta T_{lm,PF}$ . Thus, the surface area that is required to affect a heat transfer rate is smaller for the counter-flow than of the parallel-flow arrangement, assuming that they have the same value of $U$.
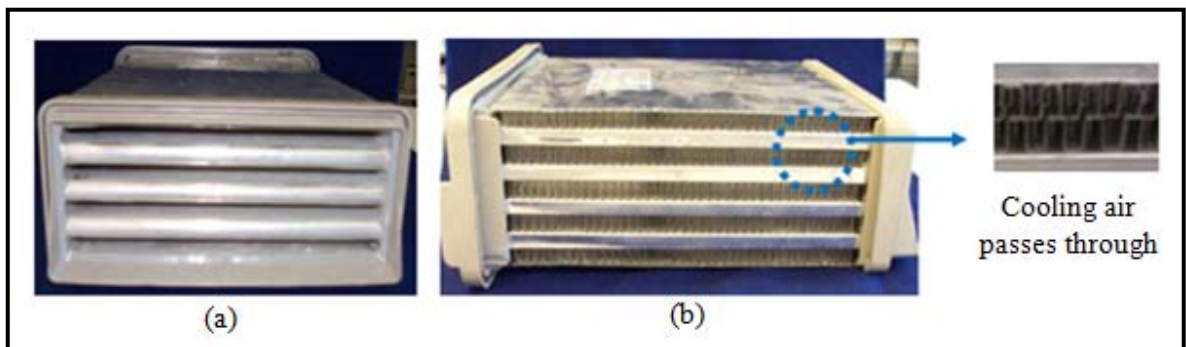


Figure 4.14. Counter-flow condenser, a. front view, b. side view

Counter-flow condenser consists of two main sections, where hot process air enters from one side and cold cooling ambient enters from the other side. Hot process air enters the condenser through the channels shown in Figure 4.14 (a). Similarly, cold ambient air enters the condenser through the fins shown in Figure 4.14 (b).

In modeling, heat exchange process inside the condenser was investigated in two parts. In the first part, it has been assumed that no condensation is occurred. In the second part of the modeling, the condensation process inside the condenser fins is taken into consideration.

Moreover, process is solved for one cell in the finite element model. These solutions are transferred to the cell next to it. Similarly, condensation process is solved iteratively for the whole condenser. Control volume for one cell with hot and cold fluids inside the condenser is shown in Figure 4.15. Red and blue colored arrows represent the directions of the hot and cold fluids respectively.
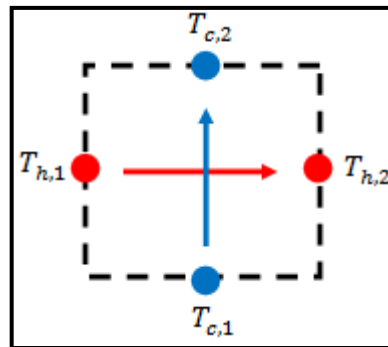


Figure 4.15. Control volume of the one cell in the condenser: (red): indicates hot process air, (blue): indicates cold ambient air

Due to the physics of the flow inside the condenser, at the inlets of the fins there non-uniform velocity exists. Flow becomes uniform after a while passing through the fins. In addition, velocity of the flow decreases near the walls and it is almost zero at the walls of the channels. Uniform and non-uniform velocity profiles of the fluid are given schematically in Figure 4.16.
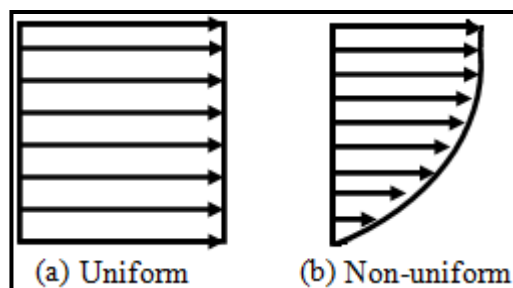


Figure 4.16. Velocity profile inside the condenser, a. uniform, b. non-uniform

For the no-condensation part mentioned, it is assumed that $w_2 = w_1$. Since, the inlet temperatures of hot and cold fluid are known, it is required to solve iteratively for the outlet temperatures shown in Figure 4.15.

Two main equations for the no-condensation part are derived by the conservation of energy expressed below:

$$q = \dot{m}_h\left(h_{h,1} - h_{h,2}\right) = \dot{m}_c Cp_{air}\left(T_{c,2} - T_{c,1}\right) \tag{4.129}$$

$$q = \dot{m}_c Cp_{air}\left(T_{c,2} - T_{c,1}\right) = UA\Delta T_{lm}F \tag{4.130}$$

The outlet temperatures $T_{c,2}$ and $T_{h,2}$ are solved simultaneously. In addition, enthalpy at the outlet of the hot fluid is temperature dependent and expressed as:

$$h_{h,2} = Cp_{air}T_{h,2} + w_2 h_{g,2} \tag{4.131}$$

Partial differentials of $h_{h,2}$ and $T_{c,2}$ are required to solve for $T_{h,2}$. Partial differential of $\partial T_{c,2}/\partial T_{h,2}$ is derived from Equation 4.129 by leaving $T_{c,2}$ alone at left hand side and partial differential $\partial h_{h,2}/\partial T_{h,2}$ is determined by differentiating Equation 4.131.

$$\frac{\partial h_{h,2}}{\partial T_{h,2}} = Cp_{air} + w_2\frac{\partial h_{g,2}}{\partial T_{h,2}} \tag{4.132}$$

$$\frac{\partial T_{c,2}}{\partial T_{h,2}} = T_{c,1} + \frac{q}{\dot{m}_c Cp_{air}} \tag{4.133}$$

For the second part mentioned where condensation takes place, it is assumed that $w_2 \neq w_1$. Specific humidity at outlet, $w_2$ is determined by:

$$w_2 = \frac{0.622\phi_2 P_s\left(T_{h,2}\right)}{P_0 - \phi_2 P_s\left(T_{h,2}\right)} \tag{4.134}$$

Relative humidity at the outlet ($\phi_2$) is determined from the Equation 4.135. In addition, $RH_{coeff}$ determines whether ($\phi_2 = \phi_1$) or ($\phi_2 = 100\%$), which will be explained later.

$$\phi_2 = \phi_1 RH_{coeff} + \left(1 - RH_{coeff}\right) \tag{4.135}$$

$$P_{v,2} = 0.622\phi_2 P_s\left(T_{h,2}\right) \tag{4.136}$$

Similarly, the partial differential of $w_2$ with respect to $T_{h,2}$ is determined. In addition, partial differential $\partial P_{v,2}/\partial T_{h,2}$ is determined by the subroutine, which was mentioned before.

$$\frac{\partial w_2}{\partial T_{h,2}} = \frac{0.622\dfrac{\partial P_{v,2}}{\partial T_{h,2}}P_0}{\left(P_0 - P_{v,2}\right)^2} \tag{4.137}$$

The two main equations for the condensation part are derived by the conservation of energy and expressed as:

$$\dot{m}_h\left(h_{h,1} - h_{h,2}\right) - \dot{m}_h(w_1 - w_2)h_{f,2} + \dot{m}_{cond}\left(h_{f,1} - h_{f,2}\right)$$
$$= \tag{4.138}$$
$$\dot{m}_c Cp_{air}\left(T_{c,2} - T_{c,1}\right)$$

$$q = \dot{m}_c Cp_{air}\left(T_{c,2} - T_{c,1}\right) = UA\Delta T_{lm}F \tag{4.139}$$

We can see that Equation 4.130 and Equation 4.139 are exactly the same, the only difference between condensation and no-condensation parts is the assumption of the specific humidity at the outlet $(w_2)$.

Partial differentials of $h_{h,2}$ and $T_{c,2}$ are required to solve for $T_{h,2}$. Partial differential of $\partial T_{c,2}/\partial T_{h,2}$ is derived from the Equation 4.138 by leaving $T_{c,2}$ alone at left hand side. Partial differential $\partial h_{h,2}/\partial T_{h,2}$ is same for condensation part as expressed in Equation 4.132. Moreover, partial differentials $\partial w_2/\partial T_{h,2}$ and $\partial h_{f,2}/\partial T_{h,2}$ are determined by the subroutine, which was mentioned before.

$$\frac{\partial T_{c,2}}{\partial T_{h,2}} = \frac{1}{\dot{m}_c C p_{air}} \left\{ -\dot{m}_h \frac{\partial h_{h,2}}{\partial T_{h,2}} - \dot{m}_{cond} \frac{\partial h_{f,2}}{\partial T_{h,2}} \right\}$$
$$+ \frac{1}{\dot{m}_c C p_{air}} \left\{ -\dot{m}_h \left[ (w_1 - w_2) \frac{\partial h_{h,2}}{\partial T_{h,2}} - \frac{\partial w_2}{\partial T_{h,2}} h_{f,2} \right] \right\}$$

(4.140)

Since all the required partial differentials are determined, it is possible to apply the Newton's method to solve for $T_{c,2}$ and $T_{h,2}$ simultaneously. For both condensation and no-condensation parts, the general iterative scheme is obtained as follows:

$$f = \dot{m}_c C p_{air} (T_{c,2} - T_{c,1}) ln \left( \frac{T_{h,2} - T_{c,1}}{T_{h,1} - T_{c,2}} \right) - UAF \left[ (T_{h,2} - T_{c,1}) - (T_{h,1} - T_{c,2}) \right]$$

(4.141)

$$f' = \dot{m}_c C p_{air} \left[ \frac{\partial T_{c,2}}{\partial T_{h,2}} ln \left( \frac{T_{h,2} - T_{c,1}}{T_{h,1} - T_{c,2}} \right) \right]$$
$$+ \dot{m}_c C p_{air} \left[ (T_{c,2} - T_{c,1}) \left( \frac{1}{T_{h,2} - T_{c,1}} \right) \left( \frac{\frac{\partial T_{c,2}}{\partial T_{h,2}}}{T_{h,1} - T_{c,2}} \right) \right]$$
$$- UAF \left( 1 + \frac{\partial T_{c,2}}{\partial T_{h,2}} \right)$$

(4.142)

$$T_{h,2}^{n+1} = T_{h,2}^n - \frac{f}{f'}$$

(4.143)

The only difference between no-condensation and condensation solution scheme is the $UA$ parameter. This parameter takes different values for the mentioned cases. In addition, for condensation part, initial guess is set as $T_{h,2} \cong T_{c,2}$, where cold air temperature is almost same as the hot air temperature at outlet. In the end, energy parameters such as condenser efficiency, energy consumption, heating and cooling efficiencies are determined.

It should be noted that before applying the Newton's method, it has been checked whether there is a problem at the logarithmic mean temperature difference.

## 4.8.  INPUT & OUTPUT PARAMETERS

In this section, the input and output parameters that are involved in the main program are introduced. The main program includes all the subroutines, which help the programmer in writing the code by eliminating the repetitions and degrading a unity. General input and output parameters of the main program are given in Table 4.2 and they are going to be discussed individually.

Table 4.2. General input & output parameters of the main program

| Input Parameters | Output Parameters |
|---|---|
| • Heater Algorithm | • Temperature |
| • Total Time of Drying Period | • Relative Humidity |
| • Process Air Flow Rate | • Specific Humidity |
| • Cooling Air Flow Rate | • Change in Mass of Water at the surface of Clothes |
| • Initial Conditions | • Evaporation Rate |
| • Environmental Conditions | • Condensation Rate |
| • Total Mass Transfer Coefficient | • Condensation Efficiency |
| • Heat Transfer Coefficients | • Total Energy Consumption |
| • RH_Coefficient | |
| • Air Leakage Ratios | |
| • Condenser Correction Factor | |

### 4.8.1.  Input Parameters

Working mechanism of the heater algorithm in the simulation program is similar to the actual one installed on the digital card. In actual dryers, a heater with 2000 W power consists of two parts as mentioned. First part is 600 W and the second part with a higher power level, which is 1400 W.

According to the algorithm installed on the digital card, sometimes the heater part with smaller power level is shut down and only the part with higher power level is remained working, thus 1400 W heater power is obtained.

When the two heater parts work together, 2000 W heater power is obtained. Heater algorithm in the simulation program is set to apply totally 2000 W heater power. In addition, the one with smaller power level is shut down and heater power is lowered to 1400 W periodically. At the cooling phase of the drying, both parts of the heater are shut down.

In Figure 4.17, a sample of heater algorithm of the simulation program is shown. Power levels of the heater parts and the specific periods of shutdowns can be rearranged, as it is desired. In addition, total time of the drying process is defined by the user, which is entered as an input parameter. Moreover, it can be rearranged by a loop that checks the relative humidity or the temperature at drum exit in order to determine whether drying process is achieved or not similarly in tumble dryers.
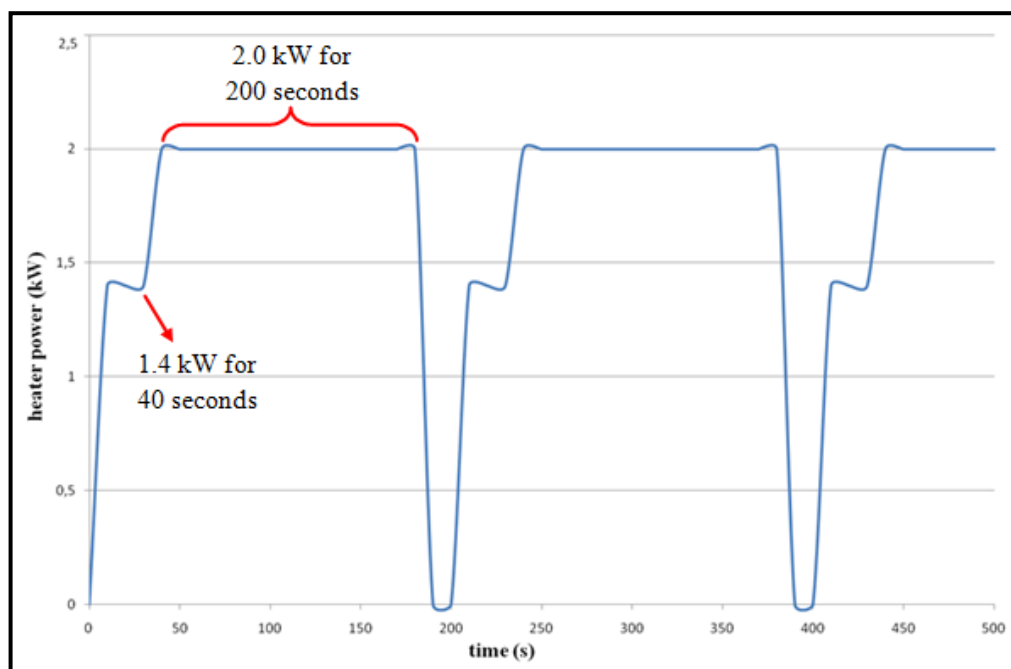


Figure 4.17. Sample of the heater algorithm for the simulation program

In addition, the user defines the mass flow rate of process air and cooling air as input parameters. Generally, mass flow rate of cooling is higher than the mass flow rate of process air. Constant parameters such as $Cp_{air}$ , $Cp_{cloth}$ and $Cp_{water}$ are defined in the beginning of the main program. Volume of the drum and heat transfer coefficient time area parameters are also the other constant parameters.

Most of the initial condition parameters are related with drum. The initial conditions that are related with drum are listed in Table 4.3.

Table 4.3. Initial condition parameters related with drum

| Initial Condition Parameters |
|---|
| • Temperature of clothes inside the drum |
| • Temperature of water on clothes inside the drum |
| • Temperature of fluid inside the drum |
| • Relative humidity in drum |
| • Specific humidity in drum |
| • Density of air inside the drum |
| • Mass of water on the clothes in drum |
| • Mass of air inside the drum |
| • Enthalpy of air inside the drum |
| • Vaporization rate at drum |

Environmental conditions, which are given in Table 4.4 are also defined in the beginning of the main simulation program.

Table 4.4. Environmental condition parameters

| Environmental Conditions |
|---|
| • Temperature |
| • Pressure |
| • Relative humidity |
| • Specific humidity |
| • Specific enthalpy |

One another important parameter is the relative humidity coefficient entered by the user, which determines the magnitude of the relative humidity at condenser exit. On the other hand, the relative humidity at condenser exit depends on the relative humidity at condenser inlet. Moreover, a constraint exists for the relative humidity coefficient, which is $0 < RH_{coeff} < 1$ . In the end, the relative humidity at the condenser exit is calculated by the Equation 4.144 given below.

$$RH_2 = RH_1 RH_{coeff} + \left(1 - RH_{coeff}\right) \tag{4.144}$$

According to the Equation 4.144, relative humidity at condenser exit is equal to the relative humidity at condenser exit when $RH_{coeff}$ is equal to one. In addition, relative humidity at condenser exit becomes 100 per cent when $RH_{coeff}$ is equal to zero.

Tumble dryer system is not a perfectly insulated system. Thus, air leakage has to be taken into consideration. There are three main locations at the dryer, which were determined by series of experiments and the amount of estimated air leakage at that locations were calculated before.

In the simulation program, the amount of air leakage is also taken into account by using the air leakage ratio parameters. Some of the total cooling air leaks from chassis into the condenser entrance. Some of the process air leaks through the chassis while blowing from the fan. Some of the process air is lost while crossing through the heater at the drum entrance. The mentioned air leakages are proportioned to the total amount of air flow rate at fan and defined in the main program as constant parameters.

For multipass and cross-flow heat exchangers, condenser correction factor is applied on the log mean temperature difference. In Equation 4.145, condenser correction factor is expressed by $F$. Condenser correction factor for shell-and-tube and cross-flow heat exchangers in the literature is represented graphically.

$$\Delta T_{lm} = F \Delta T_{lm,CF}$$

(4.145)

Heat transfer coefficients of the drying process are set as constant parameters and included in the simulation program. Heat loss in the heater and drum are also defined as constant input parameters.

In addition, the total mass transfer coefficient is included as a constant parameter in the simulation program. The experimental study on the investigation of mass transfer coefficient influences the modeling of the mass transfer process in the drum.

### 4.8.2. Output Parameters

Temperature, relative humidity and specific humidity at any location on the dryer such as condenser inlet or drum outlet can be obtained as an output parameter during the simulation.

Another parameter that is involved during the drying process in the simulation program is the change in the mass of water at the surface of the clothes. Thus, we can monitor the change in the mass of the water and realize whether the clothes are dried or not.

Simulation program also informs us about the efficiency of the drying performance. Evaporation rate and condensation rate are obtained as output parameters. Total amount of energy consumption and condenser efficiency are other useful parameters that indicate the performance of the drying process.

### 4.9. SIMULATION RESULTS AND DISCUSSION

In the process of modeling, all the components of an air-condenser tumble dryer such as fan, heater, drum and condenser are modeled by the conservation of energy and mass in the simulation program. In addition, thermodynamical properties of the specified components such as specific humidity, temperature or relative humidity are determined at any desired inlet or outlet. Complex equations involved during the modeling of the transient operation of an air-condenser tumble dryer are solved iteratively by applying the Newton's method.

Temperature at the drum outlet is one of the most important outputs of a drying process, which helps us to indicate whether clothes are dried or not. It can be stated that the clothes are dried just by looking at the overshoot before the cooling phase of the drying process. Temperature at the drum outlet is plotted in Figure 4.18 with respect to total time of drying process including both experimental and simulation data.
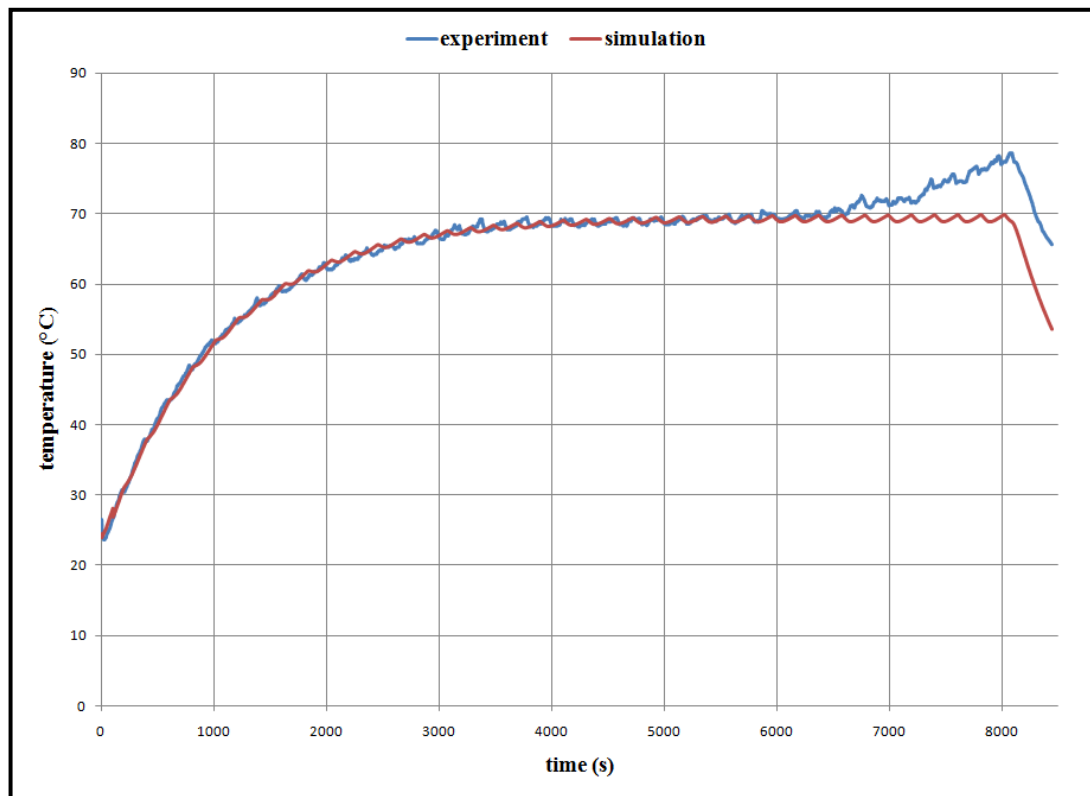
Figure 4.18. Distribution of the temperature at the drum exit

The blue line in Figure 4.18 represents the distribution of temperature at drum exit for the experimental data. Similarly, the red line in Figure 4.18 represents the distribution of temperature at drum exit for the simulation data. It can be stated that the clothes are dried sufficiently when we examine the overshoot at the end of the experimental data. As clothes dry, the amount of water at the surface of clothes decreases respectively. Hence, the temperature at the surface of clothes increases, which leads to an overshoot in the temperature at drum exit nearly at the end of the equilibrium phase. Relative humidity at the drum exit also decreases as clothes dry. The decrease in relative humidity is detected by the humidity sensors located at tumble dryers and thus, heater is shut down when cooling phase begins.

In the early stages of simulation model, the transient shut down period is difficult to simulate. Although, the relative humidity at the surface of the clothes decreases as clothes start to dry, it is remained constant for the whole drying process in the beginning of the modeling. However, simulation results are still in good agreement with the experimental results at transient heating and equilibrium phases of drying process.

The problem about the relative humidity change at the end of the equilibrium phase is handled by using the water activity parameter in the modeling. Vapor pressure is modified and thus, the relative humidity at the surface of the clothes is changed by using the water activity parameter as mentioned. Temperature distribution at drum outlet including the effect of water activity parameter is shown in Figure 4.19.
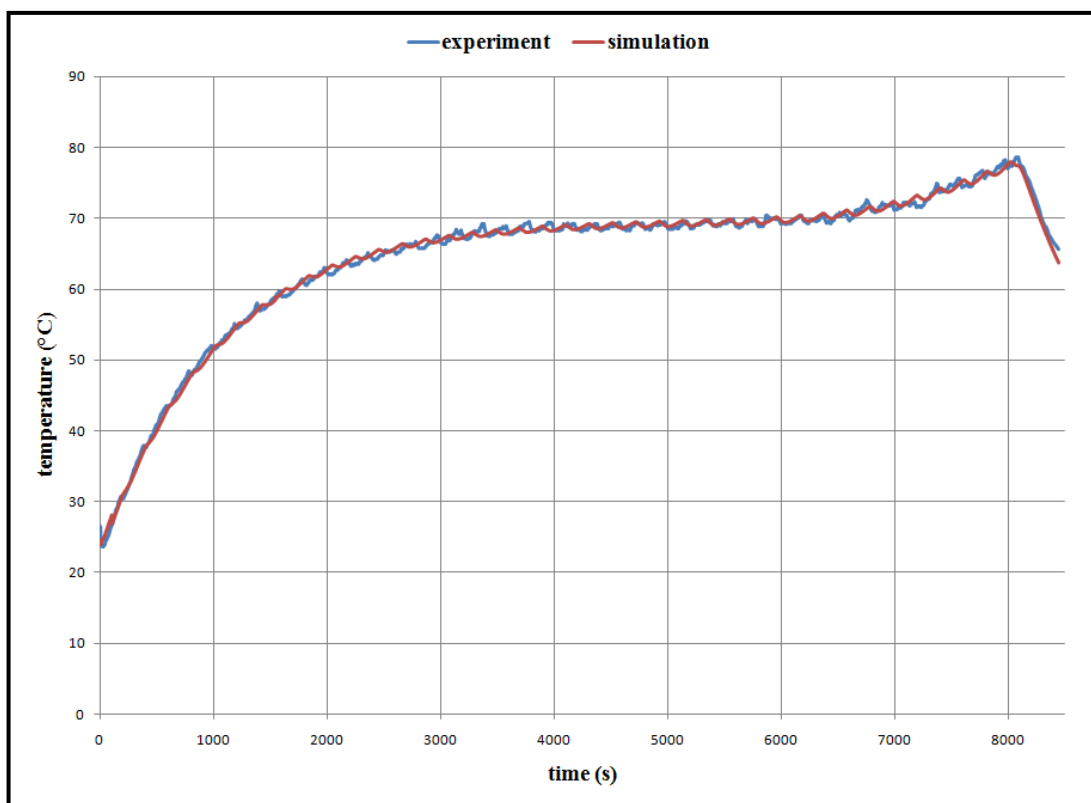


Figure 4.19. Distribution of the temperature at the drum exit including the water activity

The effect of water activity parameter on the temperature distribution at the drum exit can be examined by comparing Figure 4.18 and Figure 4.19. As a result, it is found that the simulation results are considerably in good agreement with the experimental results for all phases of the drying process. Both of the mentioned figures are corresponding to the results for 6 kg of load weight. In addition, all the parameters that are set in the simulation program are given in Appendix A.

For next step, relative humidity is investigated for both simulation and experimental data, which is shown in Figure 4.20.
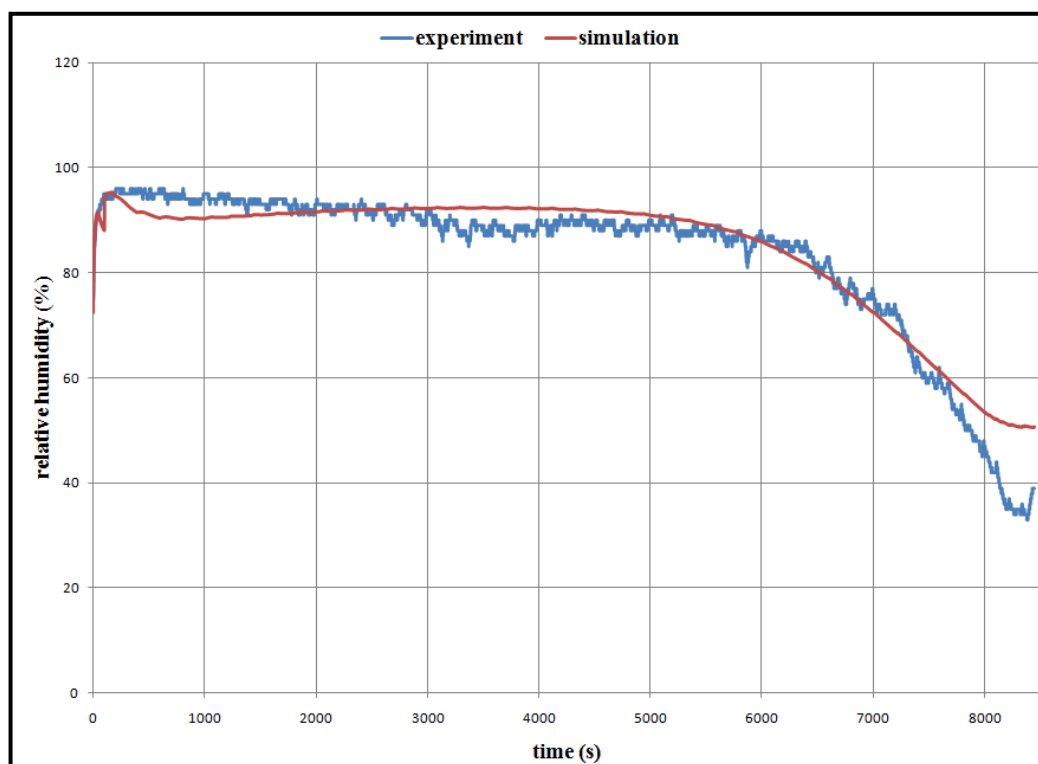
Figure 4.20. Distribution of the relative humidity at drum exit

The total mass transfer coefficient is set constant during the entire drying process as mentioned except for approximately the first 170 seconds of the heating phase. In addition, vapor pressure is modified at the end of the equilibrium phase; hence, the total mass transfer coefficient is set constant in order not to change repetitively. It is found that the relative humidity data for the simulation is in considerably good agreement with the experimental data. In addition, it should be noted that the perfect relative humidity measurement is a tough obstacle to achieve. It is hard to simulate whether you are not sure that the relative humidity measurement is handled without any question marks on the mind.

Another important parameter is the vaporization rate of the drying process, which is used in determining the efficiency of the drying process. Vaporization rate of the drying process for both simulation and experimental data can be observed by examining Figure 4.21. Vaporization rate indicates the amount of water that is extracted from the surface of the clothes during the drying process.
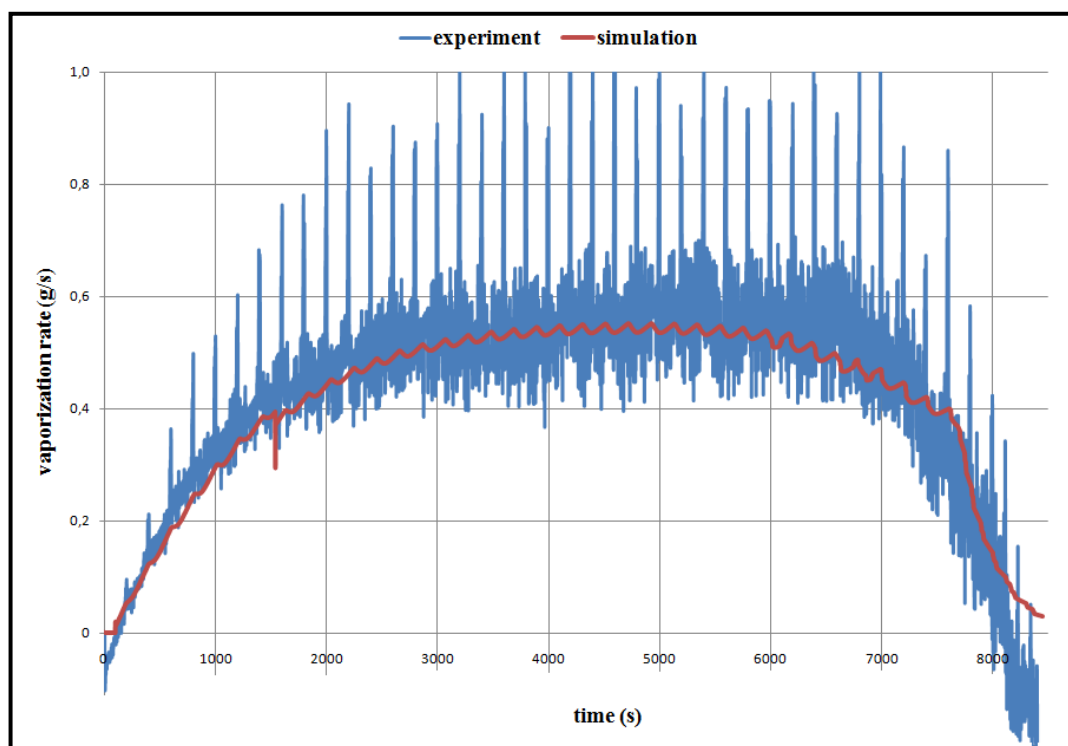
Figure 4.21. Vaporization rate of the drying process

It is found that the simulation results for vapor rate are considerably in good agreement with the experimental data when we examine Figure 4.21. Great oscillations in the experimental data for the following figure arise from the working principle of heater algorithm of the tumble dryer. In addition, heater is shut down periodically in order not to damage the equipment and thus, the oscillations in the experimental data are developed. In summary, it is clear that the simulation results are very close to the average values of the experimental data.

Before the construction of the simulation model, experimental study is carried out in order to investigate the physics of the drying process. Since the simulation results are verified so far by comparing with the experimental data, present experiments will be discussed and the difference between simulation and experimental results is going to be clarified in more detail.

In Figure 4.22, the total mass transfer coefficient data with respect to the remaining water at the surface of clothes are shown for air-vented and air-condenser tumble dryers. The data in the following figure are calculated experimentally. In addition, Terra and Luna are different types of air-condenser tumble dryers.
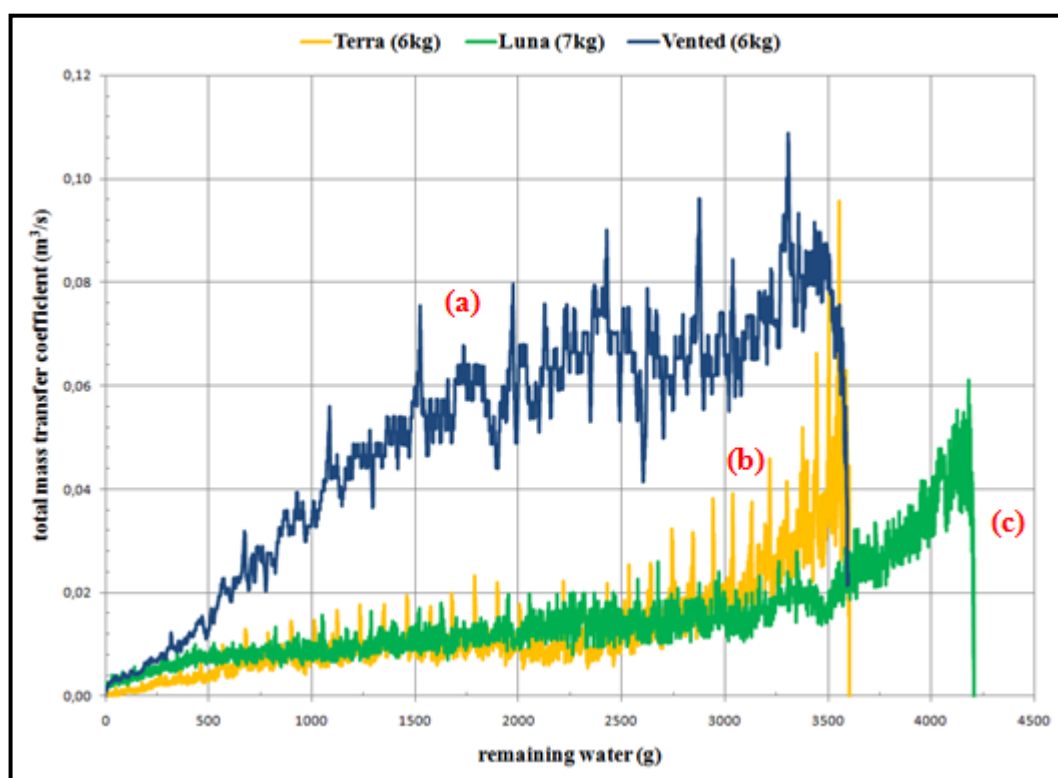


Figure 4.22. Total mass transfer coefficient for the different types of tumble dryers, a. air-vented tumble dryer, b. Terra (air-condenser), c. Luna (air-condenser)

The characteristics of the total mass transfer coefficients for different types of air-condenser tumble dryers are similar with each other. Since the graph is plotted with respect to the remaining water at the surface of the clothes, the discrepancy for the air-condenser tumble dryers at the figure is due to the difference in the weight of the clothes.

The total mass transfer coefficient is significantly higher for an air-vented tumble dryer and there is a clear difference in between air-vented and air-condenser tumble dryers. This difference may be due to the different conditions in the specific humidity data for the tumble dryers. In addition, the difference between the air-condenser and air-vented tumble dryers may originate from the drying technology.

Specific humidity is also one of the most significant parameter in determining the total mass transfer coefficient of the drying process. Specific humidity at the drum inlet is almost constant for an air-vented tumble dryer. However, for an air-condenser tumble dryer, specific humidity at the drum inlet is slightly lower than of the drum outlet. In addition, specific humidity at the drum inlet and the outlet change in similar way through the drying process for an air-condenser tumble dryer.

Specific humidity data at drum inlet and outlet for both air-vented and air-condenser tumble dryers are shown in Figure 4.23. If we examine the figure, the blue line represents the specific humidity at drum inlet for an air-vented tumble dryer, which is much lower than the specific humidity at drum outlet that is represented by the red line. In addition, the specific humidity at drum inlet is almost constant for an air-vented dryer. Moreover, the yellow and green lines on the following figure stand for the specific humidity at the drum outlet and inlet respectively. It is also found that the specific humidity at drum inlet is slightly lower than of the drum outlet for an air-condenser tumble dryer.
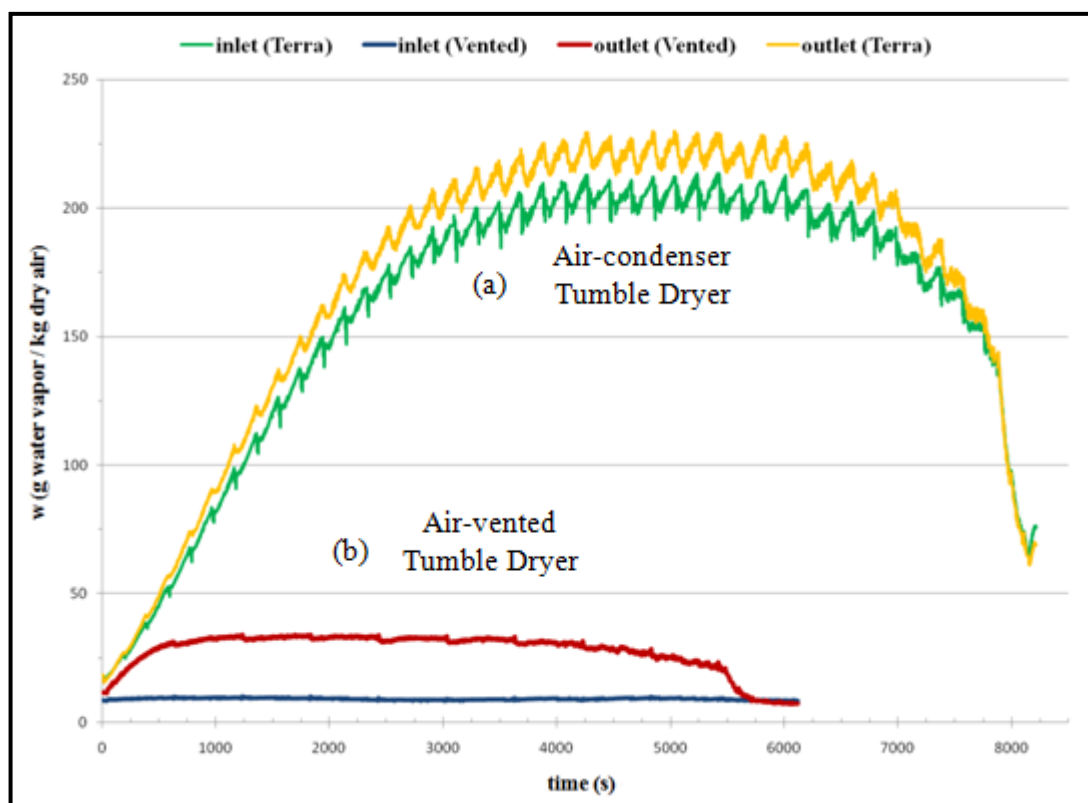


Figure 4.23. Specific humidity at drum for tumble dryers, a. air-condenser, b. air-vented

At the early beginning of the drying process, the value of the total mass transfer coefficient is significantly lower than at anywhere else during the drying process. This situation is valid for both condenser and air-vented tumble dryers, which is shown in Figure 4.24 by red circles around the respective lines. In addition, when we examine Figure 4.23 and Figure 4.20, we can easily realize that the low total mass transfer coefficient experienced at the beginning of the drying process is relatively more influencing for the relative humidity at the drum outlet than of the temperature.
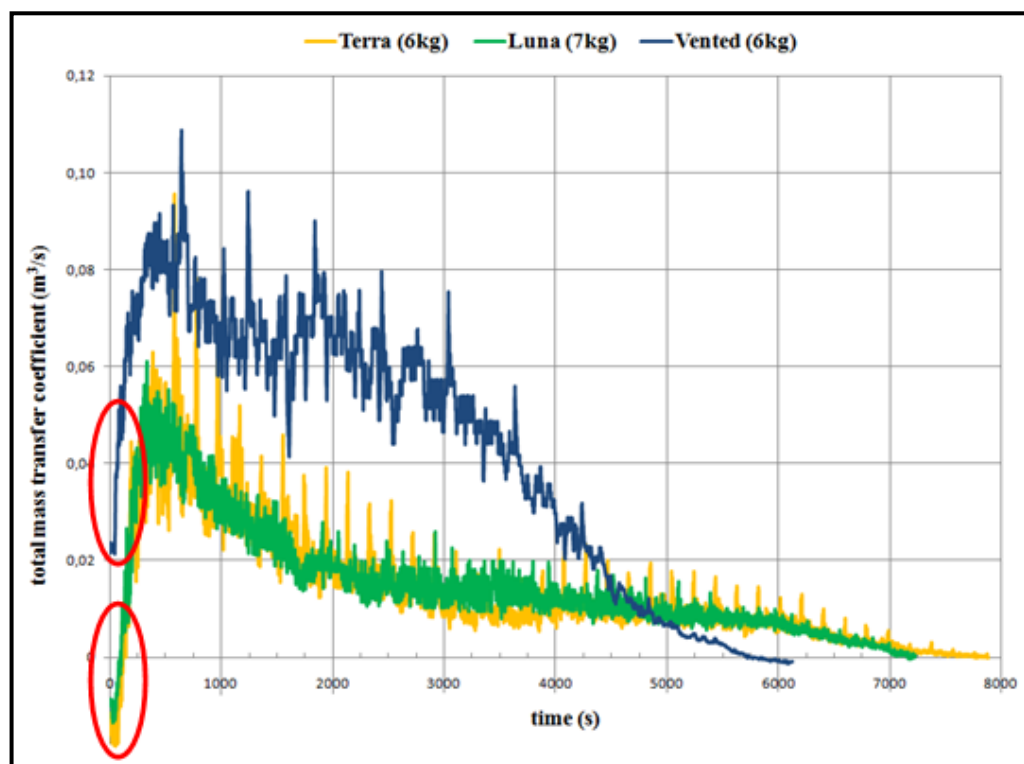


Figure 4.24. Total mass transfer coefficient at the beginning of the drying process

For both air-vented and air-condenser tumble dryers, the total mass transfer coefficient is very low for the first few minutes in the drying process. Then after five to ten minutes later, the total mass transfer coefficient makes a peak and after a while, it reaches to steady state where almost constant in magnitude for air-condenser tumble dryer. Then, it decreases with respect to time through the end of the drying process. The distribution of the total mass transfer coefficient for both tumble dryers can be monitored by examining Figure 4.24.

In addition, the low total mass transfer coefficient at the beginning of the transient heating phase is taken into consideration for the simulation program. For nearly about 170 seconds, the total mass transfer coefficient is set significantly low. Then the total mass transfer coefficient is set constant for the whole drying process. Moreover, the simulation program sometimes may fail when the low total mass transfer coefficient is ignored.

Another interesting topic is that the surface of the clothes is too cold and the hot process air does not propagate through the center of the clothes rapidly at the beginning of the heating. The propagation of hot process air from the surface through the center of the cloth is shown schematically in Figure 4.25.
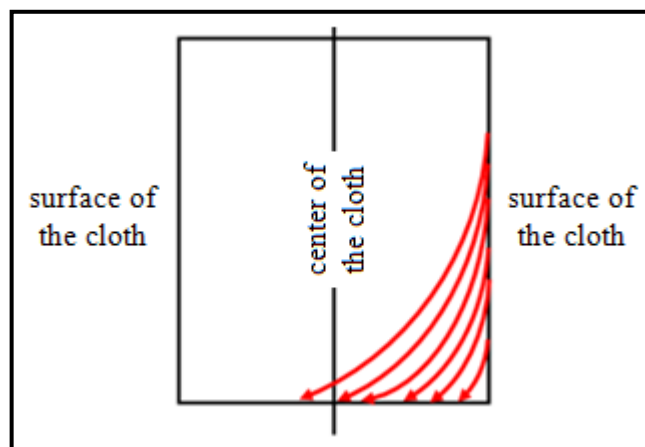


Figure 4.25. Propagation of the hot air through the cloth

In the beginning of the drying process, the surface temperature of wet clothes is very low when it is compared to the ambient air temperature. Surface temperature increases slowly as hot air arrives through the center of the clothes. The low total mass transfer coefficient experienced at the beginning of the transient heating phase is reasonable due to the slow propagation of hot air through the clothes.

It can be stated that the propagation of hot air through the center of the clothes may not accrue as fast as it is expected. In addition, the low total mass transfer coefficient experienced at nearly hundred seconds after the dryer is operated. Thus, it can be stated that the low mass transfer coefficient for about hundred seconds does not affect the performance of drying process significantly.

## 5. CONCLUSION

In this project, the entire transient operation of tumble dryers is investigated from the start transient to the steady-state operation and to the shutdown period. One of the main purposes is to gain an understanding of the mass transfer process in the drum of tumble dryers. At first, the present study was conducted experimentally and then the whole tumble dryer was modeled and simulated.

In the beginning of the experimental study, mass transfer process in the drum is investigated at an air-vented tumble dryer. The air-vented dryer, which has no condenser, eliminates the complicate process of condensation, making it easier to investigate the mass transfer process in the drum. Temperature and relative humidity are measured at drum outlet and at the upstream of the heater, whose data will give information at the drum inlet. The preliminary results of air-vented tumble dryer experiments show that the total mass transfer coefficient mainly depends on the amount remaining water at the surface of the clothes.

The design of experiment (DOE) method is employed in order to conduct more extensive study on which factors influence the total mass transfer coefficient. The effects of flow rate, load weight, initial moisture content and heater power are studied by series of experiments. It is found that the amount of remaining water at the surface of the clothes is the most influencing parameter on the total mass transfer coefficient. Moreover, it appears that the amount of remaining water at the surface of the clothes is less influencing the total mass transfer coefficient during the transient heating (start transient) period than during the steady state period.

In addition, mechanical movement of clothes, different textile type, variable fan speed and variable flow rate are investigated experimentally. Synthetic type textile has a tendency to release water easily, and thus its total mass transfer coefficient reaches to higher values than that of the cotton type textile.

It is also found that the flow rate affects the mass transfer significantly, especially during the transient heating period. Long bed sheets are often flocculated inside the drum and remain wet, affecting the mass transfer process.

Air-condenser dryers are also employed to examine the mass transfer process. General results show that the characteristics of the total mass transfer coefficient for air-condenser tumble dryer is quite similar to that of the air-vented tumble dryer. However, the total mass transfer coefficient for air-vented tumble dryer is determined to be approximately 0.06 $m^3$/s while it is about 0.01 $m^3$/s for air-condenser tumble dryer. Specific humidity at drum inlet remains constant for air-vented tumble dryer. However, specific humidity for air-condenser tumble dryer varies during drying. Different inlet conditions for specific humidity in two types of tumble dryers may have caused the discrepancy.

The present study also includes the modeling and simulation of the dryer. All components of a tumble dryer such as fan, heater, condenser and drum are modeled using equations for mass and energy conservations. The main program is written in FORTRAN and simulates the drying process from the start to the shutdown period. Water activity parameter is incorporated which influences vapor pressure on the wet clothes especially during the shutdown period. Condenser is modeled by LMTD method rather than NTU method because of complexity in finding roots for the NTU method. Newton's Method is applied for iterative root finding process. The simulation results are found to be in good agreement with the experimental data.

Simulation program enables us to observe the performance and efficiency of the drying process. In addition, temperature and humidity values, evaporation and condensation rates at any desired inlet or outlet condition can be obtained. This simulation model may be used as a practical tool in the design process of a new tumble dryer, thus helping to save time and money before constructing prototypes during the design process.

# 6.  FUTURE WORK

Developing a transient simulation model for air-condenser tumble dryers by investigating the heat and mass transfer was the main motivation of this study. As a future work, it may be necessary to expand the simulation model for the other types of tumble dryers such as air-vented or heat pump tumble dryers. In addition, the simulation model could be modified with variable heat transfer coefficients. A user-friendly graphical interface could be integrated on the simulation code written in FORTRAN in order to provide easier communication with the user.

In addition, some of the topics that are covered in the experimental study could be investigated in more detail. Thus, the effect of mechanical movement of clothes and textile type on the mass transfer process could be researched. Since relative humidity is one of the most significant parameters on the total mass transfer coefficient, variable inlet conditions for relative humidity at the drum inlet can be investigated. Moreover, the condensation in tumble dryers is a complicate process, which can be studied individually.

# APPENDIX A: SIMULATION PARAMETERS

Table A.1. Constant Parameters

| Parameter | Symbol | Value |
|---|---|---|
| Specific heat of water (kW/kg°C) | $Cp_w$ | 4.2 |
| Specific heat of clothes (kW/kg°C) | $Cp_c$ | 1.3 |
| Atmospheric pressure (kPa) | $P_0$ | 101.325 |
| Condenser correction factor | $F$ | 0.45 |
| Mass flow rate of process air (L/s) | $FR_p$ | 32 |
| Mass flow rate of cooling air (L/s) | $FR_c$ | 42 |
| Relative humidity coefficient | $RH_{coeff}$ | 0.80 |
| Total mass transfer coefficient (m³/s) | $(hA)_m$ (for 100 s) | 0.0002 |
| | $(hA)_m$ (after 100 s) | 0.03 |
| Water activity parameter constants | $\beta$ | 2 |
| | $\gamma$ | 350 |
| | $\delta$ | 1.05 |
| Heat transfer coefficient times area | $(hA_{ch})_{in}$ (W/K) | 20 |
| | $(hA_{ch})_{out}$ (W/K) | 2 |
| | $hA_{loss,heater}$ (kW/°C) | 0.0016 |
| | $hA_{loss,drum}$ (kW/°C) | 0.005 |
| | $hA_{heater}$ (kW/°C) | 0.032 |
| Air leakage ratio | $R_{fan}$ | 0.3 |
| | $R_{heater}$ | 0.05 |
| | $R_{cooling\ air}$ | 0.25 |

Table A.2. Initial Conditions and Environmental Parameters

| Parameter | Symbol | Value |
|---|---|---|
| Initial mass of water (kg) | $m_w$ | 3.6 |
| Initial temperature at drum (°C) | $T_{drum}$ | 25 |
| Initial relative humidity at drum (%) | $RH_{drum}$ | 70 |
| Initial temperature of water at drum (°C) | $T_w$ | 25 |
| Initial moisture content | $m\_c$ | 0.6 |
| Environment temperature (°C) | $T_\infty$ | 25 |
| Environment relative humidity (%) | $RH_\infty$ | 60 |

# REFERENCES

1. Old & Interesting, History of Laundry – After 1800,
   http://www.oldandinteresting.com/history-of-laundry.aspx

2. Wikipedia, Mangle (machine), http://en.wikipedia.org/wiki/Mangle_%28machine%29

3. Hartoka O., *"Design of an Efficient Condenser for Tumble Dryers",* Yeditepe University, Thesis Study, 2009.

4. Nipkow J. and E. Bush, "*Promotion of Energy Efficient Heat Pump Dryers*", Swiss Agency for Efficient Energy Use (S.A.F.E.).

5. Ecodesign of Laundry Dryers, "*Preparatory Studies for Ecodesign Requirements of Energy – using – Products (EuP) – Lot16",* Task 2 Final Version, June 2008.

6. Cochran M.P., *"A Feasibility Study of Incorporating Surface Tension Elements to Improve the Efficiency of Residential Clothes Dryers"*, Kansas State University Thesis Study, 2005.

7. Bassily A. M., *"Modeling and Optimization of Heating and Drying Processes in a Clothes Dryer",* Iowa State University, Thesis Study, 2000.

8. Haghi A. K., *"A Mathematical Model of the Drying Process",* Acta Polytechica, Vol. 41, No. 3, 2001.

9. Yadav V. and C. G. Moon, *"Fabric Drying Process in Domestic Dryers",* Applied Energy, Vol. 85, pp. 143 – 158, 2008.

10. Berghel J., L. Brunzell and P. Bengtsson, *"Performance Analysis of a Tumble Dryer",* Proceedings of the 14th International Drying Symposium, Vol. B, pp. 821 – 827, 2004.

11. Kasiri N., M. A. Hasanzzdeh and M. Moghadam, *"Mathematical Modeling and Computer Simulation of a Drum Dryer"*, Iranian Journal of Science & Technology, Transaction B, Vol. 28, No. B6, 2004.

12. T. Zeineldin, *"Modeling the Process of Drying Stationary Objects Inside a Tumble Dryer Using COSMOL Multiphysics"*, COSMOL Conference, University of Paderborn, Germany, 2008.

13. Stawreberg L. and L. Nilsson, *"Modeling of Specific Moisture Extraction Rate and Leakage Ratio in a Condensing Tumble Dryer"*, Applied Thermal Engineering 30, pp. 2173 – 2179, 2010.

14. Sensiron Sensor Company, web url: www.sensiron.com

15. D. Sonntag, *"Important New Values of the Physical Constants of 1986, Vapor Pressure Formulations Based on the ITS-90, and Psychrometer Formulae"*, Z. Meteorol. 70, pp. 340 – 344, 1990.

16. Orlando A. F., J. D. Brionizio and L. A. Lima, *"Calculation of Humidity Parameters and Uncertainties Using Different Formulations and Softwares"*.

17. Conde M. R., *"Energy Conservation with Tumbler Drying in Laundries"*, Applied Thermal Engineering 17, pp. 1163 –1172, 1997.

18. Deans J., *"The Modeling of a Domestic Tumbler Dryer"*, Applied Thermal Engineering 21, pp. 977 – 990, 2001.

# REFERENCES NOT CITED

"*Format for Theses*", The Institute of Graduate Studies in Science and Engineering, Yeditepe University Press, Istanbul, 2004.

Incropera F. P., D. P. DeWitt, T. L. Bergman and A.S. Lavine, "*Fundamentals of Heat and Mass Transfer*", Fifth Edition, WILEY, 2002.

Çengel Y. A. and M. A. Boles, "*Thermodynamics: An Engineering Approach*", Fourth Edition, McGraw-Hill, 2002.

Heath M. T., "*Scientific Computing: An Introductory Survey*", Second Edition, McGraw-Hill, 2005.

Adams R. A., "*Calculus: a Complete Course*", Fifth Edition, Adams, 2003.

Greenberg M. D., "*Advanced Engineering Mathematics*", Second Edition, Prentice Hall, 1998.

Holman J. P., "*Heat Transfer*", Sixth Edition, McGraw-Hill, 1986.

Moran M. J. and Shapiro H. N., "*Fundamentals of Engineering Thermodynamics*", Fifth Edition, Wiley, 2006.

Çengel Y. A. and J. M. Cimbala, "*Fluid Mechanics: Fundamentals and Applications*", Second Edition, McGraw-Hill, 2005.

Altaç Z. and M. Tekkalmaz, "*Mühendisler için FORTRAN 90/95 Programlama Dili ve Teknikleri*", Osmangazi University, 2005.